Louie Silver

Assessment of diatom assemblage responses to an alkalinity enhancement experiment in the Ria Formosa saltmarsh

UNIVERSIDADE DO ALGARVE

Faculdade de Ciências e Tecnologia

2024

Louie Silver

Assessment of diatom assemblage responses to an alkalinity enhancement experiment in the Ria Formosa saltmarsh

Mestrado em Biologia Marinha

Supervisor:
Isabel Maria de Paiva Pinto Mendes
Co-supervisor:
Ana Isabel de Sousa Horta Dias Gomes

UNIVERSIDADE DO ALGARVE

Faculdade de Ciências e Tecnologia
2024

Declaração de autoria de trabalho

Declaro ser o(a) autor(a) deste trabalho, que é original e inédito. Autores e trabalhos consultados estão devidamente citados no texto e constam da listagem de referências incluída.

Statement of authorship

I declare that I am the author of this work, which is original and unpublished. Authors and works consulted are duly cited in the text and are included in the list of references.

Declaração de direitos de autor

Copyright statement

Acknowledgements

To Isabel Mendes, I would like to thank you for your dedicated support and motivation throughout the project. It has been a pleasure to get to know you and to be inspired by your drive for your passions. Your education in marine ecology and oceanography has been vital for supplementing areas of knowledge I was still lacking. I appreciate the opportunity to have contributed to your team, especially including all the days stuck in the mud and cold!

To Ana Gomes, I am extremely grateful for the hours of dedication to bring me into your world of diatoms. Being able to utilise classical methods for viewing and classifying diatoms is a unique and beautiful tool, that gave me an insight into life in a different world. You have also helped me with disseminating information in a more structured form, to enable understanding a wider audience. These tools will be valuable for the future.

I am grateful to my colleagues on the projects team, especially Julia Lübbers, for their training, support and humour to keep me going.

This thesis was conducted as part of the RECAP (REduce atmospheric Carbon by Alkalinity enhancement in intertidal environments: Potential and impacts) project, funded by Fundação para a Ciência e a Tecnologia (FCT) - https://doi.org/10.54499/PTDC/CTA-CLI/1065/2021 The conceptual framework developed by the RECAP team significantly informed the approach taken in this thesis.

The equipment, resources, and facilities provided through CIMA (Centre for Marine and Environmental Research) were instrumental in completing this work.

Additional thanks go to any friends, family and loved ones that have supported me through this journey. Although they cant help directly, the emotional guidance allowed continued motivation.

Resumo

O aquecimento climático é um dos maiores desafios que a humanidade enfrentará nos próximos anos, sendo impulsionado principalmente pelos gases de efeito estufa, como o dióxido de carbono (CO_2), que absorvem a radiação solar refletida e retêm calor. A concentração de CO_2 na atmosfera aumentou drasticamente desde a revolução industrial, levando ao aumento das temperaturas globais, mudanças nos padrões climáticos e inúmeros impactos nos ecossistemas e sociedades humanas. Para enfrentar estes desafios, estão a ser desenvolvidas estratégias modernas de remoção de dióxido de carbono (CDR). Uma abordagem promissora é o aumento da alcalinidade oceânica (OAE), que utiliza o intemperismo de rochas e minerais máficos para aumentar a capacidade do oceano de absorver e armazenar CO_2 atmosférico, mitigando, assim, a acidificação oceânica e promovendo o sequestro de carbono a longo prazo. Este processo envolve a dissolução de minerais silicatados compostos principalmente por magnésio, cálcio e ferro, que reagem com o CO_2 para formar iões bicarbonato estáveis.

Embora os benefícios químicos do OAE sejam promissores, estes materiais são estranhos aos ecossistemas naturais e podem ter impactos ecológicos, geoquímicos e biológicos. Por exemplo, a olivina contém quantidades traço de níquel, que, em concentrações suficientemente elevadas, já demonstrou ser prejudicial para organismos marinhos, como fitoplâncton e zooplâncton. Consequentemente, é fundamental avaliar estes potenciais impactos para reduzir os riscos ambientais. Embora estudos laboratoriais tenham testado amplamente o OAE, avaliações em campo são essenciais para validar os resultados laboratoriais em ecossistemas reais e compreender como a variabilidade natural e os fatores ambientais podem influenciar os resultados. Os potenciais benefícios do OAE devem ser equilibrados com os riscos ecológicos, e este equilíbrio é particularmente importante ao considerar ecossistemas costeiros frágeis, como os sapais.

Este estudo faz parte do projeto RECAP (REduce atmospheric Carbon by Alkalinity Enhancement in intertidal environments: Potential and impacts), que investiga o uso de dois materiais silicatados, olivina e basalto, para o OAE, a fim de capturar CO_2 da atmosfera (Mendes et al., 2023). A área de estudo é a Ria Formosa, numa zona de sapal intertidal com marés semi-diurnas e um clima quente e seco durante a maior parte do ano. Os sapais estão entre os ecossistemas mais produtivos do mundo, com elevadas taxas de sequestro natural de carbono, tornando-os ideais para estudos *in-sit* de aumento da alcalinidade. Além da sua capacidade de sequestro de carbono, os sapais proporcionam importantes habitats para diversas

espécies, incluindo peixes, aves e invertebrados, e desempenham um papel crucial na proteção das costas contra a erosão. Esta combinação única de produtividade e sensibilidade faz dos sapais um excelente campo de testes para avaliar os impactos ecológicos do OAE.

As diatomáceas, produtores primários cruciais nos ecossistemas marinhos, desempenham um papel-chave no ciclo de nutrientes e na fixação de carbono. Elas formam a base de muitas teias alimentares marinhas e contribuem significativamente para o sequestro de carbono através da bomba biológica, um processo no qual o carbono orgânico produzido pelas diatomáceas afunda no fundo do oceano após a sua morte. A sua sensibilidade às mudanças ambientais torna-as excelentes bioindicadores para o estudo dos efeitos ecológicos do OAE. Compreender como as comunidades de diatomáceas respondem ao OAE é essencial para avaliar tanto as consequências ecológicas quanto os impactos mais amplos nas cadeias alimentares marinhas e no ciclo de carbono. Experiências laboratoriais já demonstraram que as populações de diatomáceas aumentam em resposta à disponibilidade de silício e ferro provenientes do intemperismo de silicatos, embora isso dependa das condições ambientais específicas. No entanto, as investigações sobre as respostas das associações de diatomáceas à olivina e ao basalto em ambientes naturais são escassas, particularmente em ecossistemas diversos e dinâmicos como os sapais.

O objetivo deste estudo foi avaliar o impacto de dois tamanhos de grão de olivina e de basalto nas associações de diatomáceas móveis vivas no sapal da Ria Formosa ao longo de sete meses. A experiência foi desenhada para avaliar como diferentes tratamentos de materiais silicatados afetam as comunidades de diatomáceas e a relação entre as respostas biológicas e os parâmetros ambientais. As respostas das comunidades de diatomáceas foram avaliadas através da contagem e classificação das espécies, cálculo das concentrações, diversidade e equitatibilidade. Estes parâmetros biológicos foram depois relacionados com fatores físico-químicos da água superficial, tais como pH, oxigénio dissolvido, salinidade, temperatura e alcalinidade. A amostragem decorreu em três momentos: setembro de 2022, dezembro de 2022 e março de 2023 (15 amostras no total), captando padrões sazonais de clima e sucessão. Cada evento de amostragem incluiu cinco tratamentos: um controlo, olivina fina (OF), olivina grosseira (OG), basalto fino (BF) e basalto grosseiro (BG). Ao incluir tamanhos de grão fino e grosseiro, o estudo procurou capturar possíveis diferenças nas taxas de intemperismo e efeitos biológicos devido à área reativa disponível para reações químicas.

Técnicas multivariadas, incluindo a análise de clusters hierárquicos, análise de componentes principais (PCA), análise de componentes descentrados (DCA) e análise de redundância canónica (RDA), foram usadas para explorar a relação entre variáveis ambientais e a estrutura

da comunidade de diatomáceas. Estas abordagens estatísticas permitiram uma compreensão abrangente de como as mudanças na química da água superficial, como o aumento da alcalinidade, poderiam influenciar as associações de diatomáceas ao longo do tempo. Com base na literatura, esperava-se que a olivina mostrasse mudanças mais cedo do que o basalto devido à sua taxa de dissolução mais rápida. Embora o basalto tenha um maior teor de cálcio e ferro, e menor de magnésio comparado à olivina, os efeitos dessas mudanças na composição química sobre as diatomáceas e outros organismos ainda não estão claros na literatura, pois poucos estudos abordaram este aspeto do OAE em ecossistemas naturais. Esperava-se que os tamanhos de grão mais finos se intemperizassem mais rapidamente devido à sua maior área reativa, potencialmente levando a mudanças mais rápidas na composição e abundância das comunidades de diatomáceas.

Os resultados revelaram que o tratamento BF teve o menor impacto na estrutura e composição das comunidades de diatomáceas, mantendo, no entanto, uma alcalinidade mais elevada em março (2.592 mM) do que o controlo (2.520 mM) e o BG (2.491 mM). Houve mudanças mínimas nas concentrações, diversidade e composição das espécies sob o tratamento BF, sugerindo que o basalto pode ser um material menos disruptivo para o OAE neste ecossistema. Em contraste, o tratamento BG foi o que mais se aproximou do controlo em termos de espécies dominantes em dezembro e março, embora a análise DCA tenha revelado mudanças significativas nas espécies não dominantes, indicando que, embora as principais espécies fossem estáveis, estavam a ocorrer mudanças mais subtis na composição da comunidade. Isto sugere que até pequenas alterações nas condições ambientais podem levar a alterações nas espécies menos abundantes, o que pode ter consequências ecológicas a longo prazo.

O tratamento OF mostrou o maior impacto na composição das espécies, com este efeito a tornar-se mais pronunciado ao longo do tempo, acompanhado de uma diminuição nas concentrações de diatomáceas em comparação com o controlo. Isto sugere que a olivina de grão fino pode causar maior perturbação nas comunidades de diatomáceas, possivelmente devido às taxas de dissolução mais rápidas e às mudanças associadas na química da água. O tratamento OG teve o impacto mais substancial na estrutura da comunidade de diatomáceas, com aumentos significativos nas concentrações e reduções na diversidade. Este efeito coincidiu com grandes mudanças na composição das espécies, conforme demonstrado pela DCA, embora estas mudanças parecessem diminuir até março. As perturbações iniciais podem ter sido moderadas ao longo do tempo à medida que o sistema se ajustava às novas condições ambientais.

Estas descobertas destacam a necessidade de estudos a longo prazo para determinar se as mudanças nas comunidades são temporárias ou permanentes. Investigando o conteúdo de nutrientes e metais, juntamente com a composição da macrofauna e flora, ajudaria a esclarecer quais os aspetos dos materiais silicáticos que estão a causar as mudanças observadas. Incluir parâmetros físico-químicos da água intersticial poderia melhorar a relevância dos resultados da RDA, fornecendo uma melhor compreensão do ambiente das diatomáceas bentónicas. Além disso, examinar os efeitos em outros níveis tróficos poderia esclarecer os impactos ecológicos mais amplos não capturados neste estudo.

Finalmente, é crucial expandir estas descobertas para além dos ecossistemas de sapal para avaliar os potenciais impactos do OAE em outros ambientes marinhos. Esta pesquisa oferece informações valiosas sobre como diferentes tamanhos de grão de olivina e basalto influenciam as comunidades de diatomáceas, com implicações mais amplas para o ciclo de carbono

Abstract

Ocean alkalinity enhancement (OAE) is a novel approach to reducing atmospheric CO_2 by enhancing the carbon sequestration capacity of seawater through the weathering of mafic rocks and minerals. While laboratory research has extensively explored this, field tests under natural conditions are still limited. This study forms part of project REduce atmospheric Carbon by Alkalinity Enhancement in intertidal environments: Potential and impacts, which investigates the use of two silicate substrates, olivine and basalt, for OAE as a measure to capture CO_2 from the atmosphere. The current study aimed to assess the impact of olivine and basalt on assemblages of living motile diatoms in the Ria Formosa salt marsh over seven months. Diatom community responses were assessed through species counting, classification, and specific responses, to then calculate concentrations and diversity. These biological parameters were then related to key surface water physiochemical factors, such as pH, dissolved oxygen, salinity, temperature, and alkalinity. Sampling started in 2022 and included the months of September, December, and March 2023 (15 samples in total). Each sampling event included five conditions: a control, olivine fine (OF), olivine coarse (OC), basalt fine (BF), and basalt coarse (BC). The data was analysed using multivariate techniques, including hierarchical clusters, principal component analysis (PCA), detrended component analysis (DCA), and canonical redundancy analysis (RDA). Results revealed that the BF treatment had the least impact on diatom community structure and composition compared to the control scenario. Conversely OF had the largest impacts on species composition. Future work should consider the reactions by the diatom community over a longer time scale to determine the recovery potential of the system to these changes. These findings provide insights into the role of different grain sizes of olivine and basalt in shaping diatom communities and broader implications for carbon cycling and ecosystem processes in saltmarsh systems.

Table of Contents

Table of figures

Table of tables

List of abbreviations

- ATP – Adenosine triphosphate
- BC – Basalt coarse
- BF – Basalt fine
- C – Control
- CCM – Carbon concentrating mechanisms
- CDR – Carbon dioxide removal
- DCA – Detrended component analysis
- DSi – Dissolved silicon
- DO – Dissolved oxygen
- EW – Enhanced weathering
- OAE – Ocean alkalinity enhancement
- OC – Olivine coarse
- OF – Olivine fine
- PAST – Palaeontological statistics
- PCA – Principal component analysis
- RDA – Redundancy analysis
- RECAP - Reduce atmospheric Carbon by Alkalinity enhancement in intertidal environments: Potential and impacts

1 | Introduction

1.1 | Project overview and motivations

Total global anthropogenic emissions of carbon have more than doubled during the past 60 years, from 4.6 GtC yr^{-1} during the 1960s to an average of 10.6 GtC yr^{-1} during 2011–2020, now exceeding 40 Gt CO_2 annually (Friedlingstein et al., 2022). This translates to significant increases in global warming through the trapping and reflection of infrared radiation in the atmosphere. The 2015 Paris agreement, signed by 194 parties and the European Union, accepted the goal set by the Intergovernmental Panel on Climate Change to limit the average temperature increase to between 1.5 ºC and well below 2 ºC above preindustrial levels (Bach et al., 2019). If we are to meet these goals, it is suggested that up to 5 Gt CO_2 should be removed from the atmosphere annually (Rogelj et al., 2018). Even with very optimistic techno-economic assessments of the RCP 2.6 scenarios (representative concentrations pathways leading to ≤2.6 W/m^2 radiative forcing), it is not possible to remain on target with decarbonization alone (Yamagata et al., 2018). This highlights the necessity for research into carbon dioxide removal (CDR) measures. Ocean alkalinity enhancement (OAE) is one of the suggested CDR methods that involves improving the oceans natural carbon sequestration capacity whilst alleviating the associated acidification (Vandeginste et al., 2024). Each CDR has its own economic and geospatial limitations; therefore, a variety of methods are necessary for carbon dioxide removal at a large scale. Few CDR methods have progressed beyond the laboratory due to lack of funding, legal framework, and social acceptance (Fuss et al., 2018). One important concern is related to the lack of understanding of ecological responses to these artificial changes (Lenzi, 2018).

The focus of this thesis makes up a small component of a larger project named “Reduce atmospheric Carbon by Alkalinity enhancement in intertidal environments: Potential and impacts” (RECAP). The project began in September 2022 and is using a small-scale, two-year, in situ field trial to assess the potential and impacts of alkalinity enhancement as a measure to capture more CO_2 from the atmosphere (Mendes et al., 2023). In this context, alkalinity refers to a parameter that characterises the buffering capacity of the water (Qiu et al., 2024), specifically, the number of moles of hydrogen ion equivalent to the excess of proton acceptors over proton donors in 1kg of seawater sample (Dickson, 1981). Increasing the local alkalinity of the environment requires the introduction of alkaline earth metals such as magnesium and calcium into the water. For this purpose, two substrates were chosen to assess suitability for

potential use on a larger scale. Olivine has a high capacity to sequester carbon (around 1 t CO_2 per 1 t olivine; Renforth and Henderson, 2017), but it contains hypothetically toxic trace elements (e.g. Ni, Cr). Basalt has a CO_2 sequestering capability 30 % less efficient than olivine, however, it contains more valuable nutrients and essential elements (e.g. P, Ca, Mg) as well as less potentially toxic elements (Strefler et al., 2018). If alkalinity enhancement is to be used on large and long-term scale it is important to minimise the initial carbon costs for deployment. This highlights the need for research into the net CO_2 sequestration by multiple grain sizes and alkaline substrates.

Research on OAE is informed by the comprehensive understanding of oceanic biogeochemical processes related to pH and alkalinity. The majority of studies on OAE to date are theoretical, focused on computational studies that largely estimate the global climate effects (Fakhraee et al., 2023a, 2023b; Fennel et al., 2023; Wang et al., 2023). Whilst modelling offers a cost-effective, flexible (spatially and temporally) and comprehensive approach, it comes with challenges such as data uncertainty, and potential overreliance on models without sufficient validation (Köhler et al., 2013; Hauck et al., 2014). Natural OAE analogue studies based in laboratories or microcosms are becoming more common and have already demonstrated potential and impacts on systems (Hangx and Spiers, 2009; Prigiobbe et al., 2009; Schuiling and De Boer, 2010; Wang et al., 2023). Some of this research was already done on the use of olivine to enhance CO_2 sequestration and fewer into the potential of basalt as a silicate feedstock (Gysi and Stefánsson, 2012; Xiong et al., 2018; Rinder and von Hagke, 2021). The next step to gather knowledge in this field of research is to do small-scale, in-situ experiments to test how these substrates behave in natural systems.

As atmospheric CO_2 levels rise, there is a range of associated detrimental impacts to coastal marine biota. These can affect the entire ecosystem from primary producers such as diatoms to higher trophic levels such as invertebrates or fish (Morzaria-Luna et al., 2014). A decreased pH reduces the availability of carbonate ions which are essential for shell formation, thereby elevating the energetic demands of calcification (Wootton et al., 2008). This has the potential to impair reproductive success and developmental rates in calcifying organisms, inducing cascading effects on the carbon cycle (Raven & Crawfurd, 2012). Contrary to this, some organisms like seagrasses and macroalgae may experience enhanced growth rates from the increased availability of CO_2 for photosynthesis (Macreadie et al., 2017). The consequent impact on the ecosystem, however, is complex, with potential harmful algal blooms and shifts in ecological dominance influencing trophic dynamics and ecosystem functionality.

The RECAP project will measure the responses of a range of microbiota including bacteria,

diatoms, foraminifera and meiofauna. Currently, there are a few studies that consider the response of either specific species of important phytoplankton groups (Hutchins et al., 2023; Li et al., 2024) or invertebrates (Jankowska et al., 2024), or consider the controlled response of varied taxa grown in microcosms (Ferderer et al., 2022; Ren et al., 2022; Gately et al., 2023; Xin et al., 2024) or on media (Rønning et al., 2024). These responses may be vastly different in the presence of other organisms (competition) or with the variance of environmental conditions that occur naturally. Additionally, the consideration of organisms such as foraminifera is almost absent from the literature. Important ecosystem engineers like diatoms also require more attention, especially considering basalt. In this way, the RECAP project will contribute to the understanding of these complex interactions in the context of a salt marsh.

1.1 | Present study motivations and objectives

Diatoms are a highly diverse and abundant group of unicellular autotrophic eukaryotes, contributing significantly to phytobenthic biomass in coastal areas (Hashioka et al., 2013). Phytoplankton represent around 45% of global primary production, however only 1% of the Earths photosynthetic biomass (Field et al., 1998). Being photosynthetic, they use their pigments to convert energy from the sun into chemical energy, this important ecosystem service sequesters about 20% of global carbon (Karlusich et al., 2021). The organic carbon generated by diatoms then supports production by bacteria and higher trophic levels (Khairy et al., 2014). This forms the basis of coastal food webs through biogeochemical cycling of elements and habitat formation. It is therefore vital to consider the behaviour of diatom assemblages when implementing any artificial change to the environment.

The diversity, distribution and abundance of diatom taxa are closely related to the response of abiotic and biotic factors. Nitrogen and phosphorous are essential for diatom growth, having consequences for the synthesis of proteins, nucleic acids, adenosine triphosphate (ATP), cell membranes, and chlorophyll (Armbrust, 2009; Falkowski and Raven, 2013). Silicon is also essential for the construction of part of the diatom exoskeleton called frustule, a complex structure that ensures the functioning of vital processes, including; protection from predation, filtration, control of light absorption, metabolism and buoyancy regulation (Cvjetinovic et al., 2023). Due to the high turnover rates (1-3 days; Lewin and Hellebust, 1978), and clear species-specific responses to physiochemical gradients (Blanco, 2024), diatoms can be very useful tools in assessing the impacts of environmental change (Tornés et al., 2007).

The objective of the present study is to assess the impact of alkalinity enhancement using olivine and basalt across a seven-month period on the community of motile living assemblages

of benthic diatoms in a high productivity intertidal area. This will be achieved through collecting, counting and classifying diatoms across three sampling periods, representing different seasons, that have been exposed to the alkaline substrates, and combining this with environmental data to assess any differences in assemblages compared to a control situation.

1.2 | Ocean alkalinity enhancement

1.2.1 | *How does it work?*

Despite concerns, it is crucial to evaluate the potential environmental risks of CDR measures before implementing them. Enhanced Weathering (EW) and OAE are two interconnected principles resulting in CDR. The concept involves speeding up the natural process of rock weathering by: (i) choosing silicate rocks with high dissolution rates (ii) processing into smaller particles therefore increasing the reactive surface area and dissolution rate (iii) distributing in areas with a capacity for high erosion. Theoretical studies using earth system models have demonstrated that implementing EW and OAE on an appropriate scale has the potential to significantly alleviate the impacts of climate change (Feng et al., 2017; Lenton et al., 2018).

Enhanced weathering of selected substrate promotes an increase in total alkalinity (TA) leading to permanent removal of atmospheric CO_2 from the ocean (Figure 1.1). To understand this concept, it is important to consider the equilibrium of the ocean carbonate system:

$$CO_2 + H_2O \rightleftharpoons H_2CO_3 \rightleftharpoons HCO_3^- + H^+ \rightleftharpoons CO_3^{2-} + 2H^+$$

A shift towards bicarbonate (HCO_3^-) and carbonate (CO_3^{2-}) coincides with lower available aqueous CO_2 therefore promoting an influx of CO_2 from the atmosphere. This shift can be initiated by the dissolution of alkaline minerals such as olivine (Mg_2SiO_4), since there is a consumption of H^+ ions which are replaced by conservative ions, in this case Mg^{2+}. There is also a release of OH^- which combines with CO_2 to form HCO_3^-, directly increasing alkalinity:

$$(Mg,Fe)_2SiO_4 + 4H_2O + 4CO_2 \rightarrow 2(Mg,Fe)^{2+} + 4HCO_3^- + H_4SiO_4$$

The magnesium released during weathering combines in the oceans with the CO_3^{2-} to form calcium carbonate ($CaCO_3$), which is a major sink for CO_2 (Schuiling and Krijgsman, 2006). Theoretically, 4 mol of protons are consumed for each mole of olivine, thus absorbing 4 mol of CO_2, equivalent to 1.25 tonnes of CO_2 per tonne of olivine (Köhler et al., 2013). However, the consequences of olivine or basalt dissolution on the carbon cycle are more intricate, as both dissolved inorganic carbon (DIC) and total alkalinity (TA) are altered, resulting in a new CO_2 concentration. Consequently, the ratio of CO_2 sequestration relative to olivine dissolution will fluctuate according to the initial conditions of the marine carbonate system and the quantity of olivine that undergoes dissolution. The figure of 1.25 tonnes of CO_2 per tonne of olivine represents an upper theoretical boundary (Köhler et al., 2013).

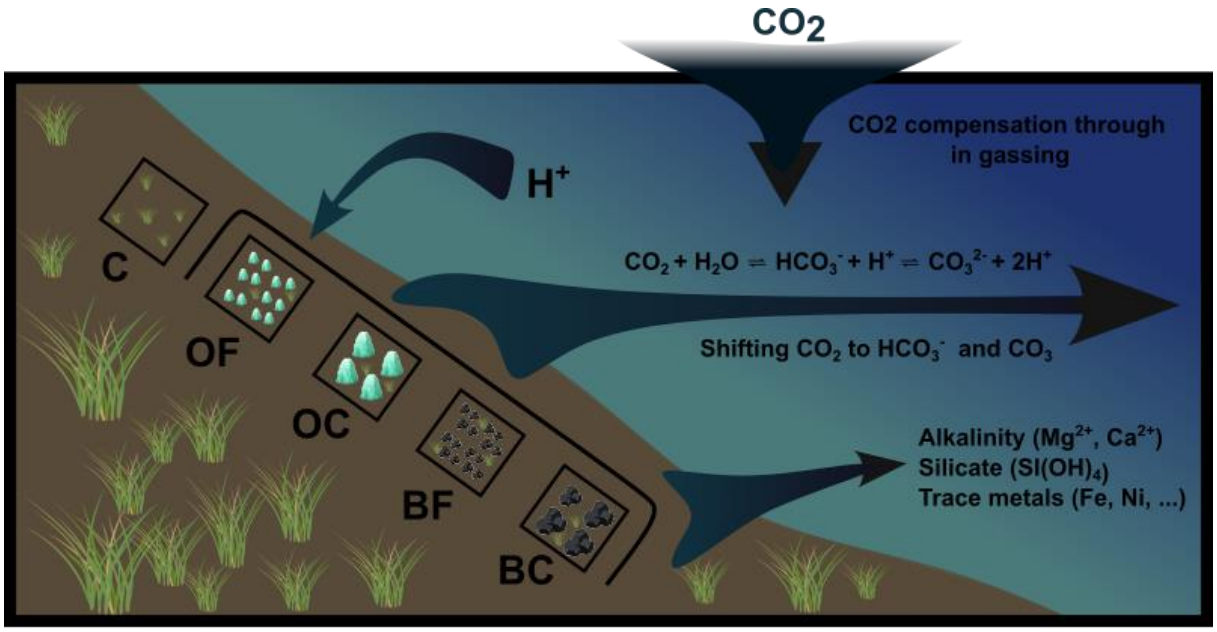

Figure 1.1 – Schematic representation of study design, with a summary of CDR through weathering. Abbreviations represent the different conditions of the experiment; Control (C), Olivine fine (OF), Olivine Coarse (OC), Basalt fine (BF) and Basalt coarse (BC). Olivine and Basalt consume protons (H^+) shifting the equilibrium away from CO_2. This draws more CO_2 due to undersaturation in the water relative to the atmosphere. Alkaline earth metals dissociate into water and bind to carbonate ions reducing their availability, further promoting CO_2 drawdown.

1.2.2 | *What do we already know?*

The reserves of natural source rocks containing basalt, olivine, or other suitable minerals are sufficient to store thousands of gigatons of CO_2 (Taylor et al., 2016). The extra mining efforts required to eliminate several gigatons of CO_2 annually are comparable to the activities of the global cement industry, which currently mines around 7 Gt of source materials each year (Renforth and Henderson, 2017). The initial cost evaluations indicate that they fall within the cost range of other CDR methods (£10–400 per ton of CO_2; Bach et al., 2019). Therefore, if the anticipated revenues from carbon taxes are allocated to support CDR, EW could emerge as a financially feasible alternative for achieving negative emissions in the twenty-first century.

EW in combination with OAE has a high potential for large-scale implementation. Firstly, CDR through EW is a natural phenomenon that already absorbs 1.1 Gt CO_2 annually (Bach et al., 2019). Secondly, EW would not necessitate its own land, nutrients, or freshwater (Meysman and Montserrat, 2017). Consequently, unlike many other CDR strategies, it is generally not in competition with other sustainable development goals such as global food and water security but could potentially even be beneficial to them. This sets it apart from other CDR since counteracting ocean acidification can provide a quasi-natural way to restore fragile habitats such as coral reefs.

One important uncertainty for OAE using olivine lies in the possibility of secondary reactions (e.g. clay production, sepiolite formation, or carbonate precipitation), that could substantially diminish the uptake of CO_2 by reducing the quantity of alkalinity released (Meysman and Montserrat, 2017). Additionally, the dissolution of silicate substrates can release potentially toxic trace elements such as (e.g. Ni and Cr), which could impact the environment or biological community (Hutchins et al., 2023). This demonstrates the necessity for field studies assessing the dissolution of silicate feedstocks and their associated alkalinity within the full context of sedimentary biogeochemical cycling.

1.2.2.1 | *Coastal weathering*

Coastal applications of EW seem favourable due to the ease of access and potential combination with existing processes such as harbour construction and beach sand nourishment (Montserrat et al., 2017). A natural turbulence in coastal areas will also allow increased weathering of larger grind sizes. Under *in situ* conditions, there will also be an interplay between microbial metabolism and macrofaunal bioturbation that could substantially increase weathering effects. Pfeffer et al. (2012) found that in "electro-active" sediments (globally common in coastal zones), long, filamentous bacteria can perform long-distance electron transport, acidifying surface sediments down to pH~5. Areas with these acidic sediments could therefore be a good target location for EW due to faster dissolution rates.

The geochemical cycling within coastal applications of silicate minerals releases a range of products into the water column. Magnesium is one of the elements released and has a high background concentration in seawater and so is not expected to pose any concern (Meysman and Montserrat, 2017). Dissolved iron is also released and is a limiting nutrient for phytoplankton due to its role in chlorophyll formation and nitrogen assimilation. In a coastal setting, however, under oxic conditions, ferrous iron is oxidised to iron hydroxides, however under anoxic conditions it can get trapped in the soil as iron sulphides (Morel et al., 2008). This suggests that CO_2 sequestration via iron fertilisation could be reduced in these environments since iron sulphides are highly insoluble and therefore less bioavailable to diatoms (Ferderer et al., 2022).

The coastal application will cause dissolution products to initially accumulate before being exported and diluted into the open ocean (Vandeginste et al., 2024). The specific environmental parameters such as bottom depth and residence time due to substrate morphology and hydrodynamics will indicate the efficiency of change to the carbonate system (Pas et al., 2023). Many of the existing studies use a closed system which will not allow olivine products to be

diluted, in a natural setting it could be expected that there would be advection causing low residence times (Bach et al., 2019). Studies in this area are still severely lacking and indicate the necessity of a combination of mesocosm and field trials given the complexity of coastal ecosystem functioning.

1.3 | Diatom ecology

This chapter will outline some important general information surrounding diatoms to enable the reader to understand their importance in the context of ecosystem health. A frustule is composed of two valves, an epitheca, and a hypotheca (Figure 1.2) that is slightly smaller and fits inside the other valve allowing for growth through the formation of girdle bands (Smol and Stoermer, 2010). Diatoms are broadly categorised into two main morphological groups, pennate or centric (Mann, 1999). These groups are markedly different in terms of their cytology, biology, and ecology, including cell wall symmetry, chloroplast morphology, and motility strategies (Round et al., 1990), which can also vary significantly within these groups. They can be vastly different in size, anywhere from 2 to 500 μm, and occupy a similarly diverse range of habitats.

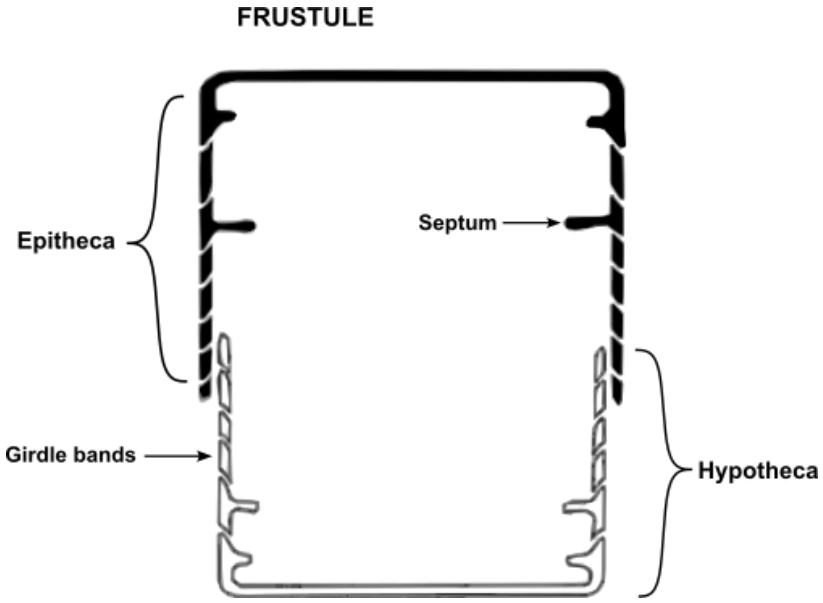

Figure 1.2 – Diagram detailing a diatom frustule and its components (adapted from Jochem, 2021).

Centric diatoms are typically planktonic, migrating vertically in the water column on the scale of tens of meters, multiple times a day (Sato and Medlin, 2006). This vertical migration allows the utilization of light and nutrients within oligotrophic systems, ascending to perform photosynthesis and descending below the nutricline for macro- and micronutrient access. This migration is achieved through buoyancy regulation involving the alteration of ionic solutes

within the vacuoles, for example, the uptake of nitrates to increase cell buoyancy (Villareal and Lipschultz, 1995).

Pennate species are usually benthic (Admiraal, 1984). Within the pennates, there is a distinction between two groups, the raphids and araphids, which means with or without raphe. A raphe is a narrow slit (Figure 1.3) that typically runs the length of one (monoraphid) or both valves (biraphid). Classically, significant features such as the raphe have been used for visual taxonomic classification (Williams and Kociolek, 2011). A stria is a row of wall perforations called pores found on the valve face (Mishra et al., 2017). The fibulae are a morphological feature of some genera that support the raphe canal, presenting as bridges that extend transapically from valve face to raphe canal (Manoylov and Ghobara, 2021). The presence of a raphe allows for directed motility known as "gliding". This creates movement parallel to the longitudinal axis of a cell when in contact with a substrate (Serôdio, 2021), through the secretion of mucilaginous extracellular polymeric substances (EPS) through the raphe (Bohórquez et al., 2017). This allows for a transient attachment to substrates during gliding but also for adhesion to substrate through stalks. Light intensity and wavelength trigger photoresponsive regions at the tips of the cells changing the movement direction depending on their position relative to the stimuli (Cohn et al., 1999).

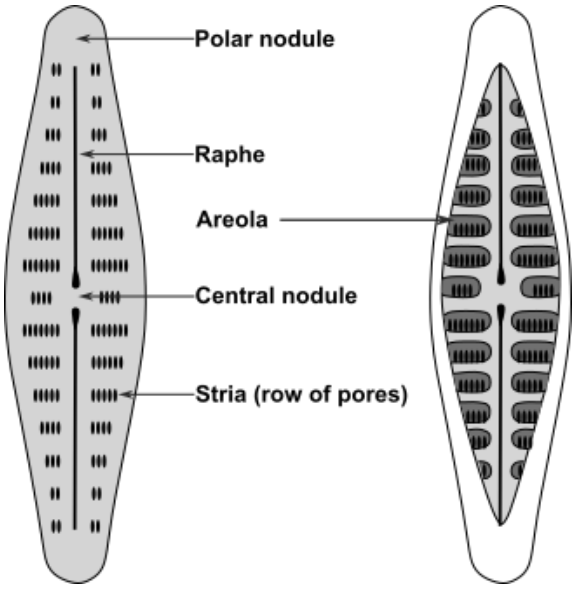

Figure 1.3 - Diagram showing the main morphological features of the valve of a pennate diatom with raphe. The left shows the exterior and right shows the interior (adapted from Cronodon, 2021).

Gravitactic responses allow for vertical migration causing a dramatic change in sediment colouration (Fischer et al., 1977), visible to the naked eye, associated with day-night and tidal cycles of mass cell movements in anticipation of sunlight or flooding (Round and Palmer,

1966). This migration affects photoaclimation and carbon assimilation patterns (Serôdio et al., 2001), as well as determining reproduction (Saburova and Polikarpov, 2003), nutrient uptake (Marques da Silva et al., 2020), and utilization of complex ecosystem resources (Nakov et al., 2018). Merz et al., 2021, discovered that this can drastically affect diatom concentrations, with up to 40% of the population migrating more than 2 cm deep for at least 8 hours a day. The considerable release of carbon-rich mucilages during diatom vertical migration represents a crucial organic carbon source for heterotrophic bacteria proliferation (Serôdio et al., 2023). Additionally, the extracellular polymeric substances (EPS) that accumulate in upper sediment layers during low tides significantly enhance sediment stability in estuarine benthic habitats (Poulsen et al., 2022), thus playing a pivotal role in ecosystem stability (Saburova and Polikarpov, 2003). Figure 1.4 details several other possible cell movements through fine sediments including cell rolling, rocking, pirouetting (Barnett et al., 2020).

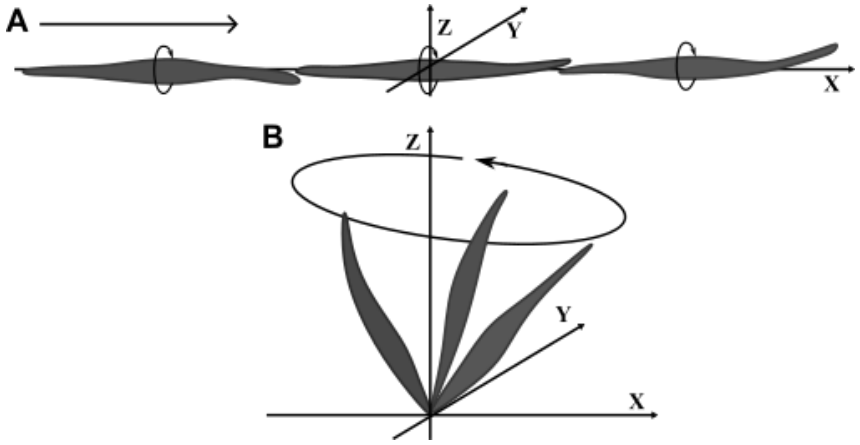

Figure 1.4 - Model of diatom movements, showing changes relative to x, y and z axes. A) Cell rolling with forward motion (corkscrew gliding). Open arrowhead indicates direction of movement. Elliptical arrows indicate direction of cell body rotation. B) Cell pirouetting. Elliptical arrow indicates precession of cell tip around the z axis (adapted from Apoya-Horton et al., 2006).

Diatoms can also utilize EPS for colony formation, allowing for a species to occupy a larger area and influencing fitness through improved nutrient acquisition and reduced predation. Colonies have been observed to split up in response to both, the presence of, and cues, from predators such as copepods (Ryderheim et al., 2022). In competition for scarce nutrients, longer chains can both create microenvironments with favourable nutrient flow dynamics (Kenitz et al., 2020), as well as resist turbulence to maintain position (Dell'Aquila et al., 2017). The myriad of life cycle strategies in diatoms demonstrates the adaptability but also the sensitivity of species to certain conditions, making them useful indicators in understanding ecological impacts of environmental change.

1.3.1 | *Reproduction*

Diatoms can reproduce both sexually and asexually. They have a diplontic life cycle where majority of the cycle is spent undergoing mitosis, reproducing asexually to produce genetically identical daughter cells with 2 complete sets of chromosomes (Giri et al., 2022). Several succeeding lateral girdle bands (Figure 1.2) create the necessary distance between rigid valves for mitotic division. Since cell walls cannot expand, the daughter cells from asexual reproduction are smaller than the parent cells (Figure 1.5) and inherit either the epitheca or the hypotheca (Figure 1.2). Consequently, each successive generation (every 1-3 days) decreases in size until a critical threshold is reached (after years of replication), triggering meiosis, forming an auxospore and restoring the maximum potential size (Frigeri et al., 2006).

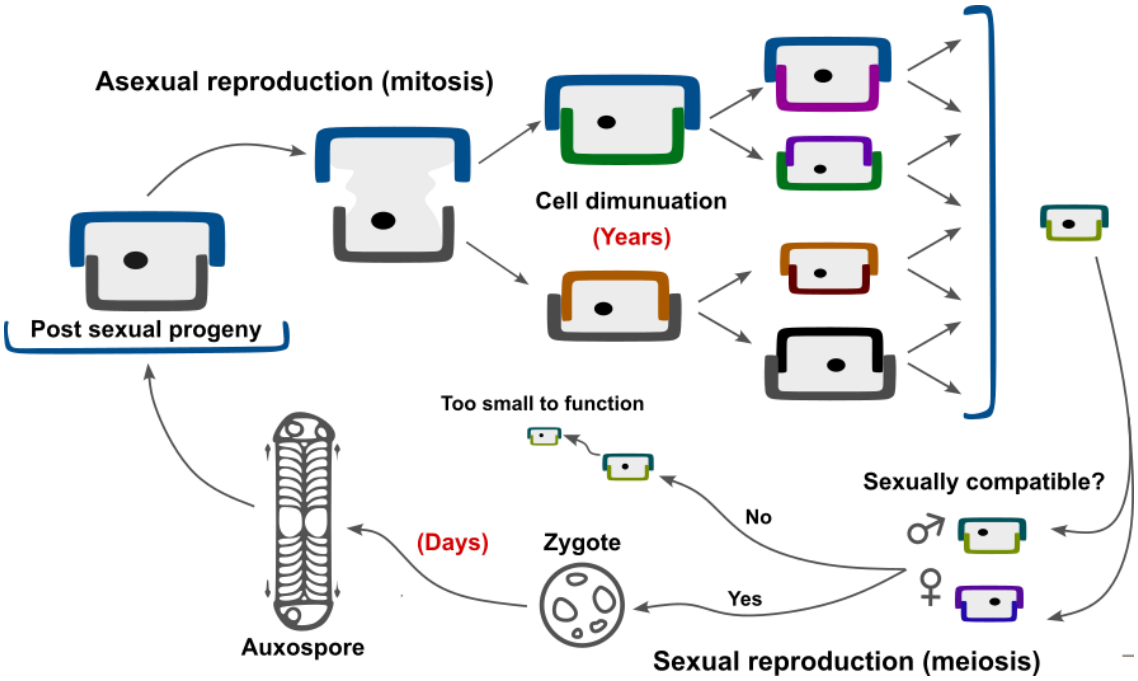

Figure 1.5 – Simplified life cycle of araphid pennate diatom. Note that post sexual progeny is several times larger than parents. Writing in red highlights that the cycle of cell division by mitosis can last years, whereas the meiosis stage only lasts a matter of days (adapted from Stock, 2019).

1.3.2 | *Response to a changing environment*

The effects of ocean acidification on diatoms are very often taxa specific, and this can even co-vary with environmental drivers to demonstrate synergistic, neutral or antagonistic effects (Li et al., 2020). A reduced pH has been shown to affect diatom nutrient absorption (Shi et al., 2015), including reduced growth under nutrient limitation (Li et al., 2018), or high irradiance (Gao et al., 2012). Latest studies show that although higher CO_2 availability could cause an increase of energy input from high photosynthetic activity, this comes with a cost of less resilience, shorter lifespans, and less diversity of algal stands, that have high carbon fixation

rates but also high export of carbon (Wada et al., 2021). Changes like this can reduce ecological complexity and total algal biomass in coastal habitats.

Intertidal environments present significant challenges to diatoms due to the vast daily variation in tides, riverine inputs, and complex hydrodynamics. These present issues including desiccation, as well as fluctuations in temperature, salinity, pH, light and nutrients. Additionally, diatoms living in the microphytobenthos, especially within biofilms, are subject to steep environmental gradients comparatively to their pelagic counterparts. Eutrophication has been demonstrated to enhance some of the effects of acidification (Cai et al., 2011), and therefore daily pH fluctuations may be exacerbated further. As such, responses of communities could be amplified under an acidified ocean scenario, indicating the pressure to discover methods of intervention.

Diatoms can also adapt to other environmental fluctuations by changing cell volume, silicification, and pore size or arrangement (Li et al., 2024). However, the extent of resilience for individual species to these shifts in regime is still unknown. These changes can be reversible or irreversible depending on the nature of the driving force. A shift driven by a gradual change tends to be permanent, whereas a stochastic event in a resilient system may be a temporary adaptation. However, slow changes to an environment can cause a decrease in resilience, making the system more vulnerable to permanent shifts from stochastic events (Scheffer et al., 2001). One of the benefits of OAE is increasing the buffering capacity of the water, therefore reducing the extent of the extreme fluctuations in pH, giving the ecosystem more time to adjust.

1.4 | Study area

Ria Formosa constitutes a vital wetland within Portuguese territory, recognized for its ecological significance, leading to the establishment of the Ria Formosa Natural Park (law-Decree 373/87, 9th December). This area supports an extensive range of habitats and species, particularly benefiting migratory birds (Fonseca et al., 2004). The Ria Formosa is a shallow coastal lagoon, averaging 2 m in depth, shielded from marine wave action by a barrier-island system comprising five islands and two peninsulas extending approximately 55 km (Moura et al., 2019). This lagoon, encompassing 18,000 hectares of salt marshes and tidal channels, facilitates the exchange of water and nutrients with the ocean through six inlets, promoting ecological vitality (Sousa et al., 2020). The diverse habitats of beaches, dunes, and salt marshes in the Ria Formosa contribute to significant biodiversity, with approximately 90% of the lagoon comprised of intertidal morphosedimentary forms, resulting in distinct phytozonation influenced by varying environmental factors such as sediment composition, salinity, thermal

amplitudes, and insolation (Moura et al., 2019; Rodrigues et al., 2021).

The Ria Formosa coastal lagoon exhibits semidiurnal tides (two high, and two low tides), that has a significant tidal amplitude ranging from 1 m to 3.6 m (Newton, 1995). However, there are also fortnightly variations in tidal amplitude due to alternation between the spring (high range) and neap (low range) tides (Gamito et al., 2012). Algarve climate is hot and dry for majority of the year with average summer temperatures of 26 °C, and winter temperatures of around 12° C (Ferreira et al., 2016). There is around 13 hours of sunlight in summer and 9.5 hours in winter, with a low annual rainfall (~490 mm/year^{-1}; Portuguese Institute for Sea and Atmosphere, IPMA, 2022) and the majority of precipitation occurring during winter months (Ferreira et al., 2016). The Ria Formosa near to Faro is well mixed with a mean salinity of 36 ppm, owed to the relatively small input of freshwater considering all inputs from rivers and wastewater (Cravo et al., 2020). The Gilão river is about 35 km away and is the closest major freshwater input with a low daily average input of 192 m^3/day, although, in summer this value can reach zero (Cravo et al., 2020). Daily tidal water exchange with the ocean is higher than all the freshwater inputs.

Salt marshes rank among the most productive ecosystems globally and possess significant ecological importance, particularly in relation to flood risk mitigation, erosion control, nutrient cycling, primary productivity, provision of wildlife habitats, and shoreline stabilization (Guimond and Tamborski, 2021). Over time, these marshes accumulate organic matter, leading to the formation of a compact layer known as peat. Peat causes a slowed decomposition due to waterlogged anaerobic conditions which prevents the release of stored carbon back into the atmosphere (Wandre, 2023). Globally, salt marshes sequester carbon at rates estimated to be between 2 to 6 metric tons of CO_2 per hectare per year (Mcleod et al., 2011). This rate is significantly higher than that of most terrestrial ecosystems, including forests (Chmura et al., 2003). When a salt marsh is compromised, typically due to anthropogenic activities, the carbon that was previously absorbed and sequestered within the ecosystem is subsequently released back into the atmosphere in the form of carbon dioxide, highlighting the importance of the protection of these systems (Macreadie et al., 2013).

The study area is colonised by two halophytes, the abundant *Spartina maritima* and the sparse *Sarcocornia fruticose* (Figure 1.6). *S. maritima* is a European cordgrass, serving as the principal producer in the lower salt marshes of Ria Formosa, acting as a primary colonist by effectively trapping and stabilizing sediment, thereby promoting ecological succession (Silva et al., 2015). *S. fruticose* is a perennial shrubby glasswort which also contributes to sediment stabilisation and creates a dense, complex structure above ground (Silva et al., 2019). *S.*

maritima dominates the lower salt marshes due to its resilience to submersion, whereas, *S. fruticose* has a high salt tolerance enabling it to thrive in the highly saline upper zones that receive more aeration and thus evaporation (Redondo-Gómez et al., 2006). Macrofauna such *Carcinus maenas* and *Uca tangeri* are also prevalent in the area, contributing to bioturbation, nutrient cycling and deposition of organic matter (Wolfrath, 1992).

Figure 1.6 – Photo of study area. The foreground shows reddish colours from *Sarcocornia fruticose*. Whereas closer to the water there is a distinct dark green zonation from *Spartina maritima*, where the present study was carried out (photography by Louie Silver, 2023).

2 | Methods

2.1 | Experimental design

A suitable location for the experimental site was selected and can be seen in Figure 2.1. The project RECAP required sediment samples for the analysis of bacteria, meiofauna, benthic diatoms and foraminifera, as well as physical sediment characteristics (density, water content, porosity, and grain size). Samples from the channel, supernatant and interstitial waters could then be used for evaluation of temperature, pH, dissolved oxygen (DO), salinity, total alkalinity, trace metals, and nutrients. Additional factors such as macrofauna, and flora coverage were also recorded.

The RECAP project has a duration of two years, with periodic sampling of water (each month) and sediments (each three months). A total of five conditions are considered including, control (C), olivine fine (OF), olivine coarse (OC), basalt fine (BF), and basalt coarse (BC). The experiment used wooden boxes to delineate the areas used to apply the different treatment conditions and controls. The boxes were made from planed pine wood boards of dimensions 600x135x18 mm. This allowed for sufficient space to take sediment samples and to fit the correct quantity of silicate substrates. The boxes were inserted to the ground to a depth of 100

mm so that 20-30 mm was showing at the surface, allowing retention of the water for surface water samples, as well as alkaline substrates, therefore, preventing loss through wave action. A total of 15 boxes were used accounting for five conditions in triplicate across three locations: Plot 1 (P1), Plot 2 (P2) and Plot 3 (P3). Triplicates help minimize the impact of random variability and errors, providing more reliable data and giving more statistical power (Vaux et al., 2012). The areas selected were determined by ensuring the ground was flat and that all boxes within each plot were at a similar distance from the water line to minimise differences from submersion time.

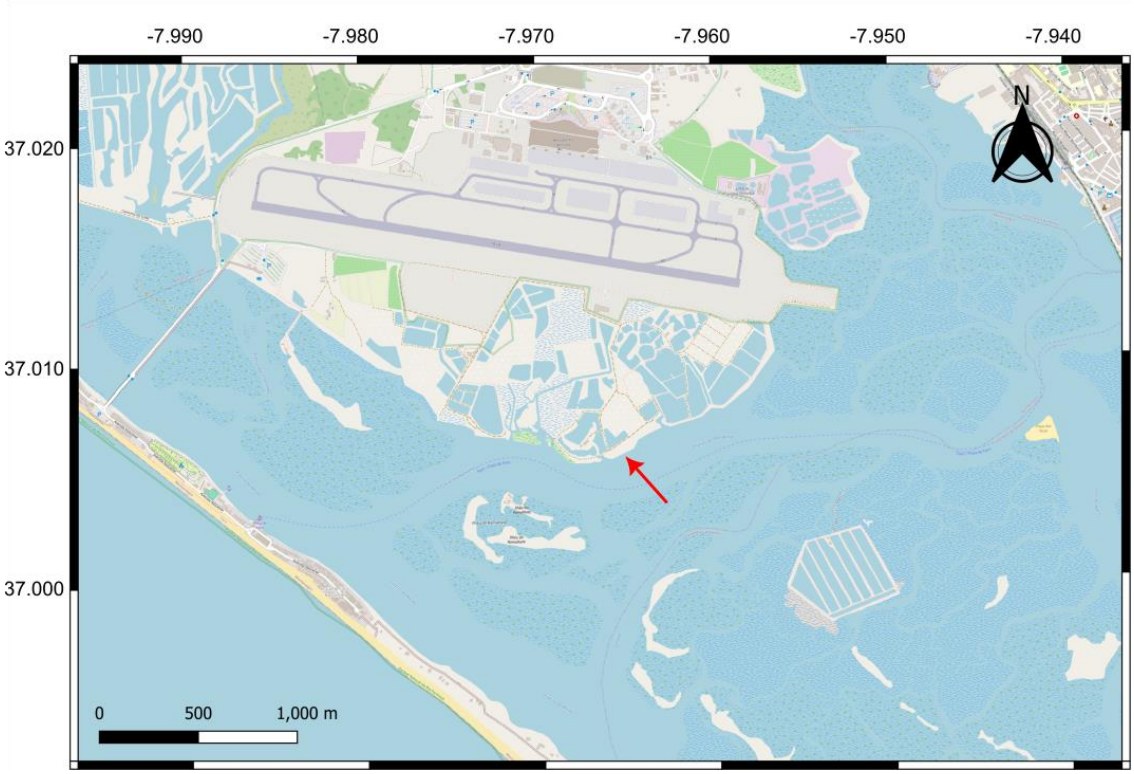

Figure 2.1– The location of the experimental site (red arrow) is on the western side of the Ria Formosa saltmarsh in south Portugal (made with QGIS by Louie Silver, 2024).

2.2 | Environmental data collection

Surface and pore water samples were collected into vials and labelled (100 ml for probe measurements, 20 ml for alkalinity lab analysis). Pore water samples were collected using standard Rhizosphere® Rhizons attached to syringes. Measurements for DO, pH, and salinity were recorded in-situ using a MultiLine® 3620 IDS - Digital multiparameter portable meter. Temperature was measured using a needle thermometer into the sediment after surface water had left.

2.3 | Sample collection for diatom analyses

For the current study, three sampling periods were considered (September and December 2022,

March 2023), and a total of 15 samples were taken. Samples were collected using a modified 5 ml syringe that was inserted into the ground to a depth of 2 cm, (2.66 cm^3 of sediment). The sample was then transferred into a pre-labelled container, and placed in a cooler for transport to the laboratory. Finally, to avoid loss of sediment volume on the study site, the hole was replaced with aquarium quartz sand. In the day before the sediment sampling, a litre of surface water from the channel was also collected and filtered in the laboratory, with a 0.45µm filter to remove any living diatoms from the water column. This was used for further preparation of diatom samples whilst minimising changes to their natural growth environment.

2.4 | Living diatom assemblage slide preparations

The sediment samples were spread in a thin layer over a petri dish. Lens-cleaning tissues were dipped into the filtered channel water and placed on top of the sediment for the living motile diatoms to colonise (Figure 2.2). Samples were then exposed to natural light for 24 hours (Yang et al., 2010a; Nagy, 2011; Yamamoto and Ohtsuka, 2020). The tissue was kept moist using drips of the filtered channel water, ensuring movement and survival of diatoms. Lens tissues were placed into individually labelled sterile containers and put into the freezer.

Later, each tissue sample was dried in an oven for 10 minutes at 80 °C. Once dry, each tissue sample was burned. Organic matter was removed from the samples using 50 ml of hydrogen peroxide (30 %) per sample (Yamamoto and Ohtsuka, 2020). Samples reacted for an hour at room temperature before moving to a hot plate to increase the reaction efficiency. Once the reaction was completed the sample could then be washed and cleaned with 10% hydrochloric acid until it turned yellow (Yang et al., 2010a). This will remove any carbonates present that may obscure the viewing of frustules. The sample was washed a further two times by removal of supernatant and addition of distilled water up to the 100 ml line, leaving to settle overnight in between washes. Tests of diatom concentration indicated that a final suspension of 50 ml would be sufficient for suitable visualisation and counting.

Samples of 50 µl were added to coverslips and allowed to dry overnight at room temperature. A second drop of 500 µl could then be added to half the slides for the option of a higher concentration of diatoms. Once all liquid had evaporated, the slides could be placed onto a preheated hotplate (~70°C), and cover slips mounted using one drop of Naphrax® resin. Diatom suspensions were labelled and retained in 20 ml vials in the fridge to avoid contamination (Tortora et al., 2007), and sustain chemical stability (Karthick et al., 2010).

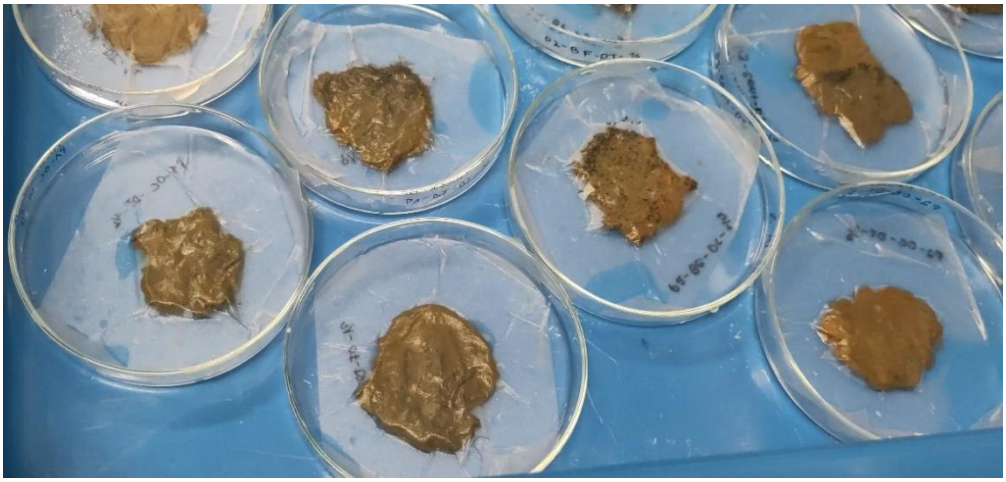

Figure 2.2 – Photo demonstrating collection of living motile diatoms from sediment samples (photography by Louie Silver, 2023)

2.5 | Diatom identification

The slides were analysed using a Leitz dialux 20 compound brightfield light microscope with a 100 x magnification oil immersion lens. Samples were systematically assessed using transversal transects (Figure 2.3), eliminating the potential bias that may occur from an over- or under-estimation of a species due to clustering in certain areas (Patil and Anil, 2005). A mechanical tally counter was used to keep track of the number of fields of view observed, which could then be used for calculations of diatom concentrations. For statistical power, it was determined to aim for a count of 300 valves for each sample (Scherer, 1994). However, one sample did not have a high enough concentration of diatoms to reach 300 valves. Fatela and Taborda (2002) demonstrated that a specimen count of 100 was sufficient to identify the dominant species. In this case, it was still considered relevant to include this sample in the analysis, with the awareness that it may have overinflated relative abundances values. When very few transects were needed to reach 100 diatom valves, the next transect was moved towards the centre of the slide also to avoid bias in the distribution of the valve in the slide (Taylor et al., 2005).

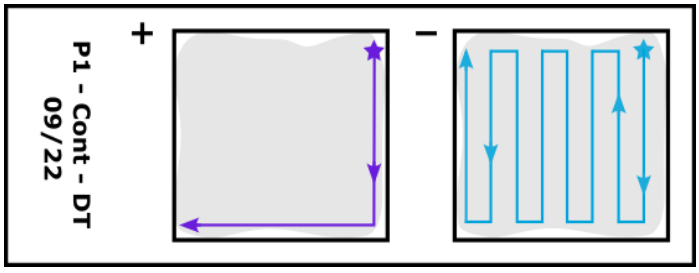

Figure 2.3 - Diagram of example microscope slide. Star indicates start location. Purple lines indicate how the total fields of view count are estimated, note that the line does not pass the edge of the sample (grey shape). Blue lines indicate how transects were used to cover the area of the slide.

Each diatom that had more than 50% of a valve would be identified and recorded on a spreadsheet, including whether the valve was in a pristine or broken condition (Ryves et al., 2009). For the identification of diatoms a range of catalogues, articles and websites were used (Krammer and Lange-Bertalot, 2000, 2003; Witkowski et al., 2000; Lange-Bertalot and Podzorski, 2001; Krammer et al., 2008; Spaulding et al., 2021; Jüttner et al., 2024; Potapova et al., 2024) to compare various morphological cues to determine each valve to the species level. These cues include valve shape, stria morphology (orientation/chambering), raphe morphology, and apical areas. Measurements were taken for the length, breadth, and stria or fibula density in 10 micra, and if the species is confirmed its tally recorded. Finally, taxonomic species classifications were updated by searching (Guiry and Guiry, 2024).

2.6 | Data Analysis

2.6.1 | *Diatoms*

2.6.1.1 | *Total species abundance and dominance*

All species counts were transformed into relative abundance values (Appendix II, Table , representing each species as a proportion of the whole population. Dominant species were any species with a relative abundance of ≥ 5%. If there were any doubts about features or if the measurements did not fit, a range of abbreviations are used to convey the confidence. The abbreviation “cf.” (confer) or “aff.” (affinis), is used when the identification is uncertain, suggesting that the specimen is similar to the referenced species(Winston and Disney, 2000). If the genus can be identified but the species is unknown, the prefix “sp.” can be used after the genus name. The final category was “unidentified (genus)” for any valves that were too broken, distorted, or not found in literature, to allow identification on the species level. To prevent loss of potential ecological information, species that contained “cf.” were agglomerated to the species with which they were most related. Species relative abundances for each condition were calculated using Microsoft Excel, and visualised using the program TILIA version 3.0.3 (Grimm, 2023). This gave initial insights to how dominant species were transforming over time and between conditions.

2.6.1.2 | *Diversity and Evenness Indices*

Understanding diversity can indicate how resilient an ecosystem might be to changes as well as highlighting more subtle responses since diversity tends to decrease before concentration is observed to be affected (Tréguer et al., 2018). Shannon-Weiner diversity index (H') is one of the most widely used methods for diversity comparisons and is calculated using the following equation:

$$H' = -\sum_{i=1}^{S} p_i \ln(p_i)$$

Where S is the total number of species, and p_i is the proportion of individuals of a given species i (Shannon, 1948). The value usually ranges from 1.5 to 3.5 and rarely exceeds 4.5 (Ortiz-Burgos, 2016).

Understanding the evenness of a population can give valuable insights to ecological stability and whether there is a dominance of resource usage by some species (Cristóbal et al., 2020). The evenness was calculated using Pielou's evenness index formula:

$$J' = \frac{H'}{\ln(S)}$$

Where H′ is the Shannon Diversity Index and S is the total number of species (Pielou, 1966). The evenness index value ranges from 0 (no evenness) to 1 (complete evenness). Formulas were input using Microsoft Excel.

2.6.1.3 | *Concentration*

Calculating the concentration of diatoms in a sample enables an understanding of the productivity of an ecosystem as well as giving insights to how a community is responding to environmental pressures (Smol and Stoermer, 2010). Diatom valve concentrations were estimated using an equation adapted from (Lapointe, 2000):

$$\frac{\left(\frac{N_{vtot}}{Vol_p}\right)\left(\frac{Vol_{tot}}{P_{tot}}\right)}{\left(\frac{C_c}{C_{tot}}\right)} = n_{vc}$$

Where N_{vtot} is the total amount of counted valves, Vol_p the volume of sample in ml, Vol_{tot} the volume of total dilution in ml, P_{tot} the total volume of sample in cm^3, C_{tot} the total number of fields, and C_c the number of counted fields, n_{vc} the number of valves per cm^3. The adaptation replaced the use of dry weight of sample (g) with volume of sample (cm^3). Concentrations were calculated using Microsoft Excel.

2.6.1.4 | *Ecological preferences*

To consider any contributing factors to species change over time, each dominant species was characterized by their salinity preferences (Freshwater, Brackish, Marine). This classification was based on the works by: Denys, 1991; Spaulding et al., 2021; Guiry and Guiry, 2024. If conflicts arose, the most recent or cited trait was selected. It was also considered important to research pH preferences, although the literature regarding this is still very limited for the species identified and thus was omitted due to lack of data.

2.6.1.5 | *Cluster analysis.*

All cluster analyses used dominant species of each sample (abundance ≥5 %). Cluster analysis is a tool used to group objects based on their associations between each other. Q-mode clusters help indicate how closely related samples are, based on their diatom composition (Legendre and Birks, 2012a). For this reason, Q-mode clusters were conducted for each sampling date to visualise how related each treatment was to the control. The R-mode control cluster gives indications to how species are clustering based on seasonality (Legendre and Birks, 2012a). R- mode clusters were conducted for each individual treatment and control separately. Clustering was carried out using the programme PAST version 4.7 (Hammer et al., 2023). Clustering used unweighted pair-group method using arithmetic averages (UPGMA) with a Bray-Curtis similarity index. This index is well suited to comparing community compositions based on ecological datasets and captures absolute differences in abundance rather than the ranks (Legendre and Birks, 2012a). To ensure more abundant species were not affecting the clustering disproportionately, all species abundances were square root transformed.

2.6.2 | *Environmental data*

2.6.2.1 | *Normality*

Environmental parameters were assessed for normality using the Shapiro-Wilk test (Appendix I, Table 2; Shapiro and Wilk, 1965). This test is widely accepted as the standard for assessing the normality of small to moderate data sets, due to its high sensitivity to skewness and kurtosis (Yap and Sim, 2011). If data is not normally distributed ($p \leq 0.05$) it is recommended to continue with a non-parametric analysis. The parameters assessed for both pore, and surface water included: salinity, pH, DO, in situ sediment temperature, and alkalinity. In the context of diatoms, it was considered that pore water measurements would be more suitable. However, for the month of September, there were several missing data for pore water. Since it was the first month of sampling, the prediction of how the tide would impact the availability of pore water was still being developed. Thus, it was decided to continue further exploration using surface water data only.

2.6.2.2 | *Correlation*

A correlation test was performed considering all environmental parameters to determine which variables were related to each other. This informed the selection of variables for use in ordination graphics. If variables are highly correlated, they will not add any extra information and may make the model interpretation more difficult (Birks et al., 2012). Since several of the

parameters did not meet assumptions of normality, it was decided to use the Spearman's rank correlation test (Spearman, 1961) since this is non-parametric and robust to non-normally distributed data. The coefficient (r) ranges from -1 (inverse correlation) to +1 (positive correlation), with 0 indicating no relationship. Values above or below +/-0.8 were considered a strong relationship and one of these variables should be removed from ordination tests. This test was carried out using PAST version 4.7 (Hammer et al., 2023).

2.6.3 | *Diatom and environmental parameter ordination*

Ordination is a term for a range of multivariate techniques which simplify a multidimensional dataset in such a way that when it is projected onto a low dimensional space, any fundamental pattern the data may possess becomes apparent upon visual inspection (Økland, 1996). Three issues may necessitate data pre-processing prior to ordination: (a) skewness may need to be mitigated if variable distributions are asymmetrical; (b) variables must be standardized to a common dimensionless format; (c) multistate qualitative variables (e.g., rare, common, abundant) may occasionally require conversion into dummy variables before ordination (Birks et al., 2012). Standardisation and ranging are the primary techniques employed to achieve dimensional elimination. For this purpose, physio-chemical data was first transformed due to high skewness using box-cox transformation, followed by Z-score normalisation (Juggins and Telford, 2012) using the formula: $Z = \frac{x-\mu}{\sigma}$. Only diatom species found in abundances of more than 1% were used for ordinations, and values were square root transformed to deal with the large variance and presence of zeros (Juggins and Telford, 2012).

2.6.3.1 | *Principal component analysis (PCA)*

PCA is a non-constrained linear dimensionality reduction technique that preserves Cartesian distances between samples (Pearson, 1901). It simplifies datasets by transforming data into a new set of variables called principal components (PC) which aim to capture the most amount of variance. Several PC's can be produced and are ranked in terms of the quantity of variance explained and each subsequent PC is orthogonal to the previous one (Legendre and Birks, 2012b). This allows for visualisation of differences between samples (points) in terms of physio-chemical parameters (biplot vectors), on a graph with each axis representing a PC. The bi-plot indicates the strength and direction of variables contributing to the PCs. If there are any samples with outlier environmental characteristics, they will be indicated visually by this graph. Outliers can then be confirmed using methods described by Lever et al., 2017; Z-scores can be applied to PCA scores, values of ± 2 are classed as moderate outliers, and ± 3 are extreme outliers.

2.6.3.2 | *Detrended correspondence analysis (DCA)*

DCA is a multivariate statistical technique used primarily in ecological and environmental studies to analyse species composition data (Hill and Gauch Jr, 1980). It is a modification of Correspondence Analysis (CA) designed to address specific issues related to the gradient lengths and arch effect that can distort the interpretation of ecological data. This permits the identification of outlier samples with unusual species associations, and to determine which method (unimodal or linear) is the most suitable for further exploration of the data (Birks et al., 2012). When the length of the gradient of the longest axis of a DCA graph is up to 3 standard deviations away then linear ordination methods can be used. If between 3 and 4 then either unimodal or linear can be used. If above 4 then only unimodal ordination methods are suitable. If a species abundance remained lower than 5% and it appeared in 3 or less samples, it was deemed suitable for removal from further investigation.

2.6.3.3 | *Canonical redundancy analysis (RDA)*

RDA is a linear dimensionality reduction technique, that contrary to PCA is constrained by the explanatory variables. This allows for assessment of how species compositions are related to physio-chemical variables. Like PCA, the ordination plot displays environmental variables as vectors whose length and angles indicate the strength and direction of relationship.

Exploration of the results used Monte Carlo permutation tests (999 permutations) to see the statistical validity of the model (Birks et al., 2012). Partial RDA tests were run to determine the percentage contribution of each environmental variable. This is done by removing a variable and calculating the difference in total explained variance and converting this value to a percentage. Pore water is more suitable to assess benthic diatom response, however due to missing data points for all parameters during the first sampling date in September, it was decided that ordination would be trailed for both situations. However, the final RDA model for pore water parameters and diatom distributions was not significant and explained less variance than the model using surface water parameters, thus only surface water ordinations will be shown in the results.

3 | Results

This section will graphically present the most relevant data from the study. For clarity, abbreviations have been used in graphs. The conditions are represented as follows: Control (C), Olivine fine (OF), Olivine coarse (OC), Basalt fine (BF) and Basalt coarse (BC). If numbers are presented after, it is in the format of month and then year. Environmental parameters are Oxygen (Oxy), Salinity (Sal), Alkalinity (Alk), and Temperature (Temp).

3.1 | Environmental characterisation

Before assessing the response of diatom assemblages, it is important to understand the way the environment is changing over time, and how these changes might be affected by the weathering of substrates in the treatments. Table 3.1 summarises the recorded physiochemical parameters in surface water across the 3 sampling times and 15 samples. September control samples were characterised by high temperatures (28.9 °C), high salinity (36.4 ppt), moderate alkaline pH (7.950), well oxygenated waters (7.16 mg/l), and low alkalinity (2.129 mM). The main deviations from these values were associated with basalt. BF had a higher temperature of (30.1 °C), and lower DO (6.28 mg/l). Both BF and BC had comparatively higher alkalinity (2.453, and 3.134 respectively).

December control samples were characterised by the lowest temperature (20.5 °C), lowest salinity (33.8), lowest pH (7.774), lowest DO (5.90 mg/l) and higher alkalinity than September (2.506 mM). The treatments followed the same pattern for temperature and salinity. The largest deviations from the normal state were observed in OC which had lower DO levels, (3.80 mg/l), pH (7.412), and the highest alkalinity seen during the study (3.146 mM). The condition OF also had slightly lower pH (7.412). Alkalinity was higher in all treatments compared to the control. March control samples had moderate temperatures (23.0 °C), and high salinity comparable to September (36.5), highest pH (8.082), highest DO (7.44 mg/l) and similar alkalinity to December (2.506 mM). Temperatures, salinity and DO were consistent with control. The pH for OF and OC were lower than control (8.022 and 8.055 respectively) but was higher in BF and BC (8.109 and 8.115 respectively). Alkalinity was similar to control in OF and BC, however it was higher in the OC and BF treatments (2.595 and 2.592 respectively).

Figure 3.1 highlights the main correlation between the physiochemical variables. DO had significant strong positive correlations between salinity ($p = 4.35E5$, $r_s = 0.86$), and pH ($p = 1.41E6$, $r_s = 0.92$). Salinity and pH also had a strong positive correlation ($p = 1.21E5$, $r_s = 0.88$). There was a significant negative correlation between temperature and alkalinity although this was only moderate ($p = 0.043$, $r_s = -0.53$).

Table 3.1 – Summary of the recorded surface water values for all 5 physiochemical variables across 15 samples from three sampling dates.

Sample date	Condition	O^2 (mg/l)	Sal (ppt)	pH	Alk (mM)	Temperature
September 15/09/22	C	7.16	36.4	7.950	2.129	28.9
	OF	7.04	36.5	7.960	2.129	28.6
	OC	6.74	36.5	7.860	2.087	28.8
	BF	6.28	36.4	7.770	2.453	30.1
	BC	6.88	36.4	7.850	3.134	28.4
December 12/12/22	C	5.90	33.8	7.774	2.506	20.5
	OF	6.26	33.8	7.638	2.685	20.8
	OC	3.80	33.7	7.412	3.146	20.6
	BF	5.88	33.8	7.772	2.628	20.5
	BC	6.05	33.9	7.778	2.493	20.6
March 13/03/23	C	7.44	36.5	8.082	2.520	23.0
	OF	6.96	36.5	8.022	2.476	23.2
	OC	7.35	36.5	8.055	2.595	21.0
	BF	7.56	36.5	8.109	2.592	21.8
	BC	7.40	36.5	8.115	2.491	20.0

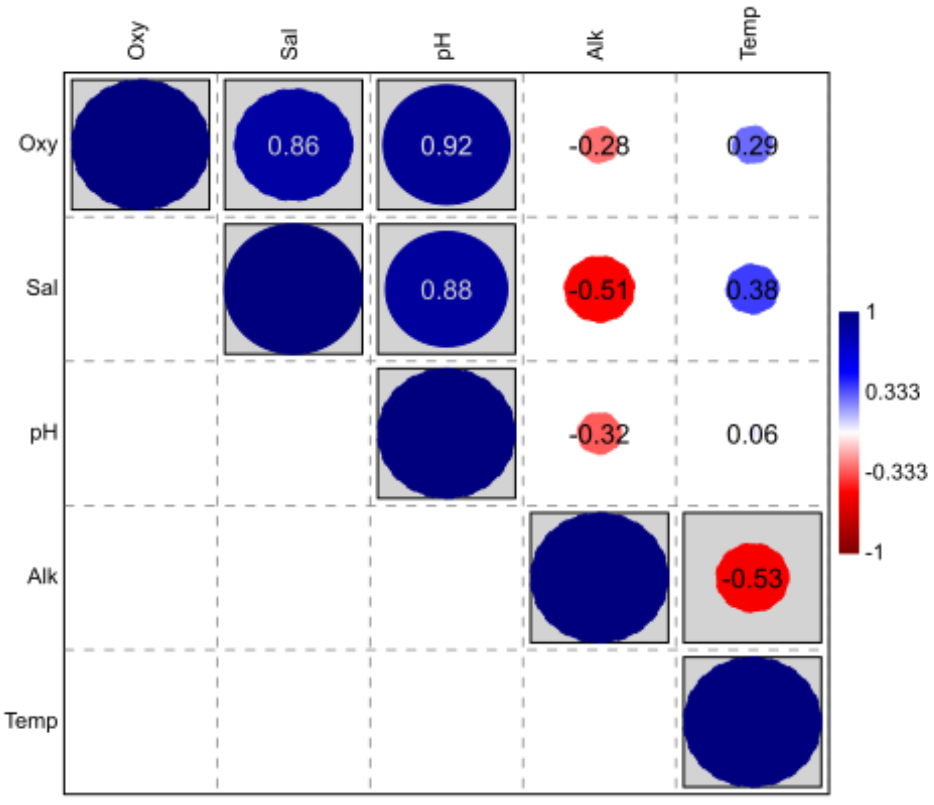

Figure 3.1 - Correlation heatmap including data from all 15 samples and 5 physiochemical parameters; oxygen, salinity, pH, alkalinity, and temperature. Boxed values indicate significance ($p \leq 0.05$). The size of circles is relative to the strength of correlation and contain associated correlation values (1 = strong positive correlation, -1 = strong negative correlation). Negative correlations are red and positive are blue.

3.2 | Diatom species response to seasonality and treatments

In total, 152 species (Appendix II, Tables 2 and 3), grouped in 46 genera, were counted and identified in the 15 analysed samples. Of this total, 41 species (across 23 genera) had relative abundances of more than 1 % (Appendix II, Table 2) and 18 were dominant (across 11 genera; Appendix II, Table 1), that is, they have relative abundances equal to or greater than 5 % in at least one of the analysed samples.

Figure 3.2 shows the similarity between the dominant species distribution across the September, December and March, for each condition separately. The control sample contained nine dominant species and indicated four main clusters related to the distribution of the species through time. The S1 group included species found in high abundances across all months with an increase over time. The three species characterising the S1 group were: *Nitzschia frustulum, Psammodictyon panduriforme,* and *Staurosirella guenter-grassii*. The S2 group included only one species (*Encyonema sp.*1) that was only dominant in September. The S3 group had four species that had higher abundances in September and December. The species for the S3 group included: *Navicymbula pusilla, Navicula salinicola, Navicula phylleptosoma,* and *Navicula sp.4*. The S4 group included only one species (*Nitzschia palea*) that was only dominant during the month of March. The species with black names appearing in the treatments are any species that was not found in the control cluster and were assigned to the U1 group (Figure 3.3).

All treatments contain every species of the S1 group. The OF, BC, and BF treatments all cluster S1 in a similar way, however OC indicates that *Psammodictyon panduriforme* (*Psa.pan*) was distributed in a different way through time compared to the rest of the S1 group. The S2 group was only found to remain dominant in the OC treatment, and clustered with *Navicymbula pusilla* (*Navcy.p*). From the S3 group, *Navicula phylleptosoma* (*Nav.phs*) remained dominant across all treatments, however *Navicula salinicola* (*Nav.sal*) was only found in BC. The species *Navicula sp.4* (*Nav.sp4*) was present in both BF and BC but not dominant in the olivine conditions (Figure 3.3). *Navcy.p* was found dominant in BF and OC. The OC treatment only contained one of the four species from this group. The S4 group does not appear in any of the treatment clusters. OF had a total number of six dominant species, and one U1 species. OC had nine dominant species and three U1 species. BF had ten dominant species and four U1 species. BC had nine dominant species and three U1 species. From the U1 group, only *Denticula subtilis* was present in more than one treatment.

A summary of the main aspects of diatom community structures is also shown in Figure 3.3. The concentration of the control group began at 62838 frustules/cm^3 in September, gradually

increasing over time to 202425 frustules/cm^3 in December, and finally reaching the maximum 323714 frustules/cm^3 in March. The OC treatment has very high concentrations across all months (527821 – 1073797 frustules/cm^3). The BF treatment shares a similar pattern over time to C, with each successive measurement increasing compared to the previous (76386, to 279699, to 419696 frustules/cm^3). Conversely to the concentration, the diversity of C decreased over time (3.14, to 3.04, to 2.87 H'). The BF and OF conditions followed similar patterns to the control decreasing over time. The OC treatment had the lowest diversity in September.

There are shifts in the dominant diatom species between the control and treatments. Species abundances from the S3 group in December are, in general, much lower in the treatments compared to the control. The S4 group is abundant in March for the control sample, however it is absent in all but one of the treatments in the same month. The OC treatment has some vast differences in species abundances with species such as *Tabularia fasciculata, Halamphora coffeaformis*, *Denticula subtilis*, *Nitzschia frustulum*, and *Staurosirella guenter-grassi* appearing in much higher abundances compared to the control. *Navicula phyllepta* was the only species that did not occur in the control but was found in both OC and BF.

The salinity preferences for the top 5 % most abundant species were arranged into three broader categories: marine, brackish, or freshwater. There was a total of 19 dominant species, with seven marine, eight brackish, and four freshwater species. The control has higher abundances of freshwater species than all treatments, despite maintaining a similar salinity. Majority of species are brackish across all conditions. December has higher abundances of Marine species in all treatments compared to the control, despite very similar salinity values.

Figure 3.4 shows hierarchical clustering using UPGMA algorithm and Bray-Curtis similarity index. This highlights similarities in species composition between sites. In the September samples, the most closely related are OF and OC, followed by C with this same group. For the months of December and March, C forms an outgroup with BC. September and December both show that the control holds about 75% similarity of species with the closest group. In March this value is closer to 85% similarity with BC.

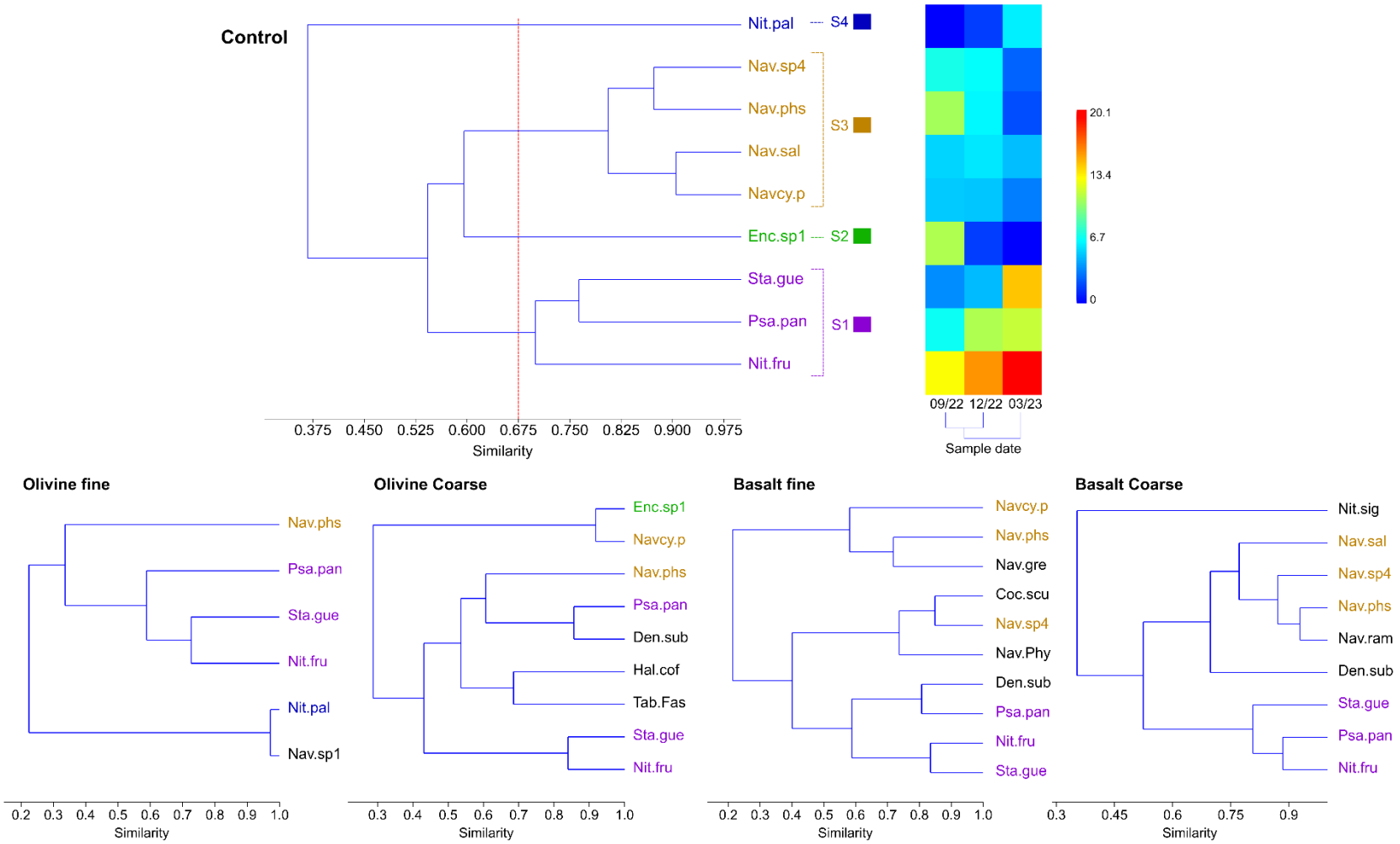

Figure 3.2 - R- mode UPGMA hierarchical clustering for control (top row) and each treatment (bottom row) including dominant diatom species (≥5 %) across three sampling times. Heat map shows abundance across each month (% abundance). Groups related to species seasonality are selected from (red line), and highlighted in, the control dendrogram: Ubiquitous across all months with skew towards March (S1 – violet), Unique for September (S2 - green), common in September and December but not for March (S3 - orange), Unique for March (S4 - blue).

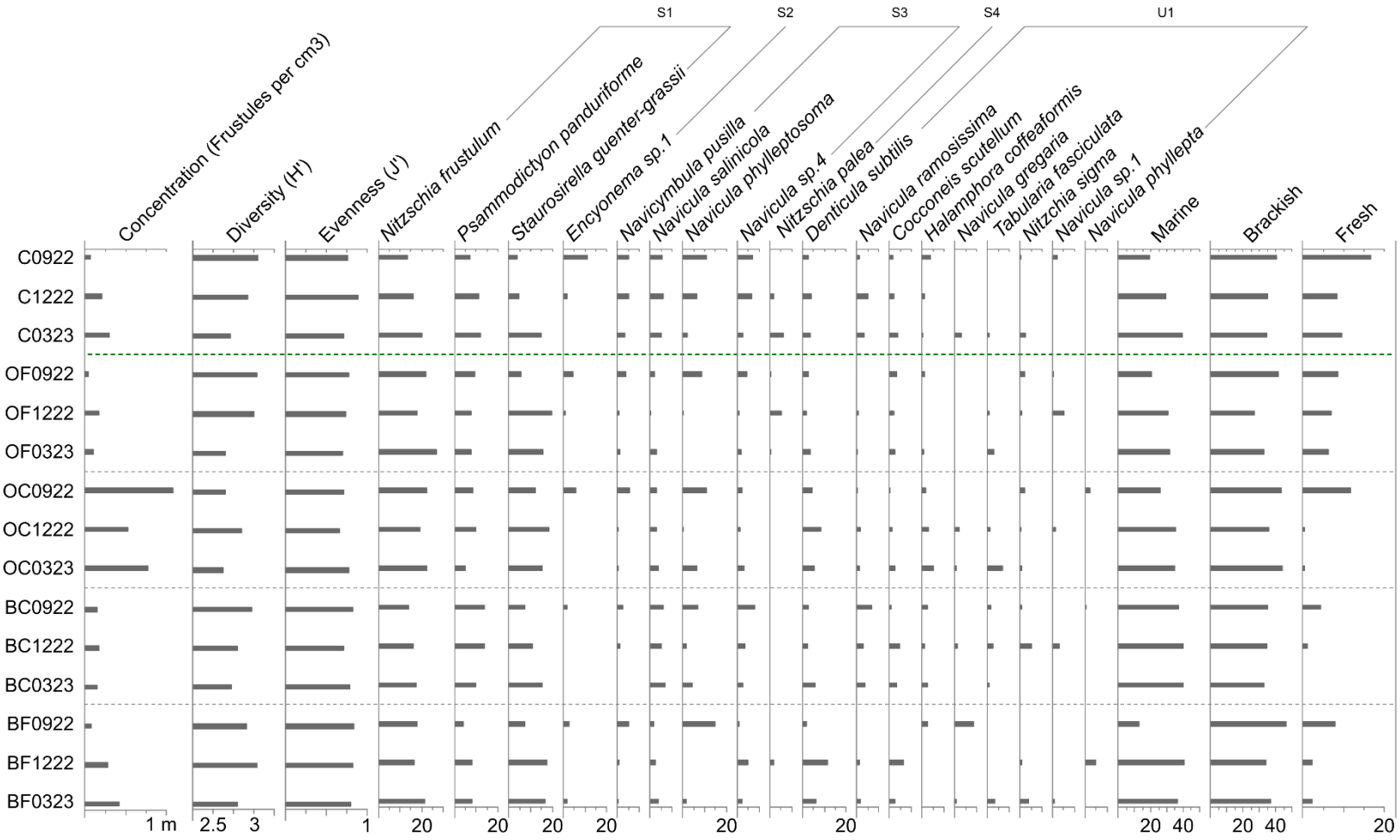

Figure 3.3 - Distribution of 18 species between 5 conditions across three sampling dates (15 samples total). The first column indicates condition and date. The first three graphs from the left show concentration, diversity, and evenness of diatoms. Dominant diatom species (≥5 % abundance) appear at the top of the graph and are grouped according to their seasonality as determined in Figure 3.2. Green dotted line separates the control samples from the rest. The final three columns indicate the percentage abundance of dominant species characteristic of brackish, marine or freshwater environments. Abundance values are shown as percentages. Concentration maximum is one million frustules per cm^3.

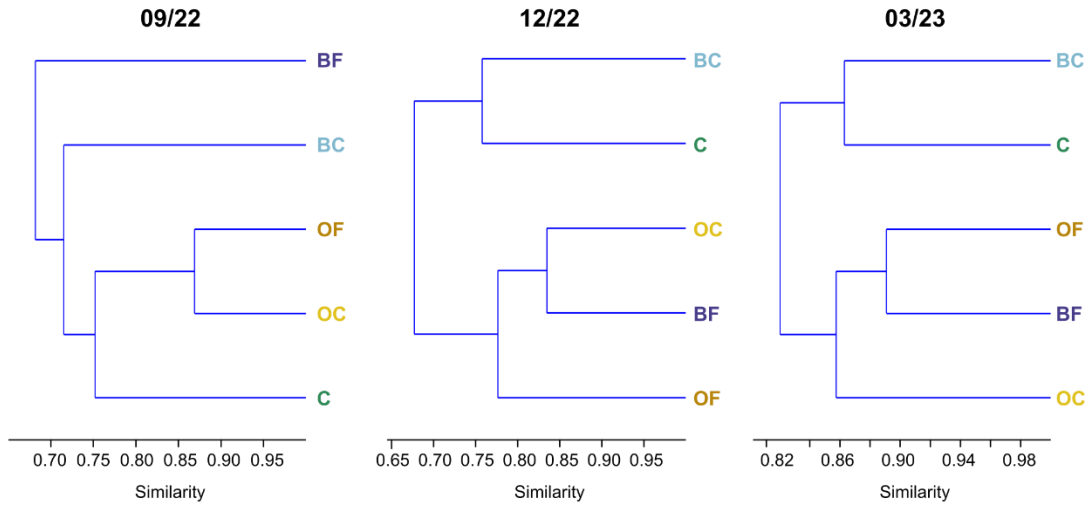

Figure 3.4 - Q-mode hierarchical clusters using UPGMA algorithm and Bray-Curtis similarity index for September, December and March including 18 species and 5 samples per cluster.

3.3 | Ordination

3.3.1 | *PCA*

The results of the PCA using surface water data indicated clear distinctions between the months. The PCA explained a total variance of 83.06% between PC1 and PC2 (Table 3.2).

Figure **3.5** displays the first two principal components plotted as the x and y axes. The DO parameter was removed from the model due to significant positive correlations with salinity and pH. Although temperature and alkalinity show a weak negative correlation, both parameters were considered to be biologically relevant for further analysis. All physiochemical parameters contribute highly to the explained variance.

Table 3.2 – Results of PCA including all five physiochemical parameters, and 15 samples.

Principal component	**1**	**2**	**3**	**4**
Eigenvalue	2.428	0.895	0.628	0.050
Percentage of explained variance (Cumulative percentage)	60.693	22.366 (83.059)	15.71 (98.769)	1.2309 (99.999)

The diagram showed that there was a clear separation in the environmental characteristics of each sampling time. However, upon visual inspection, BC0922 (light blue diamond) and OC1222 (yellow triangle), appeared to not cluster together with the rest of the samples from the same month, indicating potential outlier characteristics. BC0922 had a Z-score of 2.82 for PC3 (15% explained variance), and the score for OC1222 was -2.02 for PC1, indicating both possess outlier physiochemical characteristics which should be considered in further exploration. BC0922 has a much higher alkalinity compared to other samples in September.

OC1222 has much lower pH and DO, and higher alkalinity than other December samples.

The physiochemical parameters pH, salinity and temp directly correlate with PC1, whilst Alkalinity inversely correlates with it. This separates December samples from September and March. There is a direct correlation of Alkalinity, pH and Salinity with PC2, and temperature inversely correlates with the same axis. This clearly separates March and September samples.

September samples were characterised by higher temperatures, and lower alkalinity than other months (Table 3.1), correlating, respectively, positively and negatively with PC1 (Figure 3.5). December had the lowest values for temperature, DO, pH, and salinity, as well as the highest alkalinity scores (Table 3.1), correlating, respectively, positively and negatively with PC1 (Figure 3.5). March samples had the highest DO and pH values (Table 3.1), correlating, respectively, positively and negatively with PC1 (Figure 3.5).

3.3.2 | *DCA*

The results of the DCA indicated similar separations as the PCA (by sample month), however, they are much less pronounced (Figure 3.6). The first two axes of the DCA are plotted in Figure 3.6 and explain 49.14 % and 34.02 % of the variance respectively (83.16 % cumulatively). The September samples vaguely clustered together towards the centre of the axes. No clear separation was observed for December or March. In this case, species that appear in the two left quadrants are more characteristic of the conditions found in September samples. The species occurring towards the top and right are found more abundantly in the conditions found for December and March. Species towards the centre are generally more ubiquitous across samples, and the further away the more unique across samples. For example, *Encyonema sp.1* appeared in abundances of more than 5% in two samples with the highest values found in September, indicating its position on the far left of the plot. *Tabularia fasciculata* appears in the bottom right quadrant which is consistent with abundances mostly appearing in March (Figure 3.3). *Navicula sp.1* is found directly above the main cluster of samples, since it is found only in December in the treatments (Figure 3.3), it coincides with the separation of months observed in Figure 3.6. The results from the DCA indicated that there were three species with outlier characteristics for Axis 1 and Axis 2. These are *Karayevia nitidiformis*, *Biremis lucens*, and *Navicula* microdigiata, which is likely related to their low abundances and samples occurrences. Thus, this species can be considered outliers and be excluded from further analysis. The length of the gradient for axis 2 (longest) was 1.39 (Table 3.3). Therefore, according to (Legendre and Birks, 2012b), the data exploration could continue using linear methods (RDA).

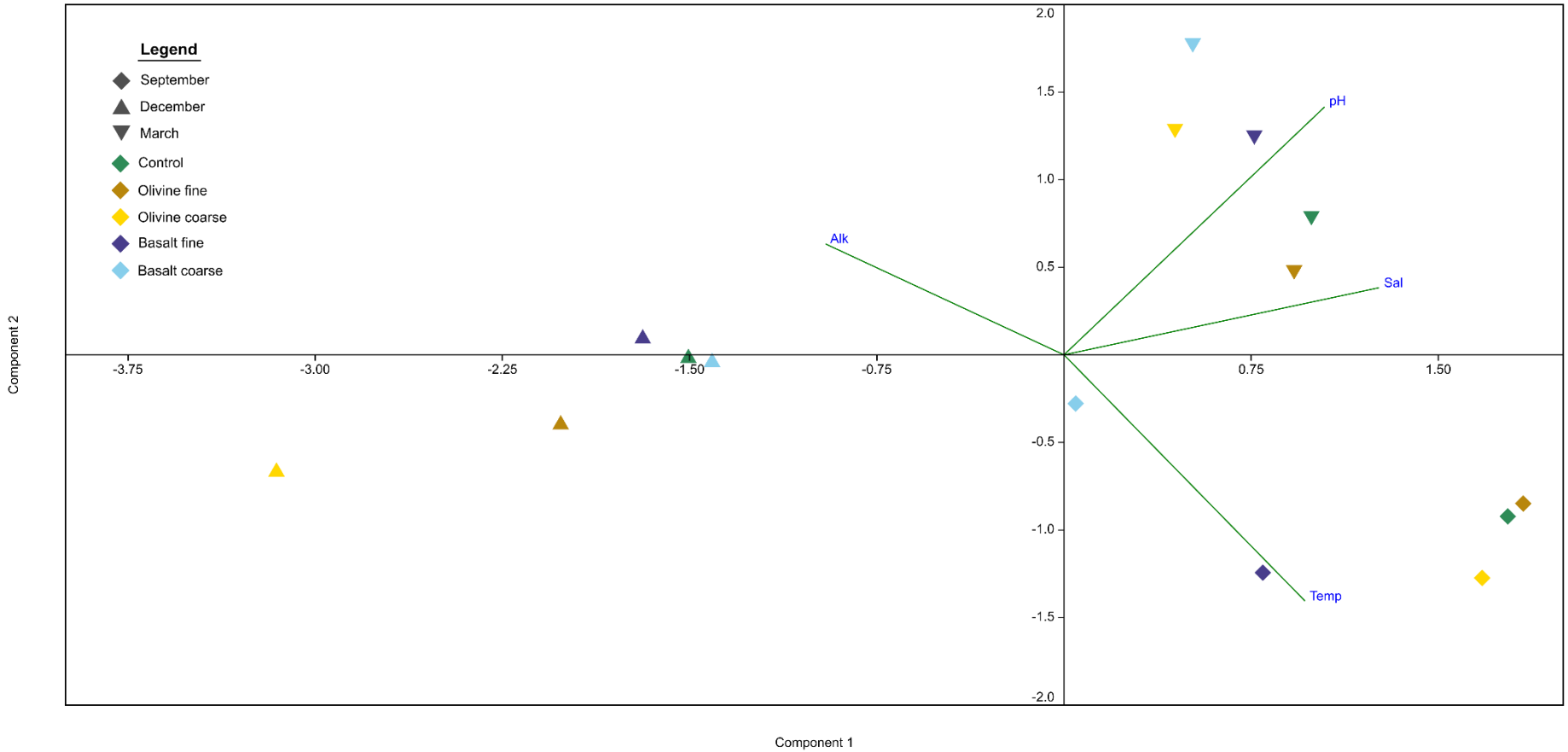

Figure 3.5 - Principal component analysis (PCA) of the first 2 principal components, including 4 physiochemical parameters (alkalinity, pH, salinity, and temperature), and 5 conditions (C, OF, OC, BF, and BC) across 3 sample dates (15 samples total). Each month is represented by a shape, and each condition is associated with a colour, both are detailed in the figure legend. Length and path of green physiochemical biplot lines indicate amount of variance explained and direction of pull.

Table 3.3 – Results of DCA including 41 species, and 15 samples.

Axis	1	2	3
Eigenvalue	0.127	0.088	0.033
Length of the gradient (standard deviation units)	1.35	1.39	0.85
Percentage of explained variance	49.14	34.02	12.78

3.3.3 | *RDA*

The RDA models' 4 environmental parameters explain a total of 39.67% of the variance across 4 axes, with the first two axes representing 20.55%, and 9.83% respectively (Table 3.4). High values of correlation between physiochemical parameters and species were found for the first three axes, ranging from 0.91 to 0.76. Monte Carlo permutation tests (999 permutations) indicated that the RDA was significant ($p = 0.013$). Alkalinity and pH positively correlate with Axis 1, whilst temperature and pH negatively correlate with the same axis (Figure 3.7). All physiochemical parameters negatively correlate with Axis 2. Temperature and alkalinity inversely correlate. All September samples are found on the negative side of the x axis, with the BC condition located away from the rest of the group (Figure 3.7). The OC samples group together for the months of December and March. The C sample for December was located far from the rest of December and March samples. For the month of September, the OC treatment correlates the closest with the C, matching the results observed in Figure 3.4. For December, all the treatment samples were located far from C with the closest treatment being OF. This is different from any observations in clusters, PCA, or DCA indicating that the two samples, while not similar in species composition alone (as shown in DCA), share common environmental drivers that cause their species assemblages to respond similarly in the RDA analysis. In March, C is most closely related to BF, matching what was observed in Figure 3.6. The results of the partial RDA series allowed contribution of each environmental variable within the total 39.67%. In Descending order, these values were 23% for salinity, 21% for temperature, 20%, for pH, and 18% for alkalinity.

Table 3.4 – Results of RDA including 38 species, 15 samples, and 4 physiochemical parameters.

Axis	1	2	3	4
Eigenvalue	3.618	1.731	0.843	0.794
Percentage of explained variance (Cumulative percentage)	20.55	9.829 (30.37)	4.788 (35.16)	4.509 (39.67)
Correlation between species and physiochemical parameters	0.9144	0.910	0.764	0.898

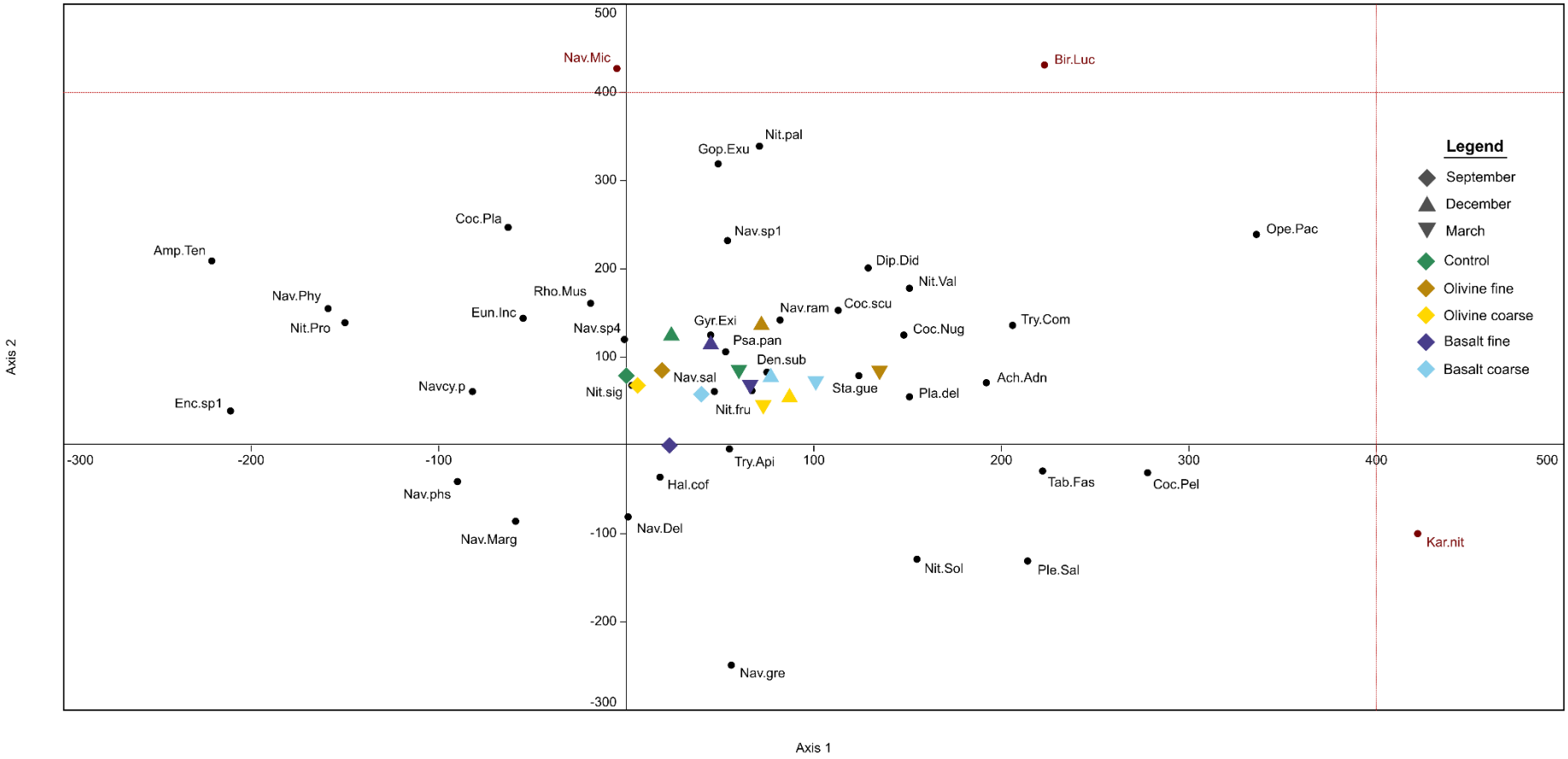

Figure 3.6 –Detrended component analysis (DCA) including 41 species across 5 conditions and 3 sampling times (15 samples total). Values on axes represent standard deviations x100. Any samples above 4 standard deviations (highlighted in red), were assessed for outlier characteristics to determine if they should be removed from further ordinations.

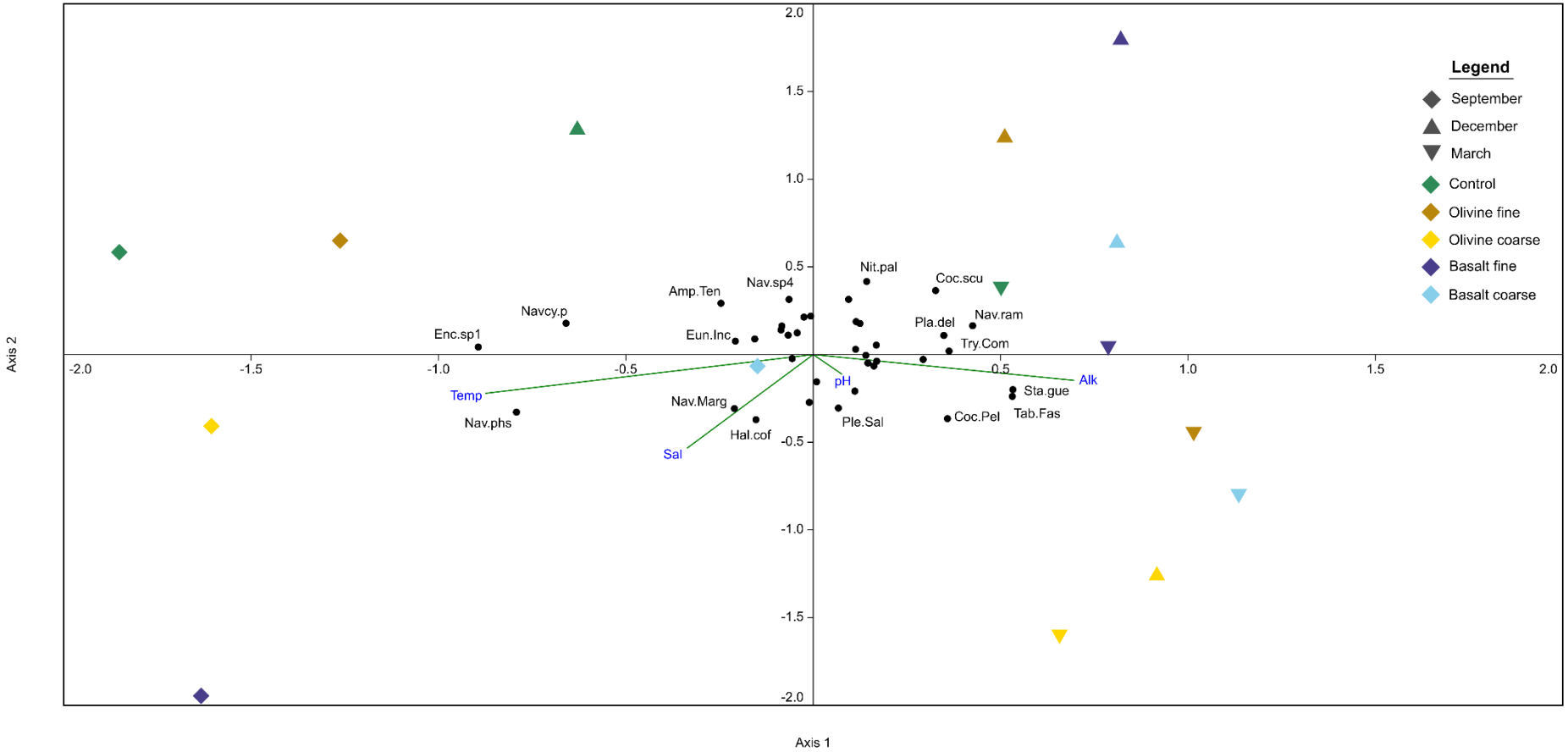

Figure 3.7 – Canonical redundancy analysis (RDA) using 4 physiochemical parameters (same as PCA), and 38 diatom species, across 5 conditions and 3 sampling dates (total of 15 samples). Only names of diatoms contributing more towards a direction were included for clarity.

4 | Discussion

To address the objectives of the study, this chapter will analyse the responses of motile living benthic diatom assemblages to the different alkalinity enhancement treatments across a seven-month period in the context of current literature. To achieve this, firstly, its necessary to consider the specific environmental changes that occurred in the control and treatment areas during the three seasons. Secondly, the changes in diatom assemblages caused by seasonality and treatments.

4.1 | Environmental change: Seasonality vs treatments

4.1.1 | *Seasonality*

The analysis of the controls environmental parameters indicates that the temperature data from this study clearly reflects seasonality (IPMA, 2022), with the highest temperatures in September (28.9 °C), lowest during December (20.5 °C) and moderate in March (23 °C). The pH also fits with what has been previously recorded in the Ria Formosa (Cravo et al., 2020), with pH following seasonal trends of photosynthesis (due to direct removal of CO_2). March had the highest pH (8.08), coinciding with higher chlorophyll-a concentrations than the other months (observed using NASA ocean colour data; Sathyendranath et al., 2023) indicating a potential phytoplankton bloom. The pH decreases from September (7.950), reaching its lowest value in December (7.774). The measured DO values were found to correlate highly with pH, as expected, due to the well documented fluctuations between respiration and photosynthesis (Cravo et al., 2020).

Dissolved oxygen and pH were also found to correlate significantly with salinity, the lowest values of which were observed in December (33.8 ppm). This low salinity is related to the higher amounts of rainfall during this month (~150 mm) compared to the other two seasons (~25mm; IPMA, 2022), this results in direct freshwater input, but may also have an indirect influence through groundwaters (Leote et al., 2008). This rainfall has a much lower pH than the Ria (Cravo et al., 2020), due to the dissociation of dissolved CO_2 in the atmosphere, resulting in a rainwater pH of between 4.5 and 5.6 (Charlson and Rodhe, 1982). The solubility of oxygen is also related to salinity, since freshwater holds less DO compared to more saline waters (Debelius et al., 2009). Cravo et al., (2020) showed that organic matter and benthic remineralization were higher after storms, periods of rainfall and land runoff in the Ria Formosa, correlating well with the observed lower DO in December (5.9 mg/l). This is also attributed to the winter shedding of leaves by many plants in the Ria Formosa, increasing

organic matter available for remineralisation, thus higher respiration (Machás and Santos, 1999).

The alkalinity was observed to be lowest in September (2.129 mM), increasing to a stable value between December (2.506 mM) and March (2.520 Mm). Since September presented the highest temperatures, it is plausible that higher evaporation concentrates the salts (echoing the high salinity observed), however CO_3^{2-} and HCO_3^{2-} (major contributors to total alkalinity) may not increase in concentration proportionally due to exchange of CO_2 with the atmosphere (Archer et al., 2004).

4.1.2 | *Environment of treatments*

The results of the PCA showed clear seasonality separations between surface water sampling times (Figure 3.5). As such, each month's treatment effects will be considered seperatly with the control. The temperatures, salinities and DO remain stable between the control and treatments during September, with the only slight deviation related to an elevated temperature for BF (30.1 °C) compared to the control (28.9 °C). This could be related to the concept that darker colours increase the absorption of heat (Stuart-Fox et al., 2017), and finer particles allow better trapping of heat (Fjeldskaar et al., 2009). These results were expected, since pH and oxygen physiochemical parameters will be slow to show impact of mineral dissolution since these changes are related to biological processes that take time to develop (water samples were collected the day after silicate substrates application). Alkalinity responses however can be much faster, since they are directly influenced by dissolution products. The results from the surface water alkalinity analysis in September for both OF (2.129 mM) and OC (2.087 mM) conditions reflected that of the control condition, however, both BF (2.453 mM) and BC (3.134 mM) had higher alkalinity values, reflecting their distance from the control in the PCA. Olivine has been reported to have faster dissolution compared to basalt (te Pas et al., 2023). Therefore, this result is most likely related to the presence of fine dust in the basalt left over from grinding processes, since source substrates were not washed to replicate a realistic application scenario. Water sampling was performed a day after silicate substrates deployment (14/09/22), and so would capture the short-term response of very fine dust dissolution. Considering that the weight of substrate deposited per box was higher in the BF (5.5 kg) and BC (4.6 kg) treatments than in OF (2.8 kg) and OC (3 kg), it is plausible that there would be more dust in the basalt treatments.

The results of sampling in December showed that temperature and salinities remained consistent with the control as expected. Dissolved oxygen measurements were stable in all but

the OC condition, which presented the lowest DO (3.8 mg/l, lower than the control by 2.1 mg/l) value across all samples. This shows that there may be increased respiration in the OC condition compared to the normal seasonal patterns (Soulsby et al., 1985). This is supported by the low pH (7.4) found in OC in December. The pH measurements for basalt were similar to the control (7.8), however, the OF treatment also showed a slightly lower pH (7.6), highlighting that both olivine treatments are impacting pH and DO more than basalt during December, and explaining the distance from the control in the PCA. The alkalinity was higher than the control (2.506 mM) in all treatments apart from BC (2.493 mM). The BF treatment shows a small increase from the control in December (2.628 mM) showing that the finer basalt treatment is releasing alkalinity products. These results fit with what we would expect considering the literature, since it is generally considered that a smaller grain size will have an increased surface area available for reaction and therefore release reaction products faster (Amann et al., 2022). However, the olivine treatments showed the opposite effect, with the OC treatment showing the largest increase in alkalinity (3.146 mM), and OF slightly less (2.685 mM). A natural setting brings several complications to the assumptions regarding grain size dissolution speed. Firstly, the study area is based in an intertidal environment and therefore tides, turbulence and bioturbation can all impact the dissolution kinetics (Montserrat et al., 2017). Larger grains can allow for more water to pass through the spaces, removing reaction products and promoting reaction efficiency (Amann et al., 2022). On the contrary, smaller grains could prevent permeability and thus reaction agents (Wilson et al., 2008). The OF condition had the smallest grain size out of all treatments (<0.063-0.125 mm). This shows that the smaller grain sizes of OF may be impeding its dissolution capabilities in this environment.

The results from March show that the salinity, pH, and oxygen values were all relatively close to the control. Basalt treatments showed very similar alkalinity results as in December. The OC (2.595 mM) treatment was still elevated above the control (2.520 mM) but OF (2.476 mM) was found to be lower, and both decreased from December values. This effect has been documented previously for olivine, since the dissolution rate diminishes over time due to the formation of surface mineral oxides (Prigiobbe et al., 2009), and solution saturation of dissolution products (Li et al., 2024). It is also known that more acidic environments such as those measured in December promote faster dissolution of minerals (Drever and Stillings, 1997). The PCA results appear to show that OF is the closest to the control in terms of physiochemical parameters, however, it seems that the main factor separating them is temperature. Both the coarse grain treatments have the lowest temperatures indicating a relation to the higher thermal conductivity of coarser grains (Midttomme and Roaldset, 1998).

4.2 | Diatom assemblage seasonality

4.2.1 | *Diatom concentration through the seasons*

March was the month with the highest concentrations of diatoms from the control group (323714 frustules/cm^3), which coincides with the with the highest values of DO and pH. The March observations fit with what is already known regarding algal blooms promoting higher diatom concentrations in spring (Assmy and Smetacek, 2009). Spring blooms are regular cycles of all oceans that occur as a result of improving conditions for photosynthetic growth. This includes increasing light availability, combined with more nutrients from deep water winter vertical mixing (Lima et al., 2022). During these early stages of the bloom, diatoms dominate due to the rapid proliferation capabilities previously described.

The lowest concentrations of diatoms were found in September (62839 frustules/cm^3). As nutrients become depleted following the autumn bloom, the dominance shifts towards smaller diatoms and other photosynthetic organisms that are able to thrive in lower nutrient concentrations (Snoeijs, 1990). At this stage, groups such as dinoflagellates and flagellates become more dominant owed to their ability to utilize organic nutrients (e.g. ammonium and urea; Spilling et al., 2018), whereas diatoms are photoautotrophic and predominantly use inorganic sources for growth (Giri et al., 2022). Therefore, shifts in taxa dominance could be causing the observed decline of the diatom population. Lower concentrations could also be linked to desiccation, thermal, and UV radiation tolerances due to the harsh summer conditions (Rijstenbil, 2002; Souffreau et al., 2010).

Concentrations of diatoms then increased in December (202425 frustules/cm^3) from the levels in September. This could be related to nutrient inputs as a result of the increased rainfall in December. Leote et al., (2008) found a link between higher submarine groundwater discharges during periods of increased rainfall in the Ria Formosa (~1.58 km from the current study site), indicating a continental origin. This groundwater was found to include nitrogen, silicon, and phosphorous (Leote et al., 2008), all of which are essential nutrients for diatom growth (Shi et al., 2015).

4.2.2 | *Diatom diversity through the seasons*

March had the lowest diversity of diatoms from the control group (2.87). If we are to consider the classical approach towards diversity indices as a monitoring metric, a lower diversity is considered to be associated with higher nutrient availability (Blanco, 2024), which appears to correlate well with the findings of increased diatom concentrations, DO, and pH.

September had the highest diversity from the control group (3.141). The successive shift in

dominance towards dinoflagellates causes a direct reduction of competitive exclusion allowing diatom diversity to increase (Spilling et al., 2018). Similar results were observed by Trigueros and Orive, (2001) investigating the variation of phytoplankton in a shallow temperate estuary, with highest diversities for diatoms found in September. Since resources are no longer abundant at this point, it allows for more species to take advantage of the different resource landscape, occupying ecological niches or utilising different strategies for accessing resources (e.g. using ammonium instead of nitrate; Chai et al., 2020).

The diversity remains high during December. Freshwater pulses have been linked to higher abundance of zooplankton, particularly copepods (Hitchcock et al., 2016). Higher grazing pressures by zooplankton has been shown to promote the diversity of phytoplankton and supress competitive exclusion processes due to modifications in physiochemical conditions and top-down control (Chícharo et al., 2006).

4.2.3 | *Diatom species seasonality*

The salinity preferences of dominant species were recorded and compared across seasons, however there appeared to be no link between species preferences and the measured salinity for each sample. The salinity was consistently high enough to be considered a marine environment in this area (33.8 - 36.5). This work shows that a revision of species ecology is required for those classified with the preference of freshwater in the literature (*N. pusilla, D. subtilis, N. palea*), since the results here indicate that they can tolerate a wider range of salinities than previously recorded. These findings were also described in the work of Gomes (2013).

The high abundance of marine species and elevated concentrations observed in March are directly associated with a dominance of the S1 group, which has the highest abundances for all associated species across the sampling period. *Nitzschia frustulum* is one of the species from this group and has been recorded to tolerate a wide range of conditions (Trobajo et al., 2004). Preferences for *S. Guenter-grassi* are limited, however one local study from the Guardiana river indicated that it was associated with sandy mudflats (Gomes, 2013), characterised by higher pH (7.38-7.91) and $CaCO_3$, but low SiO_4, and organic carbon. This correlates well with the current study which had highest pH values in March (8.08). Increased quantities of $CaCO_3$ are also generally associated with higher bivalve and gastropod abundances (Rato et al., 2022), which have seasonal reproductive patterns causing higher abundances in spring associated with warmer temperatures (Gupta and Agrawal, 2007). The preferences for *P. panduriforme* could not be found in the literature, however, considering their associations with the rest of group S1 in the present study it could be argued that they possess similar qualities to that of *N. frustulum,*

and *S. guenter-grassi.*

The S4 group is absent in September and shows highest abundances in March. This group only includes the species *Nitzschia palea*, an opportunistic and resilient species that often dominates in nutrient-rich, polluted waters (Trobajo et al., 2009). It appears that *N. palea* is benefitting from the increased nutrients in March and possess qualities that allow it to outcompete other species during this time. From the literature it is not clear what these exact preferences are, however it could be linked to silica demands (Frigeri et al., 2006), carbon concentrating mechanisms (Chrachri et al., 2018), or motility (Serôdio, 2021).

During September the S3 group showed their highest abundances. *N. phylleptosoma* has been reported to positively correlate with the aqueous silicate, orthosiliic acid ($Si(OH)_4$) as well as ammonium (NH_4^+; Du et al., 2017). Therefore, one probable cause of the increased September abundances of the S3 group could be associated with elevated silicic acid as a result of increased diatom frustule dissolution after the summer bloom and subsequent die off (Lima et al., 2022). The end of summer including September may also see elevated ammonification by bacteria as a result of the increased benthic organic matter (Asmus et al., 2000). Leote et al., (2008) measured the relative contribution of different nitrogen species from groundwater and discovered that September presented the month with highest contribution of ammonium, supporting the idea that it is contributing to the increased abundances of S3.

4.3 | Diatom assemblage response to treatments

4.3.1 | *Treatment impact on diatom concentration*

The concentrations in September increased in the BC (153,545 frustules per cm^3) and OC (1,073,797 frustules per cm^3) from the control (62,839 frustules per cm^3). This OC value is 17 times higher than control, representing a substantial increase. Since sediment samples were taken a week after the application of silicate substrates, responses by diatoms can already be seen. Both Olivine and Basalt have been shown to directly benefit growth of diatoms from the increased input of silica (Li et al., 2024), which directly supports the development of frustules. Diatoms have also been recorded to increase growth rates from supplementing Mg^{2+} (an essential ion in chlorophyl), which was found in higher quantities in the olivine (mean 11.4 % MgO) compared to the basalt (mean 48.1% MgO). Though since metals were not analysed here, this cannot be confirmed as a driver for the results observed. Therefore, the disparity between olivine and basalt here is most likely a result of the increased dissolution of olivine compared to basalt. The alkalinity results from September suggest that BC is weathering faster, though the alkalinity sampling times were a week apart from the sediment samples, therefore

the large increase in basalt from the excess dust may have already been transported or dissolved (Köhler et al., 2013).

In December, diatom concentrations were increased in the OC (527,821 frustules per cm^3) treatment compared to the control (202,425 frustules per cm^3). However, this increase was lower than concentrations in September for OC. This fits with what was mentioned previously regarding olivine dissolution slowing down over time. The BF treatment was also increase (279,699 frustules per cm^3) from the control. This also coincides with the higher alkalinity observed in BF for December compared to the control. Olivine fine had a lower concentration (175,178 frustules per cm^3), despite having a higher alkalinity. Indicating that the small grain size here is impacting the utilisation of dissolution products by olivine.

March concentrations showed higher concentrations in OC (775,359 frustules per cm^3) and BF (419,696 frustules per cm^3) compared to the control (323,714 frustules per cm^3). This follows the same pattern as December and indicates that the treatments are still significantly beneficial for diatom growth seven months after addition. Interestingly, both BC (148,517 frustules per cm^3) and OF (97,661 frustules per cm^3) were found to have lower concentrations than the control. BC had a similar alkalinity to the control at this time and so the difference could just be a result of random variation between sites. OF shows the same trend, demonstrating the need for further research into the impact on diatom growth of smaller grain sizes in a mud-sandy saltmarsh.

4.3.2 | *Treatment impact on diversity*

The diversities in September were similar to the control (3.14) for all treatments except OC which had a reduced diversity (2.82). This indicates that some species of diatoms are benefiting from the dissolution products more than others. This is reflected in the R-mode cluster results for OC (Figure 3.2), which show a reorganization of dominant species, including the first appearance of some species not found in the control (U1 group).

The variation in diversity from the control was small for December and March. The OF and BC treatments showed similar patterns to the control. This correlates with the previous discussion of small contributions to diatom concentration by OF and alkalinity by BC.

4.3.3 | *Species response to treatments*

September samples have similar trends in the DCA and RDA, with the OC and OF treatments remaining the closest to the control throughout. The distance of the Basalt conditions appears to be related to the high immediate alkalinity inputs, leading to shifts in the diatom community demonstrated by the DCA. Considering the sampling in September was

taken a week after silicate substrate application, the immediate response by diatoms will not necessarily represent long term adjustments. This concept is related both with diatom community responses over time (Gately et al., 2023), as well as the evolution of dissolution kinetics of the silicate substrates (Hauck et al., 2014). Diatom assemblage response will have an immediate phase, where sensitive species decline and opportunistic species increase (Cloern and Jassby, 2010), followed by community reorganization, and finally equilibrium (Snoeijs and Weckström, 2010). The dissolution of substrates will vary across treatments depending on chemical composition, disturbance and grain size, but overall, the impact is expected to reduce through time (Flipkens et al., 2023). This concept makes it difficult to quantify the initial impacts of the treatments. The S1 group appeared to increase in abundances from the addition of olivine and basalt, with responses visible after only one week. It has already been demonstrated that the dissolution of olivine can show immediate increases in alkalinity and dissolved silicon (DSi; Flipkens et al., 2023), with a peak after around seven days. The turbulence of the environment can then have significant impacts on how much product is released (Flipkens et al., 2023). The S2 group including only *Encyonema. sp.1,* is found in slightly lower abundances in all treatments compared to the control, however it still follows the same patterns with higher abundances in September and lower in December. Its abundance is also higher in olivine compared to basalt. Further analysis over the next year will help to understand whether this response is showing normal seasonality, or if its loss in December for the OC and BC treatments is indicative of sensitivity to olivine or basalt. However, the higher concentrations of S1 could theoretically also be impacting the success of S2.

In December the Q-mode cluster indicated that the BC dominant diatom assemblage was closest to the control. However, when the non-dominant species (<1 % abundance) are also considered in the DCA, BF appears to be more closely related. The RDA model shows that the control is very far from all the treatments. The alkalinity parameter appears to be explaining most of this difference, apart from BC which had very similar alkalinity to the control. In the case of BC, it appears to be related to the significant changes in non-dominant species. This raises the question of whether the large influx of dust alkalinity introduced in September could have longer term effects. Therefore, the closest treatment to the control in the RDA for December is OF, although the only reason BF is not closer is due to the higher temperature and lower pH found in OF. The S3 group demonstrated lower abundances across all species and treatments for December, especially in the olivine treatments. This indicates that the weathering of the minerals is starting to have a larger impact after three months in situ. Considering the relatively larger increases of abundance in the S1 group, it is likely that the S3

species are being outcompeted during this time.

March Q-mode clusters indicated that the BC condition had the closest relation to the control in terms of dominant species. However, when considering the DCA, BC is the third furthest from the control. This appears to mostly be linked to the species *N. palea* and *N. pusilla*, which were not dominant in the control but still significant in March but were not found in BC. Therefore, the closest sample in terms of full species assemblage is BF. The results of the RDA indicate that the BF condition is the closest considering environment and species composition.

The following section will highlight the species that were impacted by the treatments. The U1 group contained species that were dominant in at least one treatment but not in the control condition. *Denticula subtilis* appeared in higher abundances than the control for OC and BC across all months, and BF for the month of March. *Navicula ramosissima* was found in lower abundances in all treatments but BC. Halamphora coffeaformis showed increased abundances in December and March in the OC and BC treatments. *Tabularia fasciculata* had a higher abundance in March in the OC, OF, and BF treatments.

The species *S. guenter-grassi* appears to respond with higher abundances in all treatments across all months. The species that were found in abundances of <1 % in treatments that had not been recorded in the control scenario were *Navicula phyllepta, Karayevia nitidiformis, Diploneis didyma, Opephora pacifica,* and *Nitzschia solita*. *Cocconeis scutellum* appeared in higher abundances for both basalt conditions but not in olivine.

The species that appear to be negatively impacted by all treatments in terms of loss of abundance are, *Navicymbula pusilla, Navicula sp.4,* and *Nitzschia palea*. The species *Navicula Salinicola* and *Psammodictyon panduriforme* appear in lower abundances compared to the control in all but BC. *Navicula phylleptosoma* is found in lower abundances in OF and BF.

4.4 | Study limitations and future considerations

In-situ studies often have several uncontrollable variables, exemplified by the RDA explaining a total of only 39.67 % of the variance observed in the data. This does not mean that the study is flawed, but that these factors must be considered when interpreting findings. This allows future authors to draw their own conclusions and learn from what works and doesn't work in this complex environment.

Sediment samples collected for diatom assemblage analysis used volume of sediment for the calculations of diatom concentrations. This method fails to take water content and grain size into consideration, potentially causing an over or underestimations of diatom concentrations. This is especially relevant considering that the study uses three different classes

of grain size. A better method could be to dry and weigh samples after the lens tissue has been removed (Yang et al., 2010b). The current study only considers the living motile assemblages of benthic diatoms. There was an assumption that all diatoms will have migrated to the tissue during the 24 hours acclimation period, though this could have underestimated the abundances and concentration of some species (Hassan, 2015). Therefore, there could be a part of the community that is not considered here which could explain some of the unknown factors and give more insight into the changes in community.

Samples for the analysis of diatoms considered the top 20 mm of sediment. Vertical distribution of diatoms has been found to vary significantly depending on the species composition, for example, Saburova and Polikarpov, (2003) found that between 40-50 % of diatoms were encountered within the top 20 mm of soil, and the remaining 50-60 % was found in deeper layers with maximum recorded depths of 42 mm in clay sediments and 83 mm in sandy substrates. This means that a significant proportion of the diatom assemblage could have been overlooked in this study.

An observation made during the data collection of this study was a noticeable difference in the size of certain diatom species between samples that remained that consistent size throughout that sample. Although morphologic characteristics of diatom frustules are a vital taxonomic tool, it is not absolute, since these characters can be affected by environmental conditions (Schoefs et al., 2020). For example, *N. frustulum* has been observed to adapt morphology in response to salinity gradients, modifying the length, width and fibulae density of valves (Trobajo et al., 2004). Unfortunately, measurements were not recorded as part of this study, but it is recommended that future analysis also includes consideration of this as a tool for monitoring species responses. As discussed previously, these details could also lead to erroneous classification, as well as overlooked impacts on the community structure.

The current study was able to consider only seven months of data. For an understanding of long-term impacts, the living assemblage response should be considered for more than a year, including the month that the experiment started. Additionally, results were only considered for one of three plots that the project installed. Consideration of these plots would provide robustness by limiting effects of random variation.

5 | Conclusions

Diatoms play a crucial role in marine ecosystems as primary producers, driving nutrient cycling and contributing significantly to global carbon fixation. Their sensitivity to changes in environmental conditions makes them excellent bioindicators for studying the effects of

alkalinity enhancement. Understanding the response of diatom communities is essential not only for assessing the ecological consequences of alkalinity enhancement but also for evaluating the broader impacts on marine food webs and carbon cycling processes. This research therefore contributes to both our ecological knowledge and the development of nature-based solutions for climate change mitigation. The response of diatom assemblages to olivine and basalt in a natural setting is still severely lacking in the literature.

Therefore, to fulfil this gap, the current study aimed to understand the response of living benthic motile assemblages of diatoms to the introduction of two grain sizes of olivine and basalt, two mafic silicate substrates that are being explored for use in alkalinity enhancement projects as a carbon dioxide removal strategy over a seven-month period.

Results revealed that overall the BF treatment had the least impact on diatom community structure and composition, while still maintaining higher alkalinity in March (2.592 mM) than the control (2.520 mM) and BC (2.491 mM). There were minimal changes in diatom concentrations, diversity, and species composition under the BF treatment. In contrast, the BC treatment closely matched the control in terms of dominant species in December and March, though DCA analysis revealed significant shifts in non-dominant species. The OF treatment showed the largest impact on species composition, with this effect becoming more pronounced over time, accompanied by a decrease in diatom concentrations compared to the control. The OC treatment had the largest impact on diatom community structure, with significant increases in concentrations and reductions in diversity. This coincided with large shifts in species composition, as demonstrated by the DCA, though these shifts appeared to diminish by March.

These findings highlight the need for long-term studies to determine whether community shifts are temporary or permanent. Future research should include a longer timeframe and additional repetitions to minimize inherent variability between sites. Investigating nutrient and metal content, along with the composition of macrofauna and flora, would help elucidate which aspects of the silicate substrates are driving the observed changes. Including pore water physiochemical parameters could improve the relevance of RDA results by providing a clearer understanding of the benthic diatom environment. Furthermore, examining the effects on other trophic levels could clarify broader ecological impacts not captured in this study.

Finally, it is crucial to extend these findings beyond salt marsh ecosystems to assess the potential impacts of OAE in other marine environments. This research provides valuable insights into how different grain sizes of olivine and basalt influence diatom communities, with broader implications for carbon cycling, ecosystem processes, and the development of nature-based climate change mitigation strategies.

6 | References

Admiraal, W. (1984). The ecology of estuarine sediment-inhabiting diatoms. *Progress in phycological research* 3, 269–322.

Amann, T., Hartmann, J., Hellmann, R., Pedrosa, E. T., and Malik, A. (2022). Enhanced weathering potentials—the role of in situ CO2 and grain size distribution. *Front. Clim.* 4. doi: 10.3389/fclim.2022.929268

Apoya-Horton, M. D., Yin, L., Underwood, G. J. C., and Gretz, M. R. (2006). Movement Modalities and Responses to Environmental Changes of the Mudflat Diatom Cylindrotheca Closterium (bacillariophyceae). *Journal of Phycology* 42, 379–390. doi: 10.1111/j.1529-8817.2006.00194.x

Archer, D., Martin, P., Buffett, B., Brovkin, V., Rahmstorf, S., and Ganopolski, A. (2004). The importance of ocean temperature to global biogeochemistry. *Earth and Planetary Science Letters* 222, 333–348. doi: 10.1016/j.epsl.2004.03.011

Armbrust, E. V. (2009). The life of diatoms in the world's oceans. *Nature* 459, 185–192.

Asmus, R. M., Sprung, M., and Asmus, H. (2000). Nutrient fluxes in intertidal communities of a South European lagoon (Ria Formosa) – similarities and differences with a northern Wadden Sea bay (Sylt-Rømø Bay). *Hydrobiologia* 436, 217–235. doi: 10.1023/A:1026542621512

Assmy, P., and Smetacek, V. (2009). "Algal Blooms," in *Encyclopedia of Microbiology*, (Elsevier), 27–41. doi: 10.1016/B978-012373944-5.00001-8

Bach, L. T., Gill, S. J., Rickaby, R. E. M., Gore, S., and Renforth, P. (2019). CO2 Removal With Enhanced Weathering and Ocean Alkalinity Enhancement: Potential Risks and Co-benefits for Marine Pelagic Ecosystems. *Frontiers in Climate* 1. doi: 10.3389/fclim.2019.00007

Barnett, A., Méléder, V., Dupuy, C., and Lavaud, J. (2020). The vertical migratory rhythm of intertidal microphytobenthos in sediment depends on the light photoperiod, intensity, and spectrum: evidence for a positive effect of blue wavelengths. *Frontiers in Marine Science* 7, 212.

Birks, H. J. B., Lotter, A. F., Juggins, S., and Smol, J. P. eds. (2012). *Tracking Environmental Change Using Lake Sediments: Data Handling and Numerical Techniques*. Dordrecht: Springer Netherlands. doi: 10.1007/978-94-007-2745-8

Blanco, S. (2024). What do diatom indices indicate? Modeling the specific pollution sensitivity index. *Environ Sci Pollut Res Int* 31, 29449–29459. doi: 10.1007/s11356-024-33115-1

Bohórquez, J., McGenity, T. J., Papaspyrou, S., García-Robledo, E., Corzo, A., and Underwood, G. J. (2017). Different types of diatom-derived extracellular polymeric substances drive changes in heterotrophic bacterial communities from intertidal

sediments. *Frontiers in microbiology* 8, 234951.

Cai, W.-J., Hu, X., Huang, W.-J., Murrell, M. C., Lehrter, J. C., Lohrenz, S. E., et al. (2011). Acidification of subsurface coastal waters enhanced by eutrophication. *Nature geoscience* 4, 766–770.

Chai, Z. Y., Wang, H., Deng, Y., Hu, Z., and Zhong Tang, Y. (2020). Harmful algal blooms significantly reduce the resource use efficiency in a coastal plankton community. *Science of The Total Environment* 704, 135381. doi: 10.1016/j.scitotenv.2019.135381

Charlson, R. J., and Rodhe, H. (1982). Factors controlling the acidity of natural rainwater. *Nature* 295, 683–685. doi: 10.1038/295683a0

Chícharo, L., Chícharo, M. A., and Ben-Hamadou, R. (2006). Use of a hydrotechnical infrastructure (Alqueva Dam) to regulate planktonic assemblages in the Guadiana estuary: basis for sustainable water and ecosystem services management. *Estuarine, Coastal and Shelf Science* 70, 3–18.

Chmura, G. L., Anisfeld, S. C., Cahoon, D. R., and Lynch, J. C. (2003). Global carbon sequestration in tidal, saline wetland soils. *Global Biogeochemical Cycles* 17, 2002GB001917. doi: 10.1029/2002GB001917

Chrachri, A., Hopkinson, B. M., Flynn, K., Brownlee, C., and Wheeler, G. L. (2018). Dynamic changes in carbonate chemistry in the microenvironment around single marine phytoplankton cells. *Nat Commun* 9, 74. doi: 10.1038/s41467-017-02426-y

Cloern, J. E., and Jassby, A. D. (2010). Patterns and Scales of Phytoplankton Variability in Estuarine–Coastal Ecosystems. *Estuaries and Coasts* 33, 230–241. doi: 10.1007/s12237-009-9195-3

Cohn, S. A., Spurck, T. P., and Pickett-Heaps, J. D. (1999). High energy irradiation at the leading tip of moving diatoms causes a rapid change of cell direction. *Diatom Research* 14, 193–206.

Cravo, A., Rosa, A., Jacob, J., and Correia, C. (2020). Dissolved oxygen dynamics in Ria Formosa Lagoon (South Portugal) - A real time monitoring station observatory. *Marine Chemistry* 223, 103806. doi: 10.1016/j.marchem.2020.103806

Cristóbal, G., Blanco, S., and Bueno, G. (2020). *Modern Trends in Diatom Identification*. Springer.

Cronodon.com. (2021). *Diatoms (Bacillariophytes).* Available at: https://cronodon.com/NatureTech/diatoms.html (Accessed September 19, 2024).

Cvjetinovic, J., Luchkin, S. Y., Statnik, E. S., Davidovich, N. A., Somov, P. A., Salimon, A. I., et al. (2023). Revealing the static and dynamic nanomechanical properties of diatom frustules—Nature's glass lace. *Sci Rep* 13, 5518. doi: 10.1038/s41598-023-31487-x

Debelius, B., Gómez-Parra, A., and Forja, J. M. (2009). Oxygen solubility in evaporated seawater as a function of temperature and salinity. *Hydrobiologia* 632, 157–165.

Dell'Aquila, G., Ferrante, M. I., Gherardi, M., Cosentino Lagomarsino, M., Ribera d'Alcalà, M., Iudicone, D., et al. (2017). Nutrient consumption and chain tuning in diatoms exposed to storm-like turbulence. *Scientific reports* 7, 1828.

Denys, L. (1991). *A check-list of the diatoms in the Holocene deposits of the western Belgian coastal plain with a survey of their apparent ecological requirements*. Ministerie van Economische Zaken Brussel, Belgium. Available at: https://www.vliz.be/imisdocs/publications/ocrd/249292.pdf (Accessed June 14, 2024).

Dickson, A. G. (1981). An exact definition of total alkalinity and a procedure for the estimation of alkalinity and total inorganic carbon from titration data. *Deep Sea Research Part A. Oceanographic Research Papers* 28, 609–623. doi: 10.1016/0198-0149(81)90121-7

Drever, J. I., and Stillings, L. L. (1997). The role of organic acids in mineral weathering. *Colloids and Surfaces A: Physicochemical and Engineering Aspects* 120, 167–181. doi: 10.1016/S0927-7757(96)03720-X

Du, G., Yan, H., and Dupuy, C. (2017). Microphytobenthos as an indicator of environmental quality status in intertidal flats: Case study of coastal ecosystem in Pertuis Charentais, France. *Estuarine, Coastal and Shelf Science* 196, 217–226. doi: 10.1016/j.ecss.2017.06.031

Fakhraee, M., Li, Z., Planavsky, N. J., and Reinhard, C. T. (2023a). A biogeochemical model of mineral-based ocean alkalinity enhancement: impacts on the biological pump and ocean carbon uptake. *Environmental Research Letters* 18, 044047.

Fakhraee, M., Planavsky, N. J., and Reinhard, C. T. (2023b). Ocean alkalinity enhancement through restoration of blue carbon ecosystems. *Nature Sustainability* 6, 1087–1094.

Falkowski, P. G., and Raven, J. A. (2013). *Aquatic photosynthesis*. Princeton University Press. Available at: https://books.google.com/books?hl=en&lr=&id=kUCrAQAAQBAJ&oi=fnd&pg=PP1&dq=Aquatic+Photosynthesis+(Second+Edition).&ots=brYwleZp3y&sig=L_-B27ZCs9OUbWnLv4hUhp1iq5k (Accessed August 26, 2024).

Fatela, F., and Taborda, R. (2002). Confidence limits of species proportions in microfossil assemblages. *Marine Micropaleontology* 45, 169–174. doi: 10.1016/S0377-8398(02)00021-X

Feng, E. Y., Koeve, W., Keller, D. P., and Oschlies, A. (2017). Model-Based Assessment of the CO_2 Sequestration Potential of Coastal Ocean Alkalinization. *Earth's Future* 5, 1252–1266. doi: 10.1002/2017EF000659

Fennel, K., Long, M. C., Algar, C., Carter, B., Keller, D., Laurent, A., et al. (2023). Modeling considerations for research on Ocean Alkalinity Enhancement (OAE). *State of the Planet Discussions* 2023, 1–47.

Ferderer, A., Chase, Z., Kennedy, F., Schulz, K. G., and Bach, L. T. (2022). Assessing the influence of ocean alkalinity enhancement on a coastal phytoplankton community. *Biogeosciences* 19, 5375–5399. doi: 10.5194/bg-19-5375-2022

Ferreira, Ó., Matias, A., and Pacheco, A. (2016). The East Coast of Algarve: a Barrier Island Dominated Coast. *Thalassas* 32, 75–85. doi: 10.1007/s41208-016-0010-1

FGM Silva, M., Aníbal, J., Duarte, D., and Chícharo, L. (2015). Sarcocornia fruticosa and Spartina maritima as heavy metals remediators in an European southwestern salt marsh (Ria Formosa, Portugal). *Journal of environmental protection and ecology* 16, 1468–1477.

Field, C. B., Behrenfeld, M. J., Randerson, J. T., and Falkowski, P. (1998). Primary Production of the Biosphere: Integrating Terrestrial and Oceanic Components. *Science* 281, 237–240. doi: 10.1126/science.281.5374.237

Fischer, H., Gröning, C., and Köster, C. (1977). Vertical migration rhythm in freshwater diatoms. *Hydrobiologia* 56, 259–263.

Fjeldskaar, W., Christie, O. H. J., Midttømme, K., Virnovsky, G., Jensen, N. B., Lohne, A., et al. (2009). On the determination of thermal conductivity of sedimentary rocks and the significance for basin temperature history. *Petroleum Geoscience* 15, 367–380. doi: 10.1144/1354-079309-814

Flipkens, G., Fuhr, M., Fiers, G., Meysman, F. J. R., Town, R. M., and Blust, R. (2023). Enhanced olivine dissolution in seawater through continuous grain collisions. *Geochimica et Cosmochimica Acta* 359, 84–99. doi: 10.1016/j.gca.2023.09.002

Fonseca, V. G., Grade, N., and Cancela da Fonseca, L. (2004). Patterns of association and habitat use by migrating shorebirds on intertidal mudflats and saltworks on the Tavira Estuary, Ria Formosa, southern Portugal. *Wader Study Group Bull* 105, 50–55.

Friedlingstein, P., Jones, M. W., O'Sullivan, M., Andrew, R. M., Bakker, D. C. E., Hauck, J., et al. (2022). Global Carbon Budget 2021. *Earth Syst. Sci. Data* 14, 1917–2005. doi: 10.5194/essd-14-1917-2022

Frigeri, L. G., Radabaugh, T. R., Haynes, P. A., and Hildebrand, M. (2006). Identification of Proteins from a Cell Wall Fraction of the Diatom Thalassiosira pseudonana: Insights into Silica Structure Formation* S. *Molecular & Cellular Proteomics* 5, 182–193.

Fuss, S., Lamb, W. F., Callaghan, M. W., Hilaire, J., Creutzig, F., Amann, T., et al. (2018). Negative emissions—Part 2: Costs, potentials and side effects. *Environmental research letters* 13, 063002.

Gamito, S., Patrício, J., Neto, J. M., Marques, J., and Teixeira, H. (2012). The Importance of Habitat-type for Defining the Reference Conditions and the Ecological Quality Status Based on Benthic Invertebrates: The Ria Formosa Coastal Lagoon (Southern Portugal) Case Study. *Ecological Indicators* 19, 61–72. doi: 10.1016/j.ecolind.2011.08.004

Gao, K., Xu, J., Gao, G., Li, Y., Hutchins, D. A., Huang, B., et al. (2012). Rising CO2 and increased light exposure synergistically reduce marine primary productivity. *Nature Clim Change* 2, 519–523. doi: 10.1038/nclimate1507

Gately, J. A., Kim, S. M., Jin, B., Brzezinski, M. A., and Iglesias-Rodriguez, M. D. (2023). Coccolithophores and diatoms resilient to ocean alkalinity enhancement: A glimpse of

hope? *Sci. Adv.* 9, eadg6066. doi: 10.1126/sciadv.adg6066

Giri, T., Goutam, U., Arya, A., and Gautam, S. (2022). Effect of Nutrients on Diatom Growth: A Review. *Trends Sci* 19, 1752. doi: 10.48048/tis.2022.1752

Gomes, A. (2013). Alterações ambientais na costa algarvia durante o holocénico: um estudo com base em Diatomáceas. UALG.

Grimm, E. C. (2023). TILIA Version 3.0.3 : A pollen program for analysis and display. Available at: https://www.neotomadb.org/apps/tilia

Guimond, J., and Tamborski, J. (2021). Salt marsh hydrogeology: A review. *Water* 13, 543.

Guiry and Guiry (2024). AlgaeBase. Available at: https://www.algaebase.org/ (Accessed June 18, 2024).

Gupta, S., and Agrawal, S. C. (2007). Survival and motility of diatomsNavicula grimmei andNitzschia palea affected by some physical and chemical factors. *Folia Microbiol* 52, 127–134. doi: 10.1007/BF02932151

Gysi, A. P., and Stefánsson, A. (2012). CO2-water–basalt interaction. Low temperature experiments and implications for CO2 sequestration into basalts. *Geochimica et Cosmochimica Acta* 81, 129–152.

Hammer, Ø., Harper, D. A. T., and Ryan, P. D. (2023). PAST: Paleontological Statistics software package (Version 4.07). Available at: https://www.nhm.uio.no/english/research/infrastructure/past/

Hangx, S. J. T., and Spiers, C. J. (2009). Coastal spreading of olivine to control atmospheric CO2 concentrations: A critical analysis of viability. *International Journal of Greenhouse Gas Control* 3, 757–767. doi: 10.1016/j.ijggc.2009.07.001

Hashioka, T., Vogt, M., Yamanaka, Y., Le Quéré, C., Buitenhuis, E. T., Aita, M. N., et al. (2013). Phytoplankton competition during the spring bloom in four plankton functional type models. *Biogeosciences* 10, 6833–6850. doi: 10.5194/bg-10-6833-2013

Hassan, G. S. (2015). On the benefits of being redundant: low compositional fidelity of diatom death assemblages does not hamper the preservation of environmental gradients in shallow lakes. *Paleobiology* 41, 154–173. doi: 10.1017/pab.2014.10

Hauck, J., Köhler, P., Abrams, J., Völker, C., and Wolf-Gladrow, D. (2014). Impact of open ocean dissolution of olivine on atmospheric CO2, surface ocean pH and the biological carbon pump. Available at: https://epic.awi.de/id/eprint/37181/1/hauck_-_impact_of_open_ocean_dissolution_of_olivine.pdf (Accessed August 26, 2024).

Hill, M. O., and Gauch Jr, H. G. (1980). Detrended correspondence analysis: an improved ordination technique. *Vegetatio* 42, 47–58.

Hitchcock, J. N., Mitrovic, S. M., Hadwen, W. L., Growns, I. O., and Rohlfs, A.-M. (2016). Zooplankton responses to freshwater inflows and organic-matter pulses in a wave-dominated estuary. *Marine and Freshwater Research* 67, 1374–1386.

Hutchins, D. A., Fu, F.-X., Yang, S.-C., John, S. G., Romaniello, S. J., Andrews, M. G., et al. (2023). Responses of globally important phytoplankton species to olivine dissolution products and implications for carbon dioxide removal via ocean alkalinity enhancement. *Biogeosciences* 20, 4669–4682. doi: 10.5194/bg-20-4669-2023

Jankowska, E., Montserrat, F., Romaniello, S. J., Walworth, N. G., and Andrews, M. G. (2024). Metal bioaccumulation and effects of olivine sand exposure on benthic marine invertebrates. *Chemosphere* 358, 142195. doi: 10.1016/j.chemosphere.2024.142195

Jochem, F. (2021). FIU BOT4404 Lecture Notes. *Diatoms (Bacillariophyceae)*. Available at: http://www.jochemnet.de/fiu/bot4404/BOT4404_19.html (Accessed November 11, 2024).

Juggins, S., and Telford, Richard. J. (2012). "Exploratory Data Analysis and Data Display," in *Tracking Environmental Change Using Lake Sediments: Data Handling and Numerical Techniques*, eds. H. J. B. Birks, A. F. Lotter, S. Juggins, and J. P. Smol (Dordrecht: Springer Netherlands). doi: 10.1007/978-94-007-2745-8

Jüttner, I., Carter, C., Cox, E. J., Ector, L., Jones, V., Kelly, M. G., et al. (2024). *Freshwater Diatom Flora of Britain and Ireland*. Available at: https://naturalhistory.museumwales.ac.uk/diatoms/ (Accessed August 28, 2024).

Karlusich, J. J. P., Bowler, C., and Biswas, H. (2021). Carbon Dioxide Concentration Mechanisms in Natural Populations of Marine Diatoms: Insights From Tara Oceans. *Front. Plant Sci.* 12, 657821. doi: 10.3389/fpls.2021.657821

Karthick, B., Taylor, J. C., Mahesh, M., and Ramachandra, T. (2010). Protocols for collection, preservation and enumeration of diatoms from Aquatic habitats for water quality monitoring in India. *IUP Journal of Soil & Water Sciences* 3.

Kenitz, K. M., Orenstein, E. C., Roberts, P. L. D., Franks, P. J. S., Jaffe, J. S., Carter, M. L., et al. (2020). Environmental drivers of population variability in colony-forming marine diatoms. *Limnology & Oceanography* 65, 2515–2528. doi: 10.1002/lno.11468

Khairy, H. M., Shaltout, N. A., El-Naggar, M. F., and El-Naggar, N. A. (2014). Impact of elevated CO2 concentrations on the growth and ultrastructure of non-calcifying marine diatom (Chaetoceros gracilis F. Schütt). *The Egyptian Journal of Aquatic Research* 40, 243–250.

Köhler, P., Abrams, J. F., Völker, C., Hauck, J., and Wolf-Gladrow, D. A. (2013). Geoengineering impact of open ocean dissolution of olivine on atmospheric CO2, surface ocean pH and marine biology. *Environmental Research Letters* 8, 014009.

Krammer, K., and Lange-Bertalot, H. (2000). *The genus Pinnularia*. Ruggell/Liechtenstein: Gantner.

Krammer, K., and Lange-Bertalot, H. (2003). *Cymbopleura, Delicata, Navicymbula, Gomphocymbellopsis, Afrocymbella*. Ruggell/Liechtenstein: Gantner.

Krammer, K., Lange-Bertalot, H., and Pascher, A. (2008). *Süßwasserflora von Mitteleuropa*., Unveränderter Nachdruck. Heidelberg: Spektrum, Akademischer Verlag.

Lange-Bertalot, H., and Podzorski, A. (2001). *Navicula sensu stricto, 10 genera separated from Navicula sensu lato, Frustulia*. Ruggell/Liechtenstein: Gantner.

Lapointe, M. (2000). Modern diatom assemblages in surface sediments from the Maritime Estuary and the Gulf of St. Lawrence, Québec (Canada). *Marine Micropaleontology* 40, 43–65.

Legendre, P., and Birks, H. J. B. (2012a). "Clustering and Partitioning," in *Tracking Environmental Change Using Lake Sediments: Data Handling and Numerical Techniques*, eds. H. J. B. Birks, A. F. Lotter, S. Juggins, and J. P. Smol (Dordrecht: Springer Netherlands). doi: 10.1007/978-94-007-2745-8

Legendre, P., and Birks, H. J. B. (2012b). "From Classical to Canonical Ordination," in *Tracking Environmental Change Using Lake Sediments: Data Handling and Numerical Techniques*, eds. H. J. B. Birks, A. F. Lotter, S. Juggins, and J. P. Smol (Dordrecht: Springer Netherlands). doi: 10.1007/978-94-007-2745-8

Lenton, A., Matear, R. J., Keller, D. P., Scott, V., and Vaughan, N. E. (2018). Assessing carbon dioxide removal through global and regional ocean alkalinization under high and low emission pathways. *Earth System Dynamics* 9, 339–357.

Lenzi, D. (2018). The ethics of negative emissions. *Global Sustainability* 1, e7.

Leote, C., Ibánhez, J. S., and Rocha, C. (2008). Submarine Groundwater Discharge as a nitrogen source to the Ria Formosa studied with seepage meters. *Biogeochemistry* 88, 185–194. doi: 10.1007/s10533-008-9204-9

Lever, J., Krzywinski, M., and Altman, N. (2017). Points of significance: Principal component analysis. *Nature methods* 14, 641–643.

Lewin, J., and Hellebust, J. A. (1978). Utilization of glutamate and glucose for heterotrophic growth by the marine pennate diatom Nitzschia laevis. *Mar. Biol.* 47, 1–7. doi: 10.1007/BF00397012

Li, C., Liu, X., Li, Y., Jiang, Y., Guo, X., Hutchins, D. A., et al. (2024). The interactions between olivine dissolution and phytoplankton in seawater: Potential implications for ocean alkalinization. *Science of The Total Environment* 912, 168571. doi: 10.1016/j.scitotenv.2023.168571

Li, F., Beardall, J., and Gao, K. (2018). Diatom performance in a future ocean: interactions between nitrogen limitation, temperature, and CO2-induced seawater acidification. *ICES Journal of Marine Science* 75, 1451–1464. doi: 10.1093/icesjms/fsx239

Li, W., Wang, T., Campbell, D. A., and Gao, K. (2020). Ocean acidification interacts with variable light to decrease growth but increase particulate organic nitrogen production in a diatom. *Marine Environmental Research* 160, 104965. doi: 10.1016/j.marenvres.2020.104965

Lima, M. J., Relvas, P., and Barbosa, A. B. (2022). Variability patterns and phenology of harmful phytoplankton blooms off southern Portugal: Looking for region-specific environmental drivers and predictors. *Harmful Algae* 116, 102254.

Machás, R., and Santos, R. (1999). Sources of organic matter in Ria Formosa revealed by stable isotope analysis. *Acta Oecologica* 20, 463–469. doi: 10.1016/S1146-609X(99)00122-8

Macreadie, P. I., Hughes, A. R., and Kimbro, D. L. (2013). Loss of 'Blue Carbon' from Coastal Salt Marshes Following Habitat Disturbance. *PLOS ONE* 8, e69244. doi: 10.1371/journal.pone.0069244

Macreadie, P. I., Serrano, O., Maher, D. T., Duarte, C. M., and Beardall, J. (2017). Addressing calcium carbonate cycling in blue carbon accounting. Available at: https://repository.kaust.edu.sa/handle/10754/625940 (Accessed August 26, 2024).

Mann, D. G. (1999). The species concept in diatoms. *Phycologia* 38, 437–495. doi: 10.2216/i0031-8884-38-6-437.1

Manoylov, K., and Ghobara, M. (2021). "Introduction for a Tutorial on Diatom Morphology," in *Diatom Morphogenesis*, eds. V. Annenkov, J. Seckback, and R. Gordon (Wiley), 1–18. doi: 10.1002/9781119488170.ch1

Marques da Silva, J., Duarte, B., and Utkin, A. B. (2020). Travelling expenses: the energy cost of diel vertical migrations of epipelic microphytobenthos. *Frontiers in Marine Science* 7, 433.

Mcleod, E., Chmura, G. L., Bouillon, S., Salm, R., Björk, M., Duarte, C. M., et al. (2011). A blueprint for blue carbon: toward an improved understanding of the role of vegetated coastal habitats in sequestering CO_2. *Frontiers in Ecol & Environ* 9, 552–560. doi: 10.1890/110004

Mendes, I., Gomes, A., Lübbers, J., Cravo, A., Schönfeld, J., Correia, C., et al. (2023). Can alkalinity enhancement in intertidal environments contribute to reduce atmospheric carbon dioxide?

Merz, E., Dick, G. J., de Beer, D., Grim, S., Hübener, T., Littmann, S., et al. (2021). Nitrate respiration and diel migration patterns of diatoms are linked in sediments underneath a microbial mat. *Environmental Microbiology* 23, 1422–1435. doi: 10.1111/1462-2920.15345

Meysman, F. J. R., and Montserrat, F. (2017). Negative CO_2 emissions via enhanced silicate weathering in coastal environments. *Biol. Lett.* 13, 20160905. doi: 10.1098/rsbl.2016.0905

Midttomme, K., and Roaldset, E. (1998). The effect of grain size on thermal conductivity of quartz sands and silts. *PG* 4, 165–172. doi: 10.1144/petgeo.4.2.165

Mishra, M., Arukha, A. P., Bashir, T., Yadav, D., and Prasad, G. B. K. S. (2017). All New Faces of Diatoms: Potential Source of Nanomaterials and Beyond. *Front. Microbiol.* 8, 1239. doi: 10.3389/fmicb.2017.01239

Montserrat, F., Renforth, P., Hartmann, J., Leermakers, M., Knops, P., and Meysman, F. J. R. (2017). Olivine Dissolution in Seawater: Implications for CO_2 Sequestration through Enhanced Weathering in Coastal Environments. *Environ. Sci. Technol.* 51, 3960–3972. doi: 10.1021/acs.est.6b05942

Morel, F. M. M., Kustka, A. B., and Shaked, Y. (2008). The role of unchelated Fe in the iron nutrition of phytoplankton. *Limnology & Oceanography* 53, 400–404. doi: 10.4319/lo.2008.53.1.0400

Morzaria-Luna, H., Turk-Boyer, P., Rosemartin, A., and Camacho-Ibar, V. F. (2014). Vulnerability to climate change of hypersaline salt marshes in the Northern Gulf of California. *Ocean & Coastal Management* 93, 37–50. doi: 10.1016/j.ocecoaman.2014.03.004

Moura, D., Anibal, J., Mendes, I., and Gomes, A. (2019). "Introduction," in *Ria Formosa: challenges of a coastal lagoon in a changing environment*, eds. J. Anibal, A. Gomes, I. Mendes, and D. Moura.

Nagy, S. S. (2011). "Collecting, Cleaning, Mounting, and Photographing Diatoms," in *The Diatom World*, eds. J. Seckbach and P. Kociolek (Dordrecht: Springer Netherlands), 1–18. doi: 10.1007/978-94-007-1327-7_1

Nakov, T., Beaulieu, J. M., and Alverson, A. J. (2018). Accelerated diversification is related to life history and locomotion in a hyperdiverse lineage of microbial eukaryotes (Diatoms, Bacillariophyta). *New Phytologist* 219, 462–473. doi: 10.1111/nph.15137

National Academies of Sciences, Engineering, and Medicine; Division on Earth and Life Studies; Ocean Studies Board; Committee on A Research Strategy for Ocean-based Carbon Dioxide Removal and Sequestration (2021). *A Research Strategy for Ocean-based Carbon Dioxide Removal and Sequestration*. Washington (DC): National Academies Press (US). Available at: http://www.ncbi.nlm.nih.gov/books/NBK580045/ (Accessed August 12, 2024).

Newton, A. (1995). *The water quality of the Ria Formosa lagoon, Portugal*. Bangor University (United Kingdom). Available at: https://search.proquest.com/openview/eb2dfc179f9651c987ba0cf9510aae3c/1?pq-origsite=gscholar&cbl=51922&diss=y (Accessed September 9, 2024).

Økland, R. H. (1996). Are ordination and constrained ordination alternative or complementary strategies in general ecological studies? *J Vegetation Science* 7, 289–292. doi: 10.2307/3236330

Ortiz-Burgos, S. (2016). "Shannon-Weaver Diversity Index," in *Encyclopedia of Estuaries*, ed. M. J. Kennish (Dordrecht: Springer Netherlands), 572–573. doi: 10.1007/978-94-017-8801-4_233

Patil, J. S., and Anil, A. C. (2005). Quantification of diatoms in biofilms: Standardisation of methods. *Biofouling* 21, 181–188. doi: 10.1080/08927010500241726

Pearson, K. (1901). LIII. *On lines and planes of closest fit to systems of points in space*. *The London, Edinburgh, and Dublin Philosophical Magazine and Journal of Science* 2, 559–572. doi: 10.1080/14786440109462720

Pfeffer, C., Larsen, S., Song, J., Dong, M., Besenbacher, F., Meyer, R. L., et al. (2012). Filamentous bacteria transport electrons over centimetre distances. *Nature* 491, 218–221. doi: 10.1038/nature11586

Pielou, E. C. (1966). The measurement of diversity in different types of biological collections. *Journal of theoretical biology* 13, 131–144.

Portuguese Institute for Sea and Atmosphere, IPMA (2022). Available at: https://www.ipma.pt/en/oclima/monitorizacao/index.jsp?selTipo=m&selVar=rr&selAna=to&selAno=-1 (Accessed September 19, 2024).

Potapova, M., Veselá, J., Smith, C., Minerovic, A., and Aycock, L. (2024). Diatom New Taxon File at the Academy of Natural Sciences (DNTF-ANS), Philadelphia. Available at: http://symbiont.ansp.org/dntf/index.php (Accessed August 28, 2024).

Poulsen, N., Davutoglu, M. G., and Zackova Suchanova, J. (2022). "Diatom Adhesion and Motility," in *The Molecular Life of Diatoms*, eds. A. Falciatore and T. Mock (Cham: Springer International Publishing), 367–393. doi: 10.1007/978-3-030-92499-7_14

Prigiobbe, V., Hänchen, M., Costa, G., Baciocchi, R., and Mazzotti, M. (2009). Analysis of the effect of temperature, pH, CO2 pressure and salinity on the olivine dissolution kinetics. *Energy Procedia* 1, 4881–4884. doi: 10.1016/j.egypro.2009.02.317

Qiu, L., Jiang, K., Li, Q., Yuan, D., Chen, J., Yang, B., et al. (2024). Variability of total alkalinity in coastal surface waters determined using an in-situ analyzer in conjunction with the application of a neural network-based prediction model. *Science of The Total Environment* 908, 168271. doi: 10.1016/j.scitotenv.2023.168271

Rato, A., Joaquim, S., Matias, A. M., Roque, C., Marques, A., and Matias, D. (2022). The Impact of Climate Change on Bivalve Farming: Combined Effect of Temperature and Salinity on Survival and Feeding Behavior of Clams Ruditapes decussatus. *Front. Mar. Sci.* 9. doi: 10.3389/fmars.2022.932310

Raven, J. A., and Crawfurd, K. (2012). Environmental controls on coccolithophore calcification. *Marine Ecology Progress Series* 470, 137–166.

Redondo-Gómez, S., Wharmby, C., Castillo, J. M., Mateos-Naranjo, E., Luque, C. J., De Cires, A., et al. (2006). Growth and photosynthetic responses to salinity in an extreme halophyte, *Sarcocornia fruticosa*. *Physiologia Plantarum* 128, 116–124. doi: 10.1111/j.1399-3054.2006.00719.x

Ren, H., Hu, Y., Liu, J., Zhang, Z., Mou, L., Pan, Y., et al. (2022). Response of a Coastal Microbial Community to Olivine Addition in the Muping Marine Ranch, Yantai. *Front. Microbiol.* 12, 805361. doi: 10.3389/fmicb.2021.805361

Renforth, P., and Henderson, G. (2017). Assessing ocean alkalinity for carbon sequestration. *Reviews of Geophysics* 55, 636–674. doi: 10.1002/2016RG000533

Rijstenbil, J. W. (2002). Assessment of oxidative stress in the planktonic diatom Thalassiosira pseudonana in response to UVA and UVB radiation. *Journal of Plankton Research* 24, 1277–1288.

Rinder, T., and von Hagke, C. (2021). The influence of particle size on the potential of enhanced basalt weathering for carbon dioxide removal-Insights from a regional assessment. *Journal of Cleaner Production* 315, 128178.

Rodrigues, M., Rosa, A., Cravo, A., Jacob, J., and Fortunato, A. B. (2021). Effects of climate change and anthropogenic pressures in the water quality of a coastal lagoon (Ria Formosa, Portugal). *Science of The Total Environment* 780, 146311.

Rogelj, J., Popp, A., Calvin, K. V., Luderer, G., Emmerling, J., Gernaat, D., et al. (2018). Scenarios towards limiting global mean temperature increase below 1.5 °C. *Nature Clim Change* 8, 325–332. doi: 10.1038/s41558-018-0091-3

Rønning, J., Kofoed, Z. J., Jacobsen, M., and Löscher, C. R. (2024). Response of Marine Primary Producers to Olivine Additions. doi: 10.5194/egusphere-2023-2884

Round, F. E., Crawford, R. M., and Mann, D. G. (1990). *Diatoms: biology and morphology of the genera*. Cambridge university press.

Round, F. E., and Palmer, J. D. (1966). Persistent, vertical-migration rhythms in benthic microflora.: II. Field and laboratory studies on diatoms from the banks of the River Avon. *Journal of the Marine Biological Association of the United Kingdom* 46, 191–214.

Ryderheim, F., Hansen, P. J., and Kiørboe, T. (2022). Predator field and colony morphology determine the defensive benefit of colony formation in marine phytoplankton. *Frontiers in Marine Science* 9, 829419.

Ryves, D. B., Battarbee, R. W., and Fritz, S. C. (2009). The dilemma of disappearing diatoms: Incorporating diatom dissolution data into palaeoenvironmental modelling and reconstruction. *Quaternary Science Reviews* 28, 120–136.

Saburova, M. A., and Polikarpov, I. G. (2003). Diatom activity within soft sediments: behavioural and physiological processes. *Marine Ecology Progress Series* 251, 115–126.

Sathyendranath, S., Jackson, T., Brockmann, C., Brotas, V., Calton, B., Chuprin, A., et al. (2023). ESA Ocean Colour Climate Change Initiative (Ocean_Colour_cci): Version 6.0, 4km resolution data. doi: 10.5285/5011D22AAE5A4671B0CBC7D05C56C4F0

Sato, S., and Medlin, L. K. (2006). MOTILITY OF NON-RAPHID DIATOMS. *Diatom Research* 21, 473–477. doi: 10.1080/0269249X.2006.9705686

Scheffer, M., Carpenter, S., Foley, J. A., Folke, C., and Walker, B. (2001). Catastrophic shifts in ecosystems. *Nature* 413, 591–596. doi: 10.1038/35098000

Scherer, R. P. (1994). A new method for the determination of absolute abundance of diatoms and other silt-sized sedimentary particles. *Journal of Paleolimnology* 12, 171–179.

Schoefs, B., Van De Vijver, B., Wetzel, C. E., and Ector, L. (2020). Introduction : From diatom species identification to ecological and biotechnological applications. *Botany Letters* 167, 2–6. doi: 10.1080/23818107.2020.1719883

Schuiling, R. D., and De Boer, P. (2010). Coastal spreading of olivine to control atmospheric CO2 concentrations: A critical analysis of viability. Comment: Nature and laboratory models are different. *International Journal of Greenhouse Gas Control* 4. doi: 10.1016/j.ijggc.2010.04.012

Schuiling, R. D., and Krijgsman, P. (2006). Enhanced Weathering: An Effective and Cheap Tool to Sequester Co2. *Climatic Change* 74, 349–354. doi: 10.1007/s10584-005-3485-y

Serôdio, J. (2021). "Diatom Motility: Mechanisms, Control and Adaptive Value," in *Diatom Gliding Motility*, (John Wiley & Sons, Ltd), 159–183. doi: 10.1002/9781119526483.ch7

Serôdio, J., Bastos, A., Morelle, J., and Frankenbach, S. (2023). Light niche construction: Motility of sediment-inhabiting diatoms determines the experienced light environment. *Ecological Modelling* 481, 110379. doi: 10.1016/j.ecolmodel.2023.110379

Serôdio, J., da Silva, J. M., and Catarino, F. (2001). Use of in vivo chlorophyll a fluorescence to quantify short-term variations in the productive biomass of intertidal microphytobenthos. *Marine Ecology Progress Series* 218, 45–61.

Shannon, C. E. (1948). A mathematical theory of communication. *The Bell System Technical Journal* 27, 379–423. doi: 10.1002/j.1538-7305.1948.tb01338.x

Shapiro, S. S., and Wilk, M. B. (1965). An analysis of variance test for normality (complete samples). *Biometrika* 52, 591–611. doi: 10.1093/biomet/52.3-4.591

Shi, D., Li, W., Hopkinson, B. M., Hong, H., Li, D., Kao, S., et al. (2015). Interactive effects of light, nitrogen source, and carbon dioxide on energy metabolism in the diatom *Thalassiosira pseudonana*. *Limnology & Oceanography* 60, 1805–1822. doi: 10.1002/lno.10134

Silva, M., Duarte, D., and Chicharo, L. (2019). Metal contamination in Ria Formosa saltmarsh sediments and halophyte vegetation. *Ria Formosa. Challenges of a coastal lagoon in a changing environment*, 99–107.

Smol, J. P., and Stoermer, E. F. (2010). *The Diatoms: Applications for the Environmental and Earth Sciences*. Cambridge University Press.

Snoeijs, P. J. M. (1990). Effects of temperature on spring bloom dynamics of epilithic diatom communities in the Gulf of Bothnia. *J Vegetation Science* 1, 599–608. doi: 10.2307/3235565

Snoeijs, P., and Weckström, K. (2010). Diatoms and environmental change in large brackish-water ecosystems. *The Diatoms: Applications for the Environmental and Earth Sciences, edited by: Smol, JP and Stoermer, E F., Cambridge University Press, Cambridge*, 287–308.

Souffreau, C., Vanormelingen, P., Verleyen, E., Sabbe, K., and Vyverman, W. (2010). Tolerance of benthic diatoms from temperate aquatic and terrestrial habitats to experimental desiccation and temperature stress. *Phycologia*. doi: 10.2216/09-30.1

Soulsby, P. G., Mollowney, M., Marsh, G., and Lowthion, D. (1985). The role of phytoplankton in the dissolved oxygen budget of a stratified estuary. *Water Science and Technology* 17, 745–756.

Sousa, C. A., Cunha, M. E., and Ribeiro, L. (2020). Tracking 130 years of coastal wetland reclamation in Ria Formosa, Portugal: Opportunities for conservation and aquaculture. *Land Use Policy* 94, 104544.

Spaulding, S. A., Potapova, M. G., Bishop, I. W., Lee, S. S., Gasperak, T. S., Jovanoska, E., et al. (2021). *Diatoms.org* : supporting taxonomists, connecting communities. *Diatom Research*. Available at: https://www.tandfonline.com/doi/full/10.1080/0269249X.2021.2006790 (Accessed August 28, 2024).

Spearman, C. (1961). The proof and measurement of association between two things. Available at: https://psycnet.apa.org/record/2006-10257-005 (Accessed August 28, 2024).

Spilling, K., Olli, K., Lehtoranta, J., Kremp, A., Tedesco, L., Tamelander, T., et al. (2018). Shifting Diatom—Dinoflagellate Dominance During Spring Bloom in the Baltic Sea and its Potential Effects on Biogeochemical Cycling. *Front. Mar. Sci.* 5, 327. doi: 10.3389/fmars.2018.00327

Stock, F. (2019). Quorum sensing mediated interactions between bacteria and diatoms.

Strefler, J., Amann, T., Bauer, N., Kriegler, E., and Hartmann, J. (2018). Potential and costs of carbon dioxide removal by enhanced weathering of rocks. *Environ. Res. Lett.* 13, 034010. doi: 10.1088/1748-9326/aaa9c4

Stuart-Fox, D., Newton, E., and Clusella-Trullas, S. (2017). Thermal consequences of colour and near-infrared reflectance. *Phil. Trans. R. Soc. B* 372, 20160345. doi: 10.1098/rstb.2016.0345

Taylor, J. C., De La Rey, P. A., and Van Rensburg, L. (2005). Recommendations for the collection, preparation and enumeration of diatoms from riverine habitats for water quality monitoring in South Africa. *African Journal of Aquatic Science* 30, 65–75. doi: 10.2989/16085910509503836

Taylor, L. L., Quirk, J., Thorley, R., Kharecha, P. A., Hansen, J., Ridgwell, A., et al. (2016). Enhanced weathering strategies for stabilizing climate and averting ocean acidification. *Nature Climate Change* 6, 402–406.

te Pas, E. E., Hagens, M., and Comans, R. N. (2023). Assessment of the enhanced weathering potential of different silicate minerals to improve soil quality and sequester CO2. *Frontiers in Climate* 4, 954064.

Tornés, E., Cambra, J., Gomà, J., Leira, M., Ortiz, R., and Sabater, S. (2007). Indicator taxa of benthic diatom communities: a case study in Mediterranean streams. *Ann. Limnol. - Int. J. Lim.* 43, 1–11. doi: 10.1051/limn/2007023

Tortora, G. J., Funke, B. R., and Case, C. L. (2007). *Microbiology: an introduction*. Pearson Benjamin Cummings San Francisco, CA.

Tréguer, P., Bowler, C., Moriceau, B., Dutkiewicz, S., Gehlen, M., Aumont, O., et al. (2018). Influence of diatom diversity on the ocean biological carbon pump. *Nature Geoscience* 11, 27–37.

Trigueros, J. M., and Orive, E. (2001). Seasonal variations of diatoms and dinoflagellates in a shallow, temperate estuary, with emphasis on neritic assemblages. *Hydrobiologia* 444, 119–133. doi: 10.1023/A:1017563031810

Trobajo, R., Clavero, E., Chepurnov, V. A., Sabbe, K., Mann, D. G., Ishihara, S., et al. (2009). Morphological, genetic and mating diversity within the widespread bioindicator Nitzschia palea (Bacillariophyceae). *Phycologia* 48, 443–459. doi: 10.2216/08-69.1

Trobajo, R., Cox, E. J., and Quintana, X. D. (2004). The effects of some environmental variables on the morphology of Nitzschia frustulum (Bacillariophyta), in relation its use as a bioindicator. *nova_hedwigia* 79, 433–445. doi: 10.1127/0029-5035/2004/0079-0433

Vandeginste, V., Lim, C., and Ji, Y. (2024). Exploratory Review on Environmental Aspects of Enhanced Weathering as a Carbon Dioxide Removal Method. *Minerals* 14, 75.

Vaux, D. L., Fidler, F., and Cumming, G. (2012). Replicates and repeats—what is the difference and is it significant?: A brief discussion of statistics and experimental design. *EMBO Reports* 13, 291–296. doi: 10.1038/embor.2012.36

Villareal, T. A., and Lipschultz, F. (1995). Internal nitrate concentrations in single cells of large phytoplankton from the Sargasso Sea. *Journal of Phycology* 31, 689–696. doi: 10.1111/j.0022-3646.1995.00689.x

Wada, S., Agostini, S., Harvey, B. P., Omori, Y., and Hall-Spencer, J. M. (2021). Ocean acidification increases phytobenthic carbon fixation and export in a warm-temperate system. *Estuarine, Coastal and Shelf Science* 250, 107113. doi: 10.1016/j.ecss.2020.107113

Wandre, A. S. (2023). Investigation of the Microbial Community Structure of Peat and Saltmarsh Plant Microbial Fuel Cells. Manchester Metropolitan University. Available at: https://e-space.mmu.ac.uk/631688/ (Accessed August 22, 2024).

Wang, H., Pilcher, D. J., Kearney, K. A., Cross, J. N., Shugart, O. M., Eisaman, M. D., et al. (2023). Simulated Impact of Ocean Alkalinity Enhancement on Atmospheric CO_2 Removal in the Bering Sea. *Earth's Future* 11, e2022EF002816. doi: 10.1029/2022EF002816

Williams, D. M., and Kociolek, J. P. (2011). "An Overview of Diatom Classification with Some Prospects for the Future," in *The Diatom World*, eds. J. Seckbach and P. Kociolek (Dordrecht: Springer Netherlands), 47–91. doi: 10.1007/978-94-007-1327-7_3

Wilson, A. M., Huettel, M., and Klein, S. (2008). Grain size and depositional environment as predictors of permeability in coastal marine sands. *Estuarine, Coastal and Shelf Science* 80, 193–199. doi: 10.1016/j.ecss.2008.06.011

Winston, J. E., and Disney, H. (2000). Describing species: practical taxonomic procedure for biologists. *Nature* 405, 619.

Witkowski, A., Lange-Bertalot, H., and Metzeltin, D. (2000). *Iconographia diatomologica:*

annotated diatom micrographs diversity-taxonomy-identification. Ruggell: A.R.G. Gantner Verlag.

Wolfrath, B. (1992). Burrowing of the fiddler crab Uca tangeri in the Ria Formosa in Portugal and its influence on sediment structure. *Marine Ecology Progress Series* 85, 237–243.

Wootton, J. T., Pfister, C. A., and Forester, J. D. (2008). Dynamic patterns and ecological impacts of declining ocean pH in a high-resolution multi-year dataset. *Proc. Natl. Acad. Sci. U.S.A.* 105, 18848–18853. doi: 10.1073/pnas.0810079105

Xin, X., Faucher, G., and Riebesell, U. (2024). Phytoplankton response to increased nickel in the context of ocean alkalinity enhancement. *Biogeosciences* 21, 761–772. doi: 10.5194/bg-21-761-2024

Xiong, W., Wells, R. K., Horner, J. A., Schaef, H. T., Skemer, P. A., and Giammar, D. E. (2018). CO_2 Mineral Sequestration in Naturally Porous Basalt. *Environ. Sci. Technol. Lett.* 5, 142–147. doi: 10.1021/acs.estlett.8b00047

Yamagata, Y., Hanasaki, N., Ito, A., Kinoshita, T., Murakami, D., and Zhou, Q. (2018). Estimating water–food–ecosystem trade-offs for the global negative emission scenario (IPCC-RCP2.6). *Sustain Sci* 13, 301–313. doi: 10.1007/s11625-017-0522-5

Yamamoto, M., and Ohtsuka, T. (2020). Evaluation of three preparation methods for living diatoms at a sandy river–mouth tidal flat: conventional acid–cleaning, nuclear staining, and sieving. *Fottea* 20, 17–24.

Yang, H., Flower, R. J., and Battarbee, R. W. (2010a). An improved coverslip method for investigating epipelic diatoms. *European Journal of Phycology* 45, 191–199. doi: 10.1080/09670260903518439

Yang, H., Flower, R. J., and Battarbee, R. W. (2010b). An improved coverslip method for investigating epipelic diatoms. *European Journal of Phycology* 45, 191–199. doi: 10.1080/09670260903518439

Yap, B. W., and Sim, C. H. (2011). Comparisons of various types of normality tests. *Journal of Statistical Computation and Simulation* 81, 2141–2155. doi: 10.1080/00949655.2010.520163

Appendix I- Physiochemical parameter raw data

Table 1- Summary of four environmental parameters for pore and surface water as well as in situ temperatures for the five conditions.

		Surface water				**Pore water**				
Condition	Date	O^2 (mg/l)	Sal (ppt)	pH	Alk (mM)	O^2 (mg/l)	Sal (ppt)	pH	Alk (mM)	Temp (°C)
C	15/09/22	7.16	36.4	7.950	2.129	-	-	-		28.9
	12/12/22	5.90	33.8	7.774	2.506	6.32	32.3	6.446	2.674	20.5
	13/03/23	7.44	36.5	8.082	2.520	6.50	37.0	6.953	1.936	23.0
OF	15/09/22	7.04	36.5	7.960	2.129	-	38.8	8.110	5.067	28.6
	12/12/22	6.26	33.8	7.638	2.685	6.10	33.9	7.142	2.429	20.8
	13/03/23	6.96	36.5	8.022	2.476	6.46	37.4	6.839	2.331	23.2
OC	15/09/22	6.74	36.5	7.860	2.087	-	38.0	7.970	5.979	28.8
	12/12/22	3.80	33.7	7.412	3.146	6.23	33.5	6.883	2.933	20.6
	13/03/23	7.35	36.5	8.055	2.595	6.42	37.5	6.757	1.676	21.0
BF	15/09/22	6.28	36.4	7.770	2.453	-	38.0	7.860	5.766	30.1
	12/12/22	5.88	33.8	7.772	2.628	6.22	33.2	6.987	2.590	20.5
	13/03/23	7.56	36.5	8.109	2.592	6.59	37.3	6.743	2.011	21.8
BC	15/09/22	6.88	36.4	7.850	3.134	-	37.2	7.820	3.790	28.4
	12/12/22	6.05	33.9	7.778	2.493	6.72	33.8	7.488	2.745	20.6
	13/03/23	7.40	36.5	8.115	2.491	6.95	36.9	6.904	3.006	20.0

Table 2 – Summary statistics for environmental parameters

	Oxy	**Sal**	**pH**	**Alk**	**Temp**
N	15	15	15	15	15
Min	3.8	33.7	7.412	2.087	20
Max	7.56	36.5	8.115	3.146	30.1
Sum	98.7	533.7	118.147	38.064	356.8
Mean	6.58	35.58	7.876467	2.5376	23.78667
Std. error	0.248111	0.336679	0.050458	0.079143	1.008151
Variance	0.923386	1.700286	0.03819	0.093955	15.24552
Stand. dev	0.96093	1.30395	0.195423	0.30652	3.904552
Median	6.88	36.4	7.86	2.506	21.8
25 prcntil	6.05	33.8	7.772	2.453	20.6
75 prcntil	7.35	36.5	8.055	2.628	28.6
Mode	NA	36.5	NA	2.129	NA
Skewness	-1.8008	-0.78811	-0.81254	0.608524	0.656552
Kurtosis	4.316845	-1.60466	0.729869	0.726412	-1.54951
Geom. mean	6.49956	35.55731	7.874176	2.52077	23.50271
Coeff. var	14.60379	3.66484	2.481104	12.07914	16.41488
Shapiro-Wilk W	0.8265	0.6326	0.9236	0.8793	0.7804
p(normal)	0.008211	5.15E-05	0.2187	0.04625	0.002081

Appendix II - Diatom species and preferences

Table 1– Salinity preference of the top 5% most abundant species. Numbers are associated to the scale created by Denys, 1991. For the salinity preferences, acronyms are used to indicate water types: M (Marine), B (Brackish), F(Fresh).

Species	Salinity Preference
Navicula ramosissima	3/M-MB
Psammodictyon panduriforme var. continuum	3/M-MB
Staurosirella guenter-grassii	3/M-MB
Tabularia fasciculata	3/M-MB
Navicula salinicola	4/MB
Cocconeis scutellum	5/MB-BM
Navicula phyllepta	5/MB-BM
Nitzschia sigma	7/BM-B
Navicula gregaria	8/B
Navicula sp.1 (ribeiro 2010 tagus)	8/B
Navicula sp.4 Ana Gomes 2014	8/B
Navicula phylleptosoma	8/B
Halamphora coffeiformis	8/B
Denticula subtilis	8/B
Nitzschia frustulum	9/B-BF
Nitzschia palea	12/FB
Encyonema Sp.1	14/FR
Navicymbula pusilla	14/FR
Karayevia nitidiformis	14/FR

Table 2 – Species appearing <1 % abundance with code, full name, and (basonym author) author

Species code	Species full name (basionym author), published author
Ach.Adn	*Achnanthes adnata* Bory 1822
Amp.Ten	*Amphora tenuissima* Giffen, nom. illeg. 1967
Bir.Luc	*Biremis lucens* (Hustedt) Sabbe, Witkowski & Vyverman 1995
Coc.Nug	*Cocconeis nugalas* M.H.Hohn & J.Hellerman 1966
Coc.Pel	*Cocconeis peltoides* Hustedt 1939
Coc.Pla	*Cocconeis placentula* Ehrenberg 1838
Coc.scu	*Cocconeis scutellum* Ehrenberg 1838
Den.sub	*Denticula subtilis* Grunow 1862
Dip.Did	*Diploneis didymus* (Ehrenberg) Ehrenberg 1845
Enc.sp1	*Encyonema Sp.1*
Eun.Inc	*Eunotia incisa* W.Smith ex W.Gregory 1854
Gop.Exu	*Gomphonema exiguum* Kützing 1844
Gyr.Exi	*Gyrosigma eximium (*Thwaites) Boyer 1927
Hal.cof	*Halamphora coffeiformis* (C.Agardh) Mereschkowsky 1903
Kar.nit	*Karayevia nitidiformis* (Lange-Bertalot) Bukhtiyarova 2006
Nav.Del	*Navicula dilucida* Hustedt 1939
Nav.gre	*Navicula gregaria* Donkin 1861
Nav.Marg	*Navicula margalithii* Lange-Bertalot 1985
Nav.Mic	*Navicula microdigitoradiata* Lange-Bertalot 1993
Nav.phs	*Navicula phylleptosoma* Lange-Bertalot 1999
Nav.phy	*Navicula phyllepta* Kützing 1844
Nav.ram	*Navicula ramosissima* (C.Agardh) Cleve 1895
Nav.sal	*Navicula salinicola* Hustedt 1939
Nav.sp1	*Navicula sp.1* Ribeiro 2010
Nav.sp4	*Navicula sp.4* Ana Gomes 2014
Navcy.p	*Navicymbula pusilla* (Grunow) Krammer 2003
Nit.fru	*Nitzschia frustulum* (Kützing) Grunow 1880
Nit.pal	*Nitzschia palea* (Kützing) W.Smith 1856
Nit.Pro	*Nitzschia prolongata* Hustedt 1938

Nit.sig	*Nitzschia sigma* (Kützing) W.Smith 1853
Nit.Sol	*Nitzschia solita* Hustedt 1953
Nit.Val	*Nitzschia valdestriata* Aleem & Hustedt 1951
Ope.Pac	*Opephora pacifica* (Grunow) Petit 1889
Pla.del	*Planothidium delicatulum* (Kützing) Round & Bukhtiyarova 1996
Ple.Sal	*Pleurosigma salinarum* (Grunow) Grunow 1880
Psa.pan	*Psammodictyon panduriforme var. continuum* (Grunow) Snoeijis 1998
Rho.Mus	*Rhopalodia musculus* (Kützing) O.Müller 1900
Sta.gue	*Staurosirella guenter-grassii* (Witkowski & Lange-Bertalot) E.A.Morales, C.E.Wetzel & Ector 2019
Tab.Fas	*Tabularia fasciculata* (C.Agardh) D.M.Williams & Round 1986
Try.Api	*Tryblionella apiculata* W.Gregory 1857
Try.Com	*Tryblionella compressa* (Bailey) Poulin 1990

Table 3 – Summary of diatom species with ≥**1** % abundance

	Control			**Olivine Fine**			**Olivine Coarse**			**Basalt coarse**			**Basalt fine**		
	0922	**1222**	**0323**	**0922**	**1222**	**0323**	**0922**	**1222**	**0323**	**0922**	**1222**	**0323**	**0922**	**1222**	**0323**
Ach.Adn	0.0	0.0	0.7	0.9	0.0	4.0	1.0	2.5	0.3	0.0	1.7	0.7	0.0	1.7	0.7
Amp.Ten	1.7	0.0	0.0	3.0	0.0	0.0	0.0	0.0	0.0	0.0	0.0	0.0	0.0	3.6	0.0
Bir.Luc	0.0	1.0	0.0	0.0	1.0	1.0	0.0	0.0	0.0	0.0	0.0	0.0	0.0	0.0	0.0
Coc.Nug	0.0	0.3	0.0	1.7	1.0	0.7	0.0	0.6	0.0	0.7	1.0	1.7	0.3	0.7	2.0
Coc.Pel	0.0	0.0	1.3	0.0	0.0	1.0	0.0	1.2	2.3	0.0	0.0	2.7	0.0	0.0	0.0
Coc.Pla	0.7	1.9	0.0	0.0	1.6	0.0	0.0	0.0	0.0	2.7	0.0	0.0	0.0	1.3	1.3
Coc.scu	1.7	1.9	4.0	3.4	2.0	2.3	0.3	1.2	2.6	0.7	4.6	3.3	0.0	6.6	2.6
Den.sub	2.7	4.2	3.6	2.6	2.0	3.7	4.3	8.4	5.3	2.7	2.3	6.0	2.0	11.6	6.2
Dip.Did	0.0	0.0	0.0	2.2	1.6	1.7	1.7	1.2	0.0	0.0	1.0	0.0	0.0	1.0	0.0
Enc.sp1	11.3	1.6	0.0	4.3	1.0	0.0	6.0	0.0	0.0	2.0	0.0	0.0	2.7	0.0	2.0
Eun.Inc	0.0	2.9	1.0	0.4	0.0	0.7	1.3	0.0	0.0	0.0	0.0	0.0	0.7	0.0	0.0
Gop.Exu	0.0	2.6	0.0	0.0	0.0	0.0	0.0	1.2	0.0	0.0	1.0	0.0	0.0	0.0	0.0
Gyr.Exi	0.0	1.0	0.3	2.2	1.3	0.0	0.3	0.3	3.9	0.7	1.0	0.3	0.0	0.0	0.7
Hal.cof	3.7	1.3	0.3	1.3	0.0	0.7	1.7	3.1	4.9	2.7	1.3	2.3	2.3	0.0	0.0
Kar.nit	0.0	0.0	0.0	0.0	0.0	4.7	0.0	0.0	0.0	0.0	0.0	0.0	0.3	0.0	0.0
Nav.Del	0.0	0.0	0.7	0.0	1.0	0.0	0.0	0.0	0.0	1.7	0.3	0.0	1.7	0.0	0.0
Nav.gre	0.0	0.0	3.0	0.0	0.0	0.0	0.0	1.9	0.7	0.0	1.3	0.0	8.6	0.0	0.7
Nav.Marg	0.7	0.0	0.3	0.4	0.0	0.0	2.6	3.1	0.7	1.0	0.0	0.0	1.0	0.3	0.7
Nav.Mic	0.0	2.6	2.0	0.0	1.3	0.0	0.0	0.0	0.0	0.0	0.0	0.0	0.0	0.0	0.0
Nav.phs	11.0	6.5	2.0	8.6	0.3	0.0	10.9	0.3	6.6	7.0	1.7	4.3	15.0	0.0	1.6
Nav.Phy	0.0	0.0	0.0	0.0	0.0	0.0	2.0	0.0	0.0	0.3	0.0	0.0	0.0	5.0	0.0
Nav.ram	1.3	4.9	3.3	0.0	0.7	0.3	0.3	1.5	1.3	7.0	3.0	3.7	0.0	1.0	1.6
Nav.sal	5.6	6.1	5.0	2.2	0.3	3.0	3.0	2.8	3.6	6.0	5.3	7.0	1.7	2.3	3.9
Nav.sp1	2.0	0.0	0.0	0.4	5.2	0.0	0.0	1.2	0.0	0.0	3.0	0.0	0.0	0.0	1.0
Nav.sp4	7.3	6.8	2.6	4.3	1.0	1.7	2.3	1.2	3.0	8.0	3.6	2.7	0.7	5.0	2.3
Navcy.p	5.3	5.2	3.3	3.9	0.7	1.3	5.6	0.3	0.3	2.3	1.0	0.0	5.0	0.7	0.3
Nit.fru	13.3	16.2	20.1	22.0	17.7	26.6	22.5	19.2	22.4	14.0	16.2	17.6	17.9	16.6	21.3
Nit.pal	0.0	1.6	6.3	0.4	5.2	0.3	0.0	0.0	0.0	0.0	0.0	0.0	0.0	1.7	0.0
Nit.Pro	0.0	1.0	0.3	0.0	0.0	0.0	1.0	0.0	0.0	0.3	0.0	0.0	0.3	1.3	0.0
Nit.sig	0.3	0.0	2.6	2.2	1.0	0.0	2.0	0.3	1.0	1.0	5.0	0.0	0.0	0.7	3.9
Nit.Sol	0.0	0.0	0.0	0.0	0.0	0.7	0.3	1.5	0.7	1.7	1.3	0.0	0.7	0.0	2.6
Nit.Val	3.7	0.0	0.7	0.0	1.3	2.0	0.3	0.6	0.0	0.0	2.0	0.7	0.0	0.3	0.0
Ope.Pac	0.0	0.0	0.0	0.0	1.0	2.7	0.0	0.0	0.0	0.0	0.0	1.3	0.0	0.3	0.0
Pla.del	0.3	1.0	0.7	0.4	0.0	0.7	0.0	0.0	1.6	0.7	2.6	2.7	0.0	0.3	3.6
Ple.Sal	0.0	0.0	0.3	0.0	0.0	1.3	0.0	0.9	0.0	1.0	0.0	1.0	1.3	0.0	0.0
Psa.pan	7.0	11.3	11.9	9.5	7.5	7.6	8.3	9.9	4.9	14.0	13.9	10.0	4.0	7.9	8.2
Rho.Mus	0.0	0.3	0.0	0.9	1.0	0.0	1.3	0.0	0.7	0.0	1.3	0.0	0.0	0.0	0.7
Sta.gue	3.7	4.9	14.9	5.6	19.7	15.6	12.3	18.6	15.5	7.3	10.9	15.3	7.3	17.5	16.7
Tab.Fas	0.0	0.0	0.7	0.0	0.7	3.0	0.0	1.2	6.9	1.7	2.6	0.7	0.0	0.0	3.6
Try.Api	0.0	0.0	0.7	2.2	1.0	0.0	0.0	0.6	0.7	2.3	0.3	1.3	1.0	1.7	2.0
Try.Com	0.0	0.0	0.0	0.0	1.3	1.0	0.0	0.9	0.0	2.0	1.7	2.0	0.0	1.0	1.3

Table 4 – Diatom concentration, diversity, richness and evenness

Condition	Date	Frustule per cm^3	Shannon diversity (H')	Species richness (S)	Species evenness (J')
C	15/09/22	62839	3.141	50	0.803
	12/12/22	202425	3.043	35	0.856
	13/03/23	323714	2.872	39	0.784
OF	15/09/22	43609	3.125	47	0.812
	12/12/22	175178	3.102	49	0.797
	13/03/23	97661	2.819	37	0.781
OC	15/09/22	1073797	2.825	37	0.782
	12/12/22	527821	2.984	49	0.767
	13/03/23	775359	2.800	32	0.808
BF	15/09/22	76386	3.077	41	0.829
	12/12/22	279699	2.935	42	0.785
	13/03/23	419696	2.876	34	0.816
BC	15/09/22	153545	3.030	38	0.833
	12/12/22	167619	3.134	44	0.828
	13/03/23	148517	2.945	36	0.822

Table 5 – Species list appearing in abundances <1 %.

Species name	Species name	Species name
Achananthes brevipes	*Fragilaria brevistriata*	*Nitzschia laevis*
Achananthes c.f. parvula	*Fragilaria fasciculata*	*Nitzschia liebertruthii*
Achnanthes adnata Bory 1822	*Gophonema cf. angustatum*	*Nitzschia lorenziana*
Amphora acutiuscula	*Gophonema miutum*	*Nitzschia nana*
Amphora aff. Arenaria	*Gophonema parvulum*	*Nitzschia obtusa*
Amphora c.f. subacutiuscula	*Gyrosigma wansbeckii*	*Nitzschia pelucida*
Amphora Marina	*Mastagloia obliqua*	*Nitzschia plioveterana*
Amphora sp.1 aff strigosa	*Mastagloia psuedoexuiga*	*Nitzschia prolongata*
Amphora strigosa	*Mastogloia (nov. cf. pumila)*	*Nitzschia sigma*
Analus simonsenii	*Mastogloia Gieskesii*	*Nitzschia solita*
Ardissonea crystalina var. dalmatica	*Mastogloia paradoxa*	*Nitzschia sp.1 (aff. lorenziana)*
Bacillariophycidae gen (?) nov. 2	*Mastogloia pseudoexuiga*	*Nitzschia sp.19288*
Berkeleya aff. Scopolurum	*Mastogloia spec 84/1*	*Nitzschia sp.2 (aff. Leibetruthii)*
Berkeleya fennica	*Navicula aleksandrae*	*Nitzschia subacicularis*
Berkeleya obtusa	*Navicula antonii*	*Nitzschia tubicola*
Berkeleya sp.? Nov icons	*Navicula delucida*	*Nitzschia valdestriata*
Caloneis Westii	*Navicula digitoradiata*	*Nitzschia vexans*
Campilodiscus sp.1	*Navicula duerrenbergiana*	*Parlibelus berkeleyi*
Chamaepinnularia alexandrowiczii	*Navicula erifuga*	*Parlibelus c.f. rhombiformis*
Chamaepinnularia margaritiana	*Navicula germanopolonica*	*Pauliella taeniata*
Cocconeis multiperforata	*Navicula gregaria*	*Pinnularia quarataria va cuneata*
Cocconeis neothumensis	*Navicula gregaria*	*Placoneis anglophila*
Coconeis costata	*Navicula margalathii*	*Planothidium delicatulum*
Coconeis guttata	*Navicula veneta*	*Planothidium frequentissimum*
Coconeis pelta	*Navivula c.f. flagellifera*	*Planothidium pericavum*
Coconeis scutellum	*Nitzschia aurariae*	*Planothidium polaris*
Craticula halophila	*Nitzschia c.f debilis*	*Pseudofallacia tenera*
Craticula molestiformis	*Nitzschia capitellata*	*Psuedostaurosira sp.1*
Craticula vixnegligenda	*Nitzschia clausii*	*Stauroneis dubitabilis*
Cytotella wuethrichiana	*Nitzschia closterium*	*Staurophora amphioxys*
Delphineis c.f suirella	*Nitzschia compressa*	*Suirella cf scalaris*
Dimeregramma minus var. nanum	*Nitzschia dissipata*	*Suirella sp.1 (ribeiro)*
Diploneis elliptica	*Nitzschia flexoides*	*Surirella fastuosa*
Diploneis parca	*Nitzschia fonticola*	*Surirella atomus*
Diploneis smithii	*Nitzschia incognita*	*Trachyneis aspeira*
Fallacia forcipata	*Nitzschia incrustans*	*Tryblionella navicularis*
Fallacia sp.1	*Nitzschia intermedia*	

Appendix III - Ordination scores

Table 1 – Loadings for PCA

	PC 1	PC 2	PC 3	PC 4
C0922	1.778	-0.92254	-0.50739	0.10153
C1222	-1.5047	-0.00525	-0.86516	0.20065
C0323	0.99119	0.77966	0.26689	0.18069
OF0922	1.8399	-0.84891	-0.49204	0.058159
OF1222	-2.0164	-0.38458	-0.27587	-0.00981
OF0323	0.92207	0.47013	0.19455	-0.00201
OC0922	1.6754	-1.2738	-0.599	-0.25744
OC1222	-3.155	-0.65417	0.74071	-0.39432
OC0323	0.44491	1.2777	0.16452	-0.22055
BF0922	0.79656	-1.2438	0.67671	-0.16451
BF1222	-1.6877	0.10605	-0.53608	0.25764
BF0323	0.76261	1.2404	0.27582	0.10873
BC0922	0.046878	-0.27819	2.1778	0.28995
BC1222	-1.4097	-0.02854	-0.85519	0.18238
BC0323	0.51591	1.7657	-0.36632	-0.3311
Sal	0.59307	0.18007	0.38704	-0.68267
pH	0.49078	0.66534	-0.07923	0.55694
Alk	-0.44882	0.29751	0.82773	0.15784
Temp	0.45383	-0.6606	0.39849	0.44594

Table 2 – DCA scores

	Axis 1	Axis 2	Axis 3
C0922	0	79	76
C1222	24	127	0
C0323	60	83	0
OF0922	19	85	85
OF1222	72	139	55
OF0323	135	82	35
OC0922	6	68	25
OC1222	87	57	43
OC0323	73	43	45
BC0922	40	58	48
BC1222	77	80	63
BC0323	101	70	50
BF0922	23	0	14
BF1222	45	117	58
BF0323	66	66	81
Nit.fru	67	62	47
Sta.gue	124	79	25
Psa.pan	53	106	33
Nav.sp4	-1	120	71
Nav.phs	-90	-41	17
Nav.sal	47	61	19
Navcy.p	-82	61	-22
Nav.ram	82	142	-34
Nit.pal	71	339	-120
Enc.sp1	-211	39	180
Den.sub	75	83	50
Coc.scu	113	153	99

Nav.gre	56	-249	-78
Nav.sp1	54	232	299
Tab.Fas	222	-29	92
Nit.sig	3	68	112
Hal.cof	18	-36	-5
Nav.Phy	-159	155	-170
Kar.nit	422	-100	2
Nit.Val	151	178	20
Amp.Ten	-221	209	505
Eun.Inc	-55	144	-225
Gop.Exu	49	319	-147
Nav.Mic	-5	427	-299
Coc.Pla	-63	247	157
Bir.Luc	223	431	-80
Gyr.Exi	45	125	98
Nit.Pro	-150	139	-258
Pla.del	151	55	147
Coc.Pel	278	-31	-103
Dip.Did	129	201	98
Try.Api	55	-4	195
Coc.Nug	148	125	247
Try.Com	206	136	148
Nav.Del	1	-81	-112
Ope.Pac	336	239	68
Rho.Mus	-19	161	100
Ach.Adn	192	71	63
Ple.Sal	214	-131	-59
Nav.Marg	-59	-86	9
Nit.Sol	155	-129	118

Table 3 – RDA eigenvalues

Axis	Eigenvalue	%	Cumulative %	XY corr. (R)
Canonical				
1	3.6184	20.55	20.55	0.9144
2	1.731	9.829	30.37	0.9097
3	0.8432	4.788	35.16	0.7638
4	0.79419	4.509	39.67	0.8984
Residual				
5	2.5956	14.74	54.41	
6	1.6499	9.368	63.78	
7	1.3991	7.944	71.72	
8	1.1286	6.409	78.13	
9	1.1089	6.296	84.43	
10	0.73224	4.158	88.58	
11	0.6185	3.512	92.1	
12	0.57942	3.29	95.39	
13	0.47453	2.694	98.08	
14	0.33793	1.919	100	
15	6.54E-29	3.71E-28	100	
16	1.11E-30	6.31E-30	100	
17	5.31E-31	3.02E-30	100	
18	4.98E-31	2.83E-30	100	

Table 4 – RDA Scores

	Axis 1	Axis 2	Axis 3	Axis 4	Axis 5	Axis 6	Axis 7	Axis 8	Axis 9	Axis 10	Axis 11	Axis 12	Axis 13	Axis 14	Axis 15	Axis 16	Axis 17	Axis 18
Nit.fru	0.005	-0.118	-0.067	-0.166	0.138	-0.004	0.084	-0.016	-0.108	-0.170	0.093	-0.112	-0.136	0.101	-0.087	0.477	-0.006	-0.455
Sta.gue	0.280	-0.152	-0.192	0.053	0.315	0.004	0.054	-0.133	-0.032	-0.090	0.012	0.264	0.050	-0.123	-0.326	-0.231	-0.136	-0.038
Psa.pan	0.060	0.143	0.125	0.079	-0.039	0.051	-0.065	0.143	-0.076	-0.194	-0.077	-0.028	0.438	0.168	-0.014	0.173	-0.053	0.019
Nav.sp4	-0.034	0.239	0.250	-0.079	-0.185	-0.023	-0.269	0.034	-0.053	-0.075	-0.175	-0.035	-0.022	-0.014	0.301	0.230	-0.052	-0.186
Nav.phs	-0.416	-0.250	0.117	-0.274	-0.518	0.056	0.069	-0.186	-0.004	0.073	-0.014	-0.109	0.115	-0.237	-0.232	0.305	-0.091	0.035
Nav.sal	0.059	0.023	0.160	-0.225	-0.203	-0.014	-0.120	0.221	-0.144	-0.007	-0.037	0.097	0.181	0.099	0.016	-0.165	0.028	0.035
Navcy.p	-0.347	0.136	0.114	0.026	-0.138	-0.148	0.147	0.034	-0.039	-0.142	0.026	0.055	-0.036	0.111	0.261	-0.041	0.097	0.327
Nav.ram	0.224	0.125	0.287	0.061	-0.243	-0.004	-0.105	0.152	0.004	-0.193	-0.096	0.220	0.326	-0.001	0.007	-0.031	-0.363	-0.051
Nit.pal	0.075	0.317	0.012	0.036	0.155	-0.272	0.322	-0.165	0.270	-0.253	-0.310	0.057	0.118	0.164	0.126	0.112	-0.174	-0.041
Enc.sp1	-0.470	0.033	0.100	-0.081	-0.188	0.131	-0.193	-0.180	0.267	-0.009	0.138	0.238	-0.115	0.328	-0.119	0.303	0.265	0.259
Den.sub	0.154	-0.021	-0.138	0.019	0.058	-0.147	-0.217	-0.145	-0.234	0.094	-0.006	0.142	-0.087	0.180	-0.153	-0.017	-0.089	-0.312
Coc.scu	0.172	0.277	-0.059	-0.259	0.118	0.018	-0.088	0.004	-0.083	0.059	-0.296	-0.102	0.054	0.061	0.239	-0.124	-0.066	0.140
Nav.gre	-0.006	-0.207	0.059	0.210	-0.039	0.023	0.543	0.010	-0.237	0.498	0.017	0.119	0.037	0.053	0.097	0.071	0.004	0.004
Nav.sp1	-0.003	0.167	-0.238	0.241	0.086	0.406	0.030	0.060	0.320	0.103	-0.142	0.166	-0.007	0.169	-0.025	-0.127	0.101	-0.155
Tab.Fas	0.279	-0.181	0.231	-0.128	0.073	0.329	0.080	0.137	-0.108	-0.169	-0.001	0.012	-0.352	-0.228	0.146	0.020	-0.310	0.056
Nit.sig	-0.013	0.162	0.123	-0.107	0.110	0.380	0.091	-0.178	-0.237	-0.118	-0.179	0.203	0.287	0.036	0.132	0.121	0.192	-0.001
Hal.cof	-0.080	-0.282	-0.044	0.036	-0.261	0.044	-0.092	0.219	-0.114	0.004	-0.261	-0.128	-0.165	-0.204	-0.186	-0.033	0.165	0.082
Nav.Phy	-0.044	0.124	-0.027	0.093	0.112	-0.196	-0.252	-0.239	-0.230	-0.018	0.055	0.220	0.105	-0.397	0.111	0.027	0.202	-0.048
Nit.Val	-0.022	0.094	-0.188	-0.044	0.122	0.039	-0.057	0.405	0.188	0.079	-0.202	0.305	0.005	-0.092	0.049	0.246	0.163	-0.166
Amp.Ten	-0.129	0.222	-0.028	-0.081	0.092	-0.084	-0.266	-0.162	-0.046	0.290	-0.317	-0.204	-0.128	0.114	0.250	0.034	0.009	0.035
Eun.Inc	-0.109	0.058	-0.055	-0.085	-0.072	-0.223	0.200	0.040	-0.090	-0.273	0.214	-0.086	0.015	0.196	0.050	-0.048	0.033	0.052
Gop.Exu	0.066	0.135	-0.212	0.244	-0.154	0.019	0.048	0.150	-0.126	-0.097	0.089	-0.073	-0.005	0.255	0.057	-0.254	0.230	-0.328
Coc.Pla	0.050	0.239	0.281	0.211	-0.085	-0.014	-0.175	-0.190	0.236	-0.078	0.175	0.150	-0.110	0.053	0.222	-0.061	-0.338	0.032
Gyr.Exi	0.074	-0.003	-0.036	-0.072	-0.091	0.234	0.075	-0.204	-0.021	-0.300	-0.197	-0.294	-0.074	-0.058	-0.066	-0.178	0.034	-0.055
Nit.Pro	-0.045	0.107	0.027	0.083	-0.049	-0.216	-0.008	-0.132	-0.139	-0.087	0.119	0.121	0.094	-0.137	0.111	-0.063	0.161	-0.139
Pla.del	0.183	0.083	0.149	-0.418	-0.084	0.171	-0.047	0.077	-0.094	0.068	0.121	-0.070	0.077	0.037	0.173	-0.114	-0.083	-0.296
Coc.Pel	0.188	-0.278	-0.093	-0.214	0.014	-0.110	0.043	0.157	-0.045	-0.053	-0.282	-0.052	-0.041	0.005	-0.373	-0.037	-0.169	0.000
Dip.Did	-0.082	0.067	-0.296	0.180	0.270	0.060	-0.079	0.032	-0.060	-0.209	-0.006	-0.220	0.060	-0.029	-0.034	0.123	0.275	0.179
Try.Api	0.085	-0.050	0.247	0.066	0.060	0.078	-0.036	-0.304	0.017	0.220	-0.091	-0.242	0.253	0.025	-0.085	0.116	-0.227	-0.022
Coc.Nug	0.088	0.041	0.014	0.031	0.084	0.117	-0.104	-0.040	0.090	0.132	0.241	-0.327	0.236	0.195	-0.050	-0.076	0.009	-0.044
Try.Com	0.191	0.015	0.101	0.167	0.120	0.127	-0.194	0.109	0.106	0.073	0.200	-0.011	0.297	-0.148	-0.032	-0.152	-0.049	0.092
Nav.Del	-0.030	-0.017	0.282	0.247	-0.013	0.011	0.215	-0.019	0.145	0.064	0.002	0.009	0.228	-0.307	0.136	0.080	0.084	0.019
Ope.Pac	0.089	-0.029	-0.085	-0.111	0.175	-0.125	-0.076	0.159	0.240	-0.043	0.153	-0.130	-0.016	-0.185	-0.046	0.155	-0.022	-0.032
Rho.Mus	-0.035	0.084	-0.189	-0.088	0.006	0.250	0.066	-0.159	-0.037	-0.241	0.083	-0.055	0.018	-0.110	-0.001	-0.007	0.133	-0.020
Ach.Adn	0.077	-0.037	-0.168	-0.068	0.259	-0.006	-0.084	0.209	-0.328	-0.034	0.030	-0.079	0.037	0.154	0.002	0.205	-0.133	0.312

Ple.Sal	0.035	-0.232	0.167	0.136	0.025	-0.141	0.028	0.211	0.030	0.108	0.104	-0.116	0.143	0.002	-0.144	0.101	0.020	0.001
Nav.Marg	-0.111	-0.234	0.030	0.231	-0.014	0.029	-0.079	-0.146	-0.228	-0.003	-0.091	0.255	-0.053	0.191	-0.313	-0.010	-0.014	0.150
Nit.Sol	0.058	-0.159	0.217	0.190	0.017	0.247	0.005	0.068	-0.216	0.023	0.298	0.087	-0.106	0.012	0.101	0.184	-0.269	0.089
C0922	-3.525	0.761	0.426	-0.721	-1.350	0.350	-1.317	1.114	1.195	0.920	-0.901	1.062	-0.755	0.243	0.000	0.000	0.000	0.000
C1222	-1.201	1.698	0.744	-0.409	-3.581	-1.459	0.437	0.078	0.064	-0.965	0.822	-0.425	-0.366	0.516	0.000	0.000	0.000	0.000
C0323	0.950	0.484	0.431	-0.343	0.689	-1.409	2.400	0.205	-0.405	-0.312	-1.283	0.790	0.701	0.455	0.000	0.000	0.000	0.000
OF0922	-2.405	0.848	-0.555	-1.003	0.881	0.784	-0.351	-0.897	-0.225	-0.091	-0.731	-1.954	0.267	0.658	0.000	0.000	0.000	0.000
OF1222	0.969	1.639	-1.267	1.544	1.660	0.763	0.871	-0.963	2.846	-0.669	-0.138	0.135	0.009	-0.342	0.000	0.000	0.000	0.000
OF0323	1.928	-0.604	-1.454	-0.289	2.959	-0.997	-0.084	2.261	0.153	-0.620	0.883	-0.532	-0.871	-0.048	0.000	0.000	0.000	0.000
OC0922	-3.058	-0.544	-0.863	-0.126	0.364	-0.182	-0.561	-0.644	-1.021	-1.481	0.592	1.046	0.569	-0.387	0.000	0.000	0.000	0.000
OC1222	1.741	-1.648	-1.368	1.840	0.327	0.170	-0.463	0.602	-0.845	0.120	-0.569	0.169	-0.099	0.949	0.000	0.000	0.000	0.000
OC0323	1.247	-2.125	0.092	-1.472	-1.246	0.797	0.466	-0.891	-0.760	-0.451	-0.915	-0.248	-1.401	-0.799	0.000	0.000	0.000	0.000
BC0922	-0.286	-0.094	3.245	0.710	-1.202	0.286	-1.328	0.064	0.188	-0.664	-0.019	-0.193	0.509	-0.454	0.000	0.000	0.000	0.000
BC1222	1.539	0.850	-0.180	0.072	-0.171	2.598	0.744	1.582	-1.139	0.425	0.064	-0.092	0.667	-0.667	0.000	0.000	0.000	0.000
BC0323	2.157	-1.071	0.017	-1.330	-1.041	-0.809	-1.221	0.410	1.028	0.600	0.089	-0.364	1.239	-0.167	0.000	0.000	0.000	0.000
BF0922	-3.110	-2.604	0.695	1.100	-0.797	-0.863	2.031	-0.351	0.089	1.698	0.932	-0.324	-0.083	-0.410	0.000	0.000	0.000	0.000
BF1222	1.558	2.372	-0.880	0.635	1.887	-1.983	-1.524	-1.299	-0.996	1.019	-0.159	0.182	-0.172	-0.484	0.000	0.000	0.000	0.000
BF0323	1.495	0.039	0.917	-0.208	0.621	1.952	-0.101	-1.269	-0.171	0.471	1.332	0.748	-0.214	0.936	0.000	0.000	0.000	0.000
Sal	-0.153	-0.168	0.099	-0.134														
pH	0.035	-0.035	0.077	-0.197														
Alk	0.316	-0.046	0.070	0.132														
Temp	-0.397	-0.069	0.094	-0.007														